DETECTING CLIMATE CHANGE IMPACTS IN LONG ISLAND SOUND

Long Island Sound Study
EPA Grant Number LI96144501
NEI Job Code: 0302-005
Project Code: 2013-007

Prepared For:
U.S. Environmental Protection Agency
Long Island Sound Office
Stamford Government Center
888 Washington Blvd.
Stamford, CT 06904-2152

Prepared By:
Coastal Ocean Analytics, LLC
16 Brook Street
Noank, CT 06340

April 10th, 2016

Executive Summary

The adaptive management of the resources of Long Island Sound (LIS) requires on-going observations to characterize the variability and change of the environment and ecosystem it supports. It is critical that changes that result from local human activities (and therefore can potentially be regulated) be separated from those that are a consequence of natural cycles and global scale processes. In this project we assembled, reviewed, and analyzed existing measurements from Long Island Sound and its watershed to determine whether changes that have been observed at the global scale have discernible and important impacts in the region. We have also created a web site to share the results and distribute data that will facilitate further research on long term changes in the Long Island Sound ecosystem.

The most important results of this project are:

- Over the last century Long Island Sound has warmed at a rate consistent with global averages. The decade of the 1960s was anomalously cool. Warming since then has been faster that global trends but not inconsistent with warming that occurred between the 1940s and 1960s. (See Chapter 1 – Coastal Water Temperature)
- We find no evidence of changes in annual precipitation across the region or in the occurrence of high rates of rainfall. However, it does appear that the rainfall in the coastal Connecticut and Long Island is decreasing slightly and it is increasing at the more inland stations. (See Chapter 2 – Precipitation)
- Coastal air temperatures have increased at a rate consistent with global averages. This has appreciably lengthened the interval between spring and fall frosts. (See Chapter 3 – Coastal Air Temperatures)
- The annual stream flow in the Hudson and Connecticut Rivers is increasing due to higher flow rates in the low-flow months (June-December) and the spring freshet is arriving 8 days earlier than a century ago. (See Chapter 4 – River Discharge)
- Cloud cover over Long Island Sound in the NCEP Reanalysis-II was unusually low during year of anomalously low Chlorophyll-A. It is possible that the reanalysis products are not sufficiently highly resolved to predict the cloud cover at a coastal area like Long Island Sound. (See Chapter 5 – Cloudiness)
- The highest wind stress events each are lower magnitude than they were in the 1960s. This appears to be associated the Atlantic Multi-decadal Oscillation. (See Chapter 6 – Wind)
- Sea levels are rising and that will lead to an increase in the average frequency of flooding at the edge of the Sound. However, winter winds stress events appear to be getting weaker, partially offsetting the effects of sea level rise in the western sound. Ecosystems that are vulnerable to changes in flooding frequency will be more at risk in the eastern Sound. (See Chapter 7 – Sea Level)

Table of Contents

Chapter 1 - Coastal Water Temperature

Table of Contents

List of Figures

List of Tables

1. Ecological Driver: Coastal Water Temperature

1.1 Introduction

Hansen et al. (1996 and 2010) have clearly demonstrated that global-scale averages of observations of surface temperature in the atmosphere over both land and ocean exhibit a warming trend over the last century. However, detecting changes in coastal water temperatures at the scale of estuaries has frequently been confounded by the absence of sufficiently long data records and the presence of high amplitude variations at short time (days to years) and space ($1 - 10^5$ meters) scales. Separating the consequences of this global change from the local impacts of development and resource exploitation is critical to wise environmental management at the scale of estuaries and embayments and it is, therefore, important to make the most effective use of all available observations.

Over the last three decades, the high population density and long history of exploitation of fisheries in the estuaries of southern New England have led to the development and implementation of management regulations to improve water quality and restore fisheries populations. The harvest of American Lobster in Long Island Sound, for example, has declined substantially since 1991 (Howell et al., 2005) and it has been proposed by Camacho et al. (2006) that this is partially a consequence of physiological temperature stress that has been enhanced by warming bottom waters. Clearly, separating the effect of environmental change from that of fishing and other predation is critical to the regulation of the fishery.

Temperature clearly affects other species as well. Hare and Able (2007), for example, showed that average wintertime coastal water temperatures correlated with the abundance of Atlantic croaker the subsequent year. In Long Island Sound, Keser et al. (2003) demonstrated that the growth rate of brown algae, common in New England, is positively correlated with the mean annual water temperature. They suggested that warming will move the southern limit of this species northward to the Gulf of Maine. Stachowicz et al. (2002) studied the settlement of non-native species (Sea Squirts) on rocky substrates in Long Island Sound and demonstrated that during warmer winters, settlement of invaders occurred earlier in the year, providing them with an advantage in the competition for the space.

Recently, Howell and Auster (2012) reported an analysis of the character of fish species distributions in Long Island Sound based on a long time series of trawl surveys. They showed that there has been an increase in the number of species that are more commonly observed to the south of the Sound (warm water adapted) and a coincident reduction in the number of species characteristic of communities to the north (cold water adapted). This shift correlated with temperature change. Understanding whether this is a shift, or part of a long term cycle is a critically important question for the choice and effectiveness of management approach.

Temperature is the best observed characteristic of coastal environments. We assemble available observations to examine the characteristic of their variability in order to discern the magnitude of the local consequences of global changes. In section 1.2 we summarize existing analyses and then in Section 1.3 we describe the data sources used in our study and include a discussion of their limitations. In section 1.4 we show that the trends in temperature using the data, and quantitatively describe the covariation of the records. We then discuss the link between these

variations and global processes. We summarize our conclusions in Section 1.5 and comment on the implications.

1.2 Previous Work

The longest published record of coastal water temperatures in southern New England is that of Nixon et al. (2004). They concatenated the monthly averages reported by Bumpus (1957) and more recent measurement made in the harbor at Woods Hole, MA, between 1885 and 2005 and concluded that the monthly mean temperatures showed a warming in the winter (December, January, and February) between 1970 and 2002. The seasonal variation and spatial distribution of temperature in Long Island Sound was first depicted by Riley (1952). The data series was short (1952-60). Kaputa and Olsen (2000) describe a similar, but more consistent and on-going program of Long Island Sound (LIS) wide surveys that has resolved the seasonal variability of temperature and biogeochemical variables in LIS since 1991. We refer to this as the CTDEEP survey data. O'Donnell et al. (2014) provided a comprehensive summary of the seasonal and spatial structure of the seasonal and along Sound temperature variability using this data set.

McCardell and O'Donnell (2009) used the CTDEEP survey data to infer vertical transport rates of heat and it has also been exploited by Gay et al. (2004) and Lee and Lwisa (2008) to assess the exchange between LIS and the adjacent Block Island Sound. These papers concluded that interannual variations in salinity and temperature in LIS were significantly influenced variability in shelf properties. This conclusion was further explored by using a numerical model by Crowley (2005), Hao (2008) and Lee (2009) who agreed with this conclusion during the spring and summer. However, Lee's (2009) results indicate that the local surface heat flux is the major mechanism that controls the temperature during fall/winter.

Longer time series of temperature have been reported at the cooling water intake of the electric power generation facility at Millstone Point, Connecticut, in eastern LIS (see Figure 1.1) and used to assess the effect of temperature on ecosystem characteristics. Keser et al. (2003) describes the geography and sampling protocols employed and the variation of the temperature between 1979 and 2002. The data was used to assess the effect of temperature on *Ascophyllum nodosum*. Stachowicz et al. (2002) examined the mean winter (January-March) water temperature at Millstone Point to understand the variability of sessile marine invertebrates. They discovered that the rate of change during the 25 year interval 1976-2001 was 0.07 ºC/yr, or 7 ºC per century.

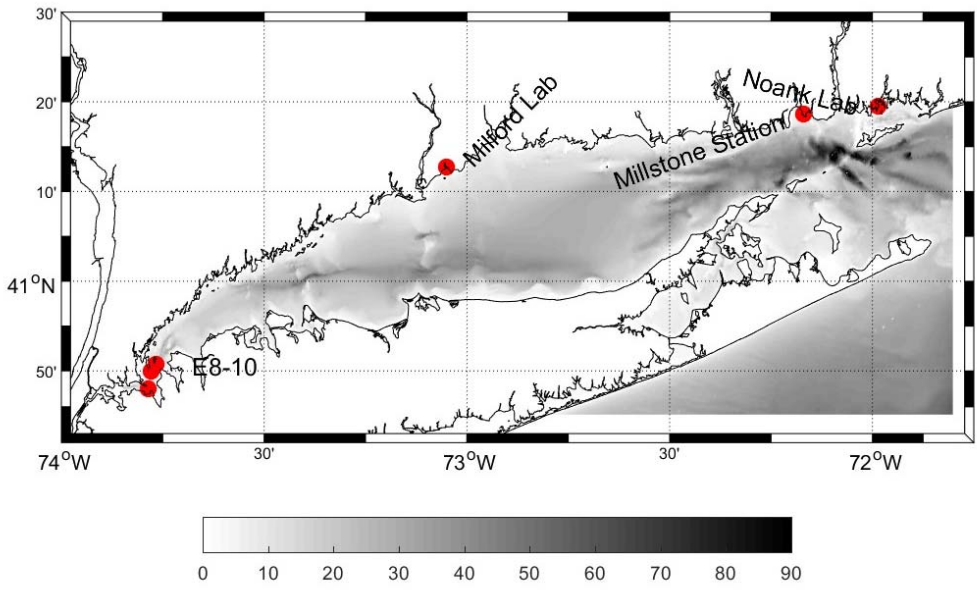

Figure 1.1. Map of the coastline and bathymetry of Long Island Sound showing the locations where the temperature measurements were obtained.

Wilson et al. (2008) reported an analysis of ship survey measurements of summertime dissolved oxygen and temperature at the western boundary of LIS, the East River (see Figure 1.1), conducted by New York City Department of Environmental Protection (DEP). They showed that the temperature of the near bottom water in July-August had decreased between at a rate of 0.03-0.04 ºC/yr between 1945 and 2005. No significant trend in the surface temperatures was reported.

Temperature in LIS is mainly dominated by seasonal variation with the minimum temperature occurring in February and the maximum in September. The annual range of the minimum and maximum temperature is higher in the western Sound (~0.7º to 22.6 ºC) than in the eastern part (1.0º–20.5 ºC). The depth-averaged temperature contains larger inter-annual variability in winter than in summer. For example, the variance of depth-averaged temperature in the central LIS is 1.9 $ºC^2$ in February and 0.2 $ºC^2$ in September (Lee and Lwiza, 2008). The magnitude and the timing of the inter-annual variations of temperature in eastern LIS do not appear to be correlated with those in the western LIS.

Long-term changes in surface temperature in LIS differ markedly between winter and summer. While winter temperatures have been shown to increase, the change for summer has been almost negligible (Lee and Lwiza, 2008). Wilson et al. (2008) reported that the increase in thermal stratification in the western LIS during summer months (July and August) from ~0.5º to 2 ºC between 1946 and 2006 was mainly due to the decrease in bottom temperature.

In this study we aggregate previously unpublished archived temperature data with more accessible observations and statistically derived temperature correlates to more completely describe the long term trends and variability in coastal water temperatures so that significance of the more recent, and well documented, changes can be placed in a broader climate context.

1.3 Data Sources and Data Quality

1.3.1 Noank Marine Laboratory

Noank Marine Laboratory is a facility near the mouth of the Mystic River at the eastern end of Long Island Sound (see Figure 1.1). To support research on shellfish, the laboratory pumped seawater from a few meters below the surface through an aquaculture facility. They monitored the water temperature approximately twice a day, and 5 days a week, beginning November 15th, 1967, and recorded values in a lab notebook. An excerpt is shown in Figure 1.2. In March 1968, water samples were taken and the salinity estimated using a refractometer. Initially the salinity estimates were not as frequent as temperature but by the end of April 1968, temperature and salinity were recorded with approximately equal frequency. The record was moved to Avery Point and measurements commenced there in January 1987 and were terminated in September 1988 when Prof. Feng retired.

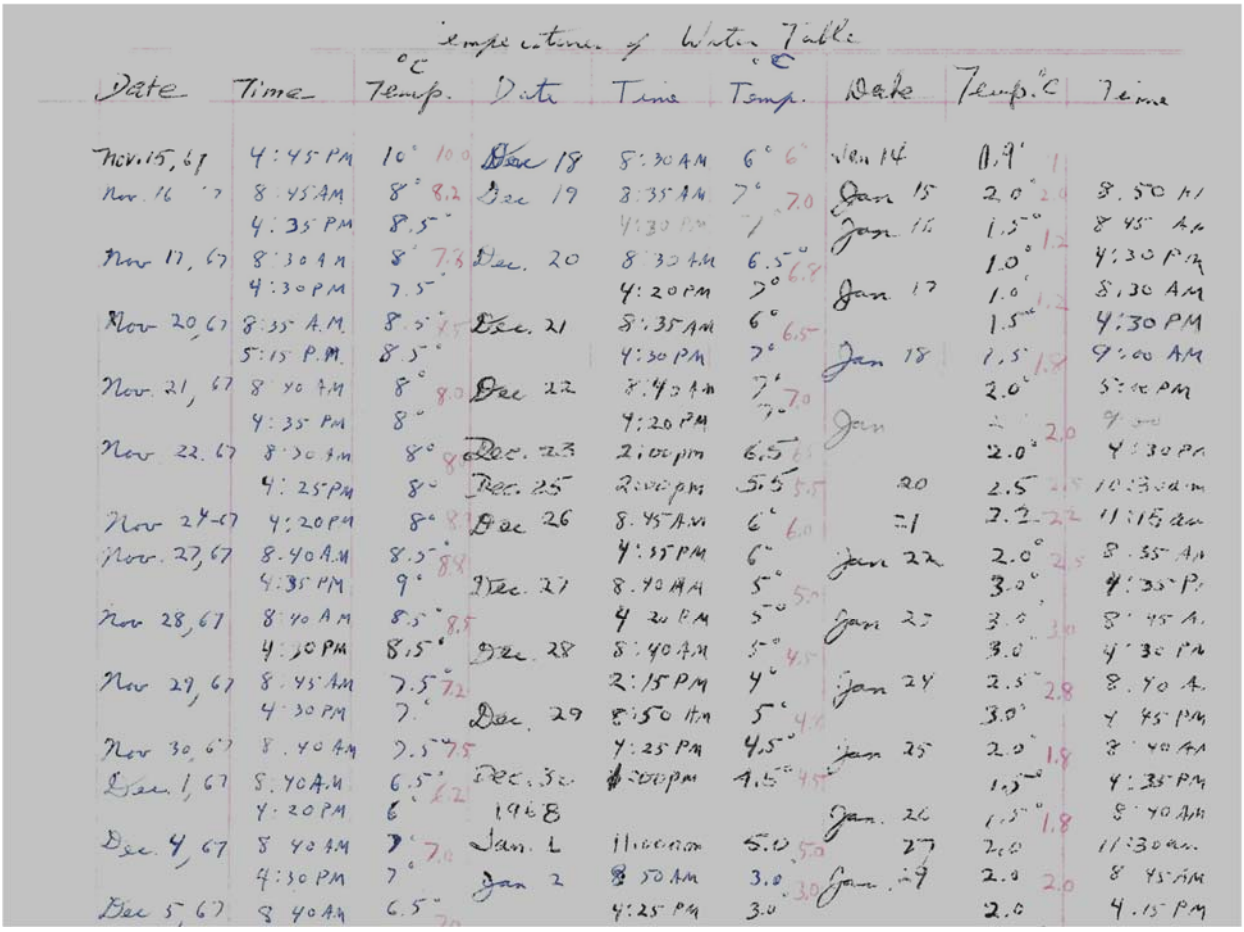

Figure 1.2. Excerpt from the water table temperature log from the University of Connecticut's Laboratory in Noank, CT, created by Prof. S. Feng and Ms. L. Haddad.

The log book was scanned to create a pdf file that could be archived and shared. An intern was employed to transcribe the text to an ASCII file format that could be converted for use with spreadsheets. Figure 1.3 shows time series of the measurements to illustrate the variability and the data density.

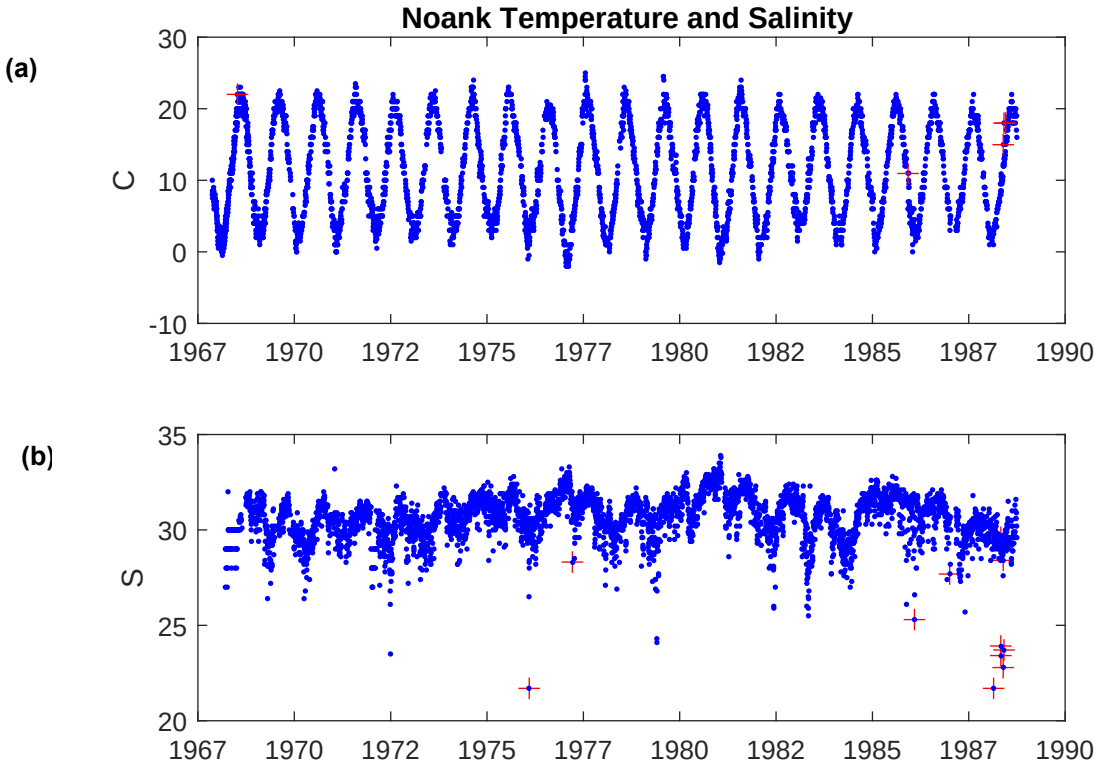

Figure 1.3. (a) Time series of the Noank Marine Laboratory intake water temperature and (b) salinity. The red '+' symbols show the samples identified by the screening process that were not corrected because they were consistent with the lab record.

Like many old data sets, the data quality is not very clear and consistency checks must be implemented to estimate the uncertainty that should be attributed to the data. When data has been transcribed manually, additional review is required. After the intern completed the data assembly, the sample times were subject to a first difference check. In a time series, the difference between the time of sample *n* and sample *n+1* should be positive. Of 4706 samples times transcribed, four were found to be incorrect. Subsequently, we developed an anomaly detection screening procedure. In the first step, we block averaged the data in 3.5 day intervals and then linearly interpolated the block averages back to the original sample times. We computed the difference between the raw and interpolated values. These series represent the high frequency fluctuations. The standard deviations of these anomalies were σ_{Temp} =0.48 ºC and σ_S = 0.49 salinity units. We then identified the samples for which the difference exceeded five times the standard deviations. In Figure 1.3, we show the raw data in blue and the points identified as anomalies by the red '+' symbols. In all, only nine temperature values and 22 salinity values were identified. Each of these was cross-checked with the original record. Four temperature and 17 salinity transcription errors were corrected. In Figure 1.3, the points that were not corrected are shown in red. The cluster in salinity in 1988 is likely a consequence of the larger salinity variance that occurs at Avery Point because of the influence of the outflow from the Thames River. The Thames has a much larger watershed and freshwater discharge than the Mystic River. Only data acquired at Noank will be used.

1.3.2 Milford Laboratory

The National Oceanic and Atmospheric Administration (NOAA) North East Fisheries Science Center (NEFSC) Milford Laboratory has also operated an aquaculture research facility that has monitored the temperature and salinity of the seawater that is pumped into the facility. The pump intake is on a dock located on the Wepawaug River, 300 meters from the connection to Long Island to the south (see Figure 1.1). From 1948 to 1975, the temperature was measured on the dock. Subsequently, the measurements were collected within the Laboratory at a filter (Dr. R. Goldberg, Pers. Com). The water was routed through a holding tank on the roof of the facility and is, therefore, likely to be biased by warming/cooling through heat exchange with the atmosphere. Some of the data has been transferred to notebooks from a Bristol chart recorder (see Figure 1.4a) and a fraction of that has been digitized to computer media.

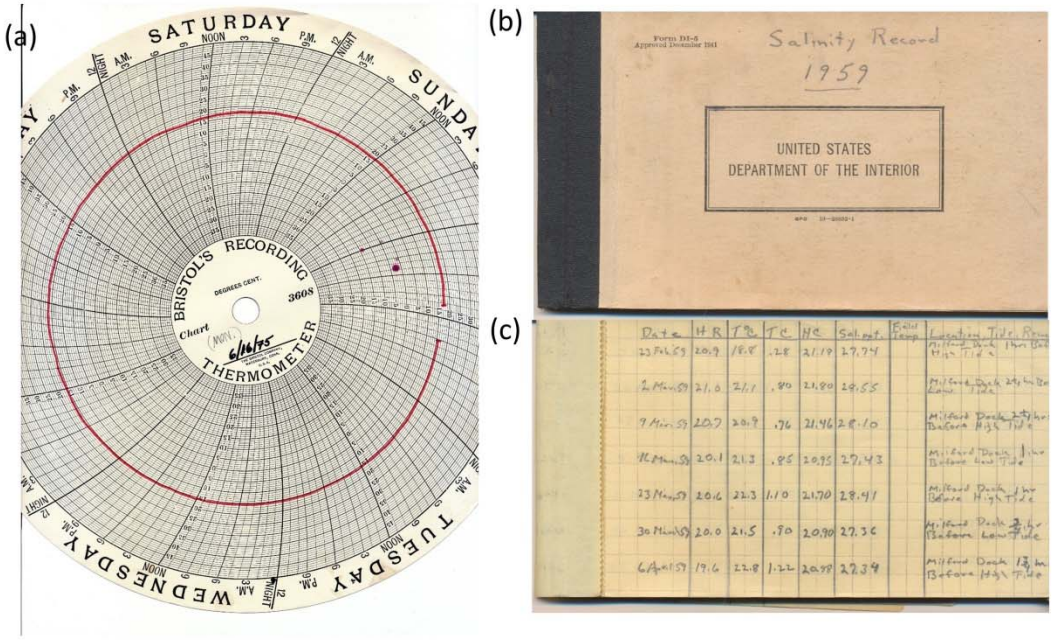

Figure 1.4. (a) An example of the Bristol temperature recorder data storage media. (b) and (c) are examples of the data logs from 1957. These record the location, time, temperature and salinity.

We acquired notebooks with tabulated date (see Figure 1.4b and c) and data files from Dr. J. Rose (NEFSC), and employed interns to transfer the data tables to computer files. An example of the data notebooks is shown in Figure 1.4(b) and (c). These did not have a standard format as the sampling plan evolved. We emphasized the temperature measurements for data entry and logged all the high and low temperatures that were recorded.

Two interns worked as a team to enter and verify the data. One read the notebook entries and the other typed the data to a spreadsheet. At the completion of each month, the data in the spreadsheet would be read by the recorder and confirmed by the reader, or corrected if necessary. In total 14 years of measurements, 1433 entries, were transcribed to Microsoft Excel spreadsheet files.

The data files were then subjected to a second review. Plotting the difference in the sample times in the series revealed a single transcription error in the month column. Subsequently, we employed the anomaly detection screening procedure described in Section 1.2. The standard deviation of these anomalies between the interpolated block averages and the raw data were σ_{Temp} =0.59 ºC and σ_S = 0.569 ºC. We then identified the samples for which the difference exceeded five times the standard deviations. In Figure 1.5, we show the raw high and low temperature data in the blue and the points identified as anomalies by the red '+' symbols. In all, only 13 high and seven low temperature values were identified as anomalies. Each of these was cross-checked with the original record and no errors in transcription were detected.

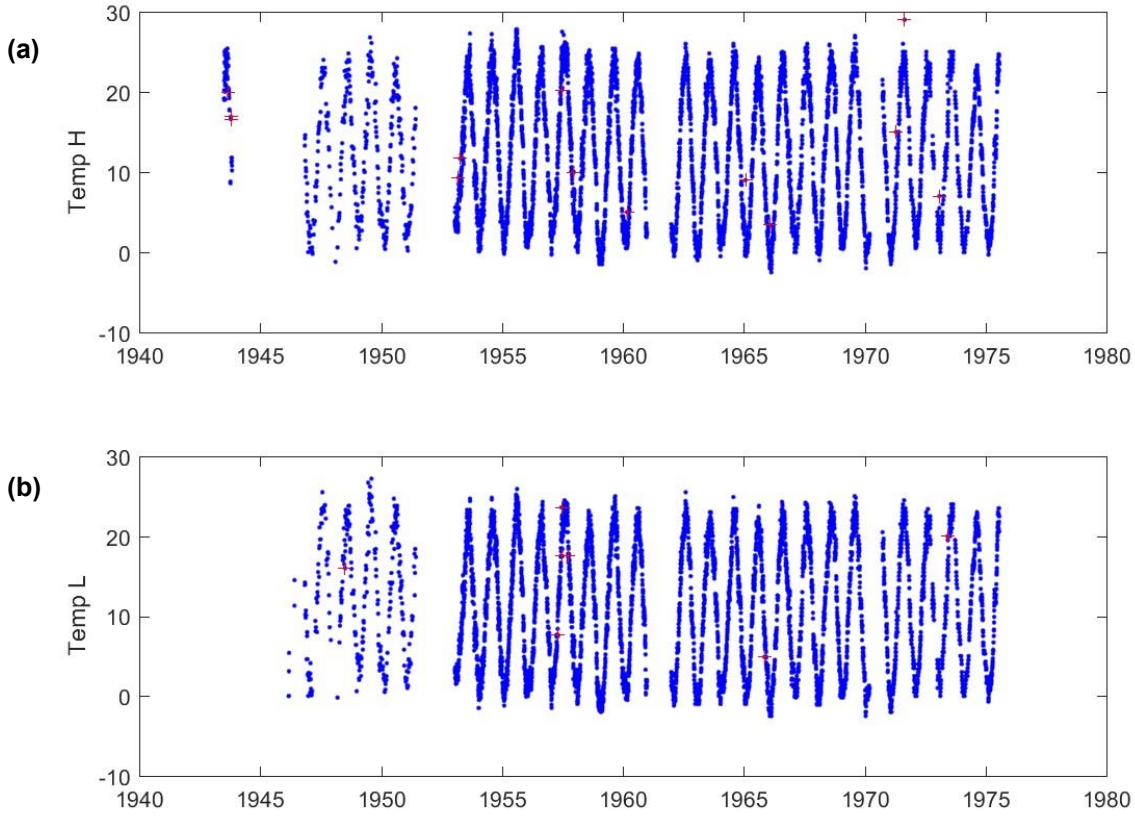

Figure 1.5. Time series of the Milford Marine Laboratory dock water temperature daily (a) high and (b) low. The red '+' symbol's show the samples identified by the screening process that were not corrected because they were consistent with the lab record.

The data from the Bristol temperature recorder at the Milford lab was digitized and provided to us in Microsoft Excel format files. The files included "daily temperature" and salinity. These are interpreted as averages. These data had been subject to verification and the quality/anomaly checks that led to several revisions prior to this project. It is important to note the Excel spreadsheet had a discrepancy in day number associated with the occurrence of leap years and the use of the `@date` function. In addition the time difference check identified 13 dates that

were clearly out of sequence, largely as a consequence of the transposition of the month and day numbers. These were corrected.

As was noted in earlier, the location in the water intake system where temperature was measured at the Milford Laboratory was changed in 1975. Data was collected at both the dock and in the sand filter which is within the lab. Figure 1.6 shows the data with the blue points depicting the earlier samples when the measurements were located on the dock. The later samples obtained at the sand filter are shown in red. The overlap interval is approximately nine months in length and there were 178 days of measurements with which the effect of the measurement location can be assessed.

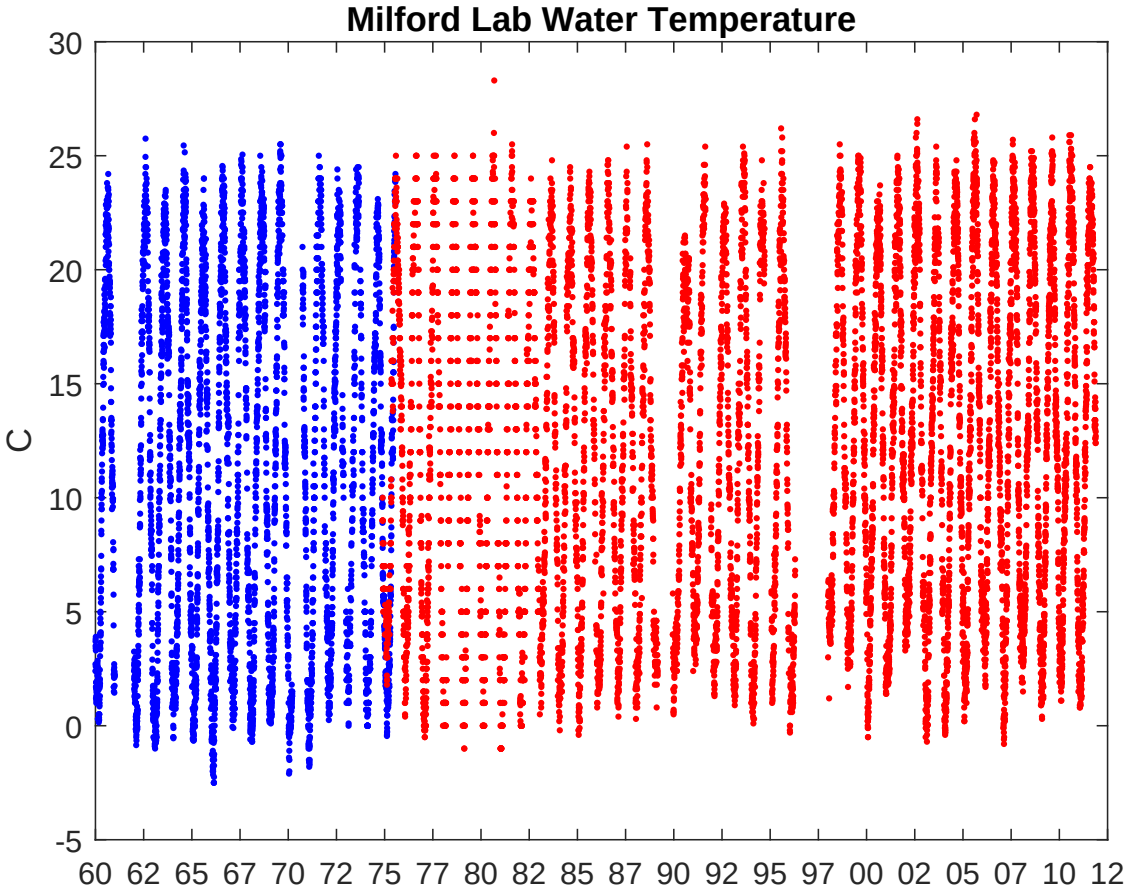

Figure 1.6. The corrected data set from Milford Laboratory. The blue points show when samples were taken at a location on the dock where the intake was located and the red dots show the measurements at the sand filter in the lab.

The temperature difference between the two measurements for the time interval when both temperatures are available (November, 1974 to August, 1975) is shown in Figure 1.7. Figure 1.7(a) shows the measurements at the sand filter in red. These are generally slightly higher than those measured on the dock, presumably due to exchange of heat with the atmosphere. The difference is largest in the spring and early summer. Figure 1.7(b) shows the time series of the

difference by the blue points. The red '+' symbols show the mean of each calendar month and the red line is the linear interpolant between them. In March, the measurements in the sand filter are an average of 3 ºC above the dock temperatures. Note that in the late summer when the monthly mean air temperature is generally close to the water temperature, and through the winter when the coastal waters are often warmer than the air temperatures, the magnitude of the bias is at its minimum, less than a degree.

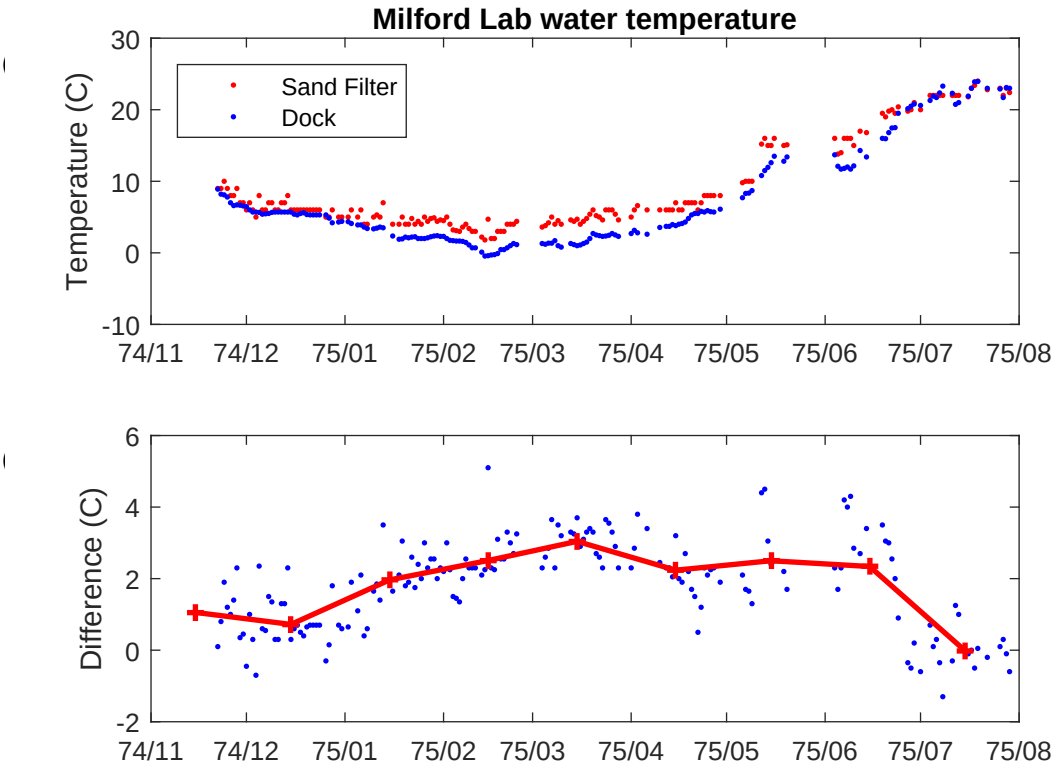

Figure 1.7. (a) The temperature measurements at the sand filter at the Milford Lab in red and the measurements at the dock in blue for the period when both measurements were being collected. (b) The difference between the two by the blue dots. The red '+' symbol show the monthly mean difference. The red line shows the linear interpolant.

To reduce the effect of the bias introduced by the change in the measurement location, we assumed that the red line in Figure 1.7 represented a periodic correction that was dependent only on day of the year. The residual error during the overlap interval is shown in Figure 1.8. It has a mean of 0.03 ºC and a standard deviation of 0.78 ºC. To apply it to the data record obtained after August, 1975, we assumed that the bias in September and October was zero. Figure 1.8 shows the "bias-corrected" data record. The maximum temperatures in the summer are reduced by 3 ºC relative to the raw values. This is quite a large adjustment; note that in the winter the bias is substantially less, so the annual minimum temperatures are not as significantly affected. A more sophisticated correction scheme that made the correction proportional to the air-water temperature difference would be straightforward, but time consuming to develop. This may be a fruitful extension of this work.

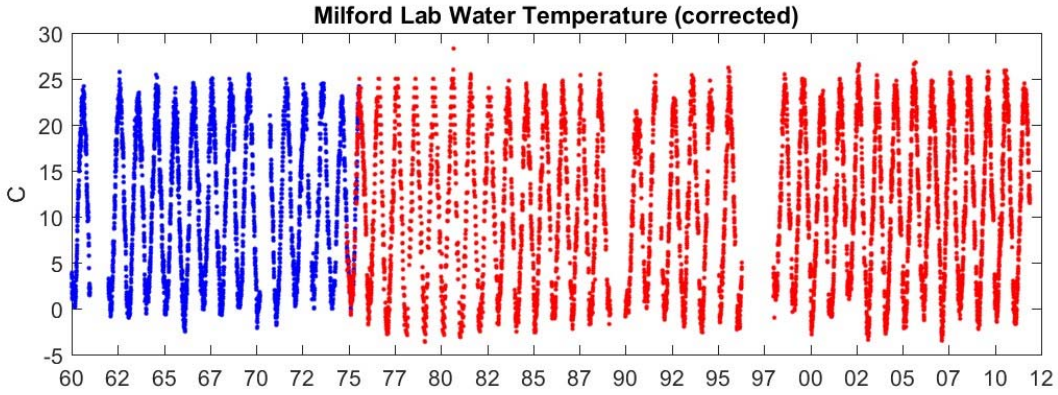

Figure 1.8. Bias-corrected time series of temperature at the Milford Laboratory.

1.3.3 Millstone Nuclear Power Plant

Millstone Nuclear Power Plant has been operating since 1970. It draws cooling water from Long Island Sound at a location to the east of the Millstone Point at approximately 1.5 m below mean low water. The temperature of the intake water is a critical factor in the safe operation of the facility and it has been monitored routinely for the lifetime of the plant. The heated water is released back to the Sound through a disused granite quarry. The design of the outfall aims to minimize the impact of the effluent on the intake and engineering studies (Northeast Utilities, 1987) have validated the design. The power generation and water use varies. Large increases occurred when a second and third reactor were brought on-line in December 1975 and April 1986. The first reactor was permanently taken off-line in July 1998. The daily average temperature since 1975 to 2013 was made available for this study and is shown in Figure 1.9(a). The blue points show the raw data. The data quality of these measurements has been assessed elsewhere. We found only eight missing measurements. These are shown by the black '+' symbols.

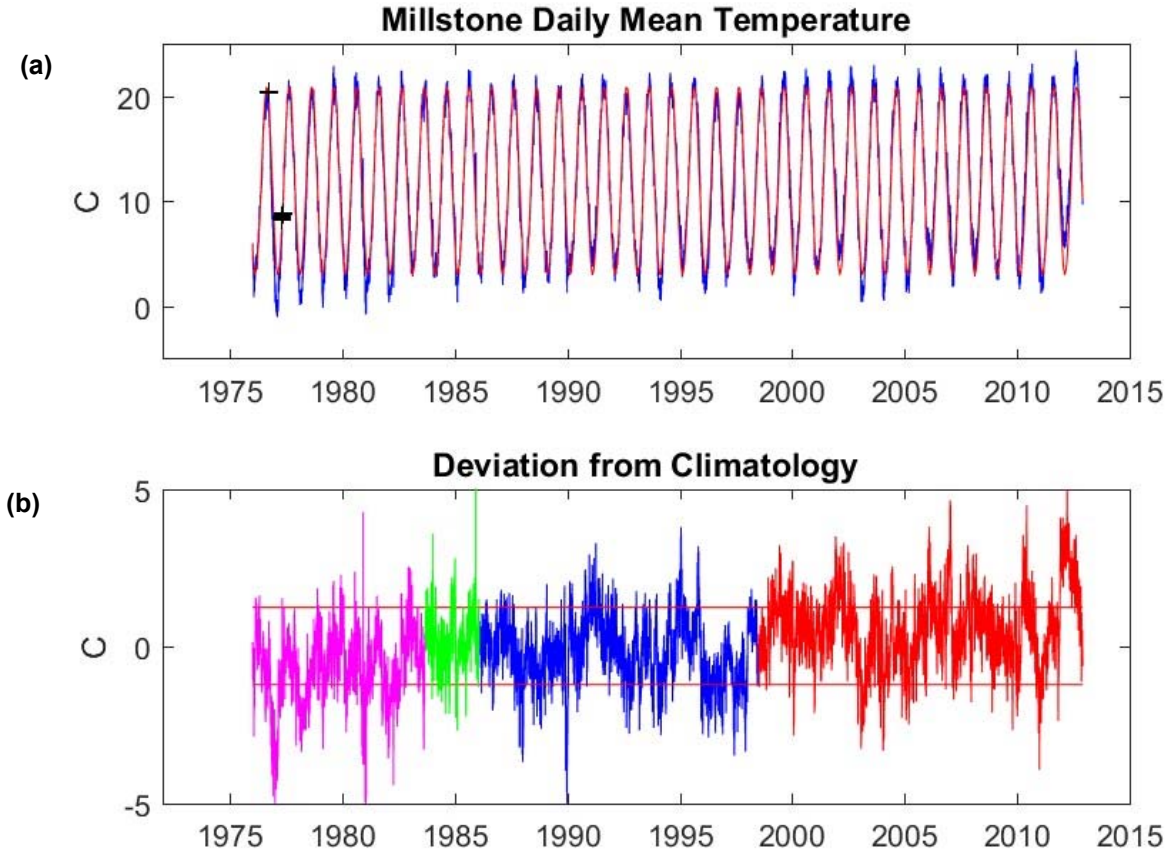

Figure 1.9. (a) The raw temperature data represented by blue dots. The red line shows the annual cycle computed by "phase averaging" by day of the year. The black '+' symbols are the eight days of missing data. (b) The deviation for the seasonal cycle with red lines showing plus and minus the standard deviation. The magenta and green points identify when only the first and second reactors were turned on. The red line shows deviations after the first reactor was retired.

The large annual temperature cycle dominates the observations though inter-annual variations are evident in the summer maxima and the winter minima. The red line in Figure 1.9(a) shows the average by day of the year of the temperature measurements. This provides an estimate of the mean annual cycle. The deviations are small. Figure 1.9(b) shows the time series with red lines at plus and minus one standard deviation (1.2 ºC). Relative to the amplitude of the annual cycle (17.9 ºC), this is only 7%.

Of most concern are the potential effects of the heated water from the cooling system on the intake water temperature. In Figure 1.9(b), the period when only one reactor was operational is shown in magenta and the green line shows the deviations from the annual mean when both unit 1 and 2 were operational. The mean deviation with one reactor was -0.75 ºC, and with two, it was 0.18 ºC. When the third (and largest) reactor was added the mean was -0.20 ºC. In July, 1998, the first reactor was decommissioned. This interval is shown in Figure 1.9(b) by the red lines. Though there has been a net warming in the record that may initially seemed to be

associated with the operation of the power plant, the fact that the warmest period is after the power generation was reduced suggests that the trends are not due to local effect.

1.3.4 Riley Observations

The first comprehensive characterization of the structure and evolution of the temperature and salinity fields in LIS was reported by Riley (1952 and 1956). Using several years of ship surveys, he established the basic spatial trends and the range of seasonal variability. The data from these cruises was archived at the New York-New Jersey Harbor Estuary Program (http://www.harborestuary.org/) with a range of other surveys. Though the study was extensive, it only lasted from 1952 to 1960 and stations were not revisited very frequently. We selected the stations shown by the green square in Figure 1.10 for inclusion in our study because they were sampled for multiple years.

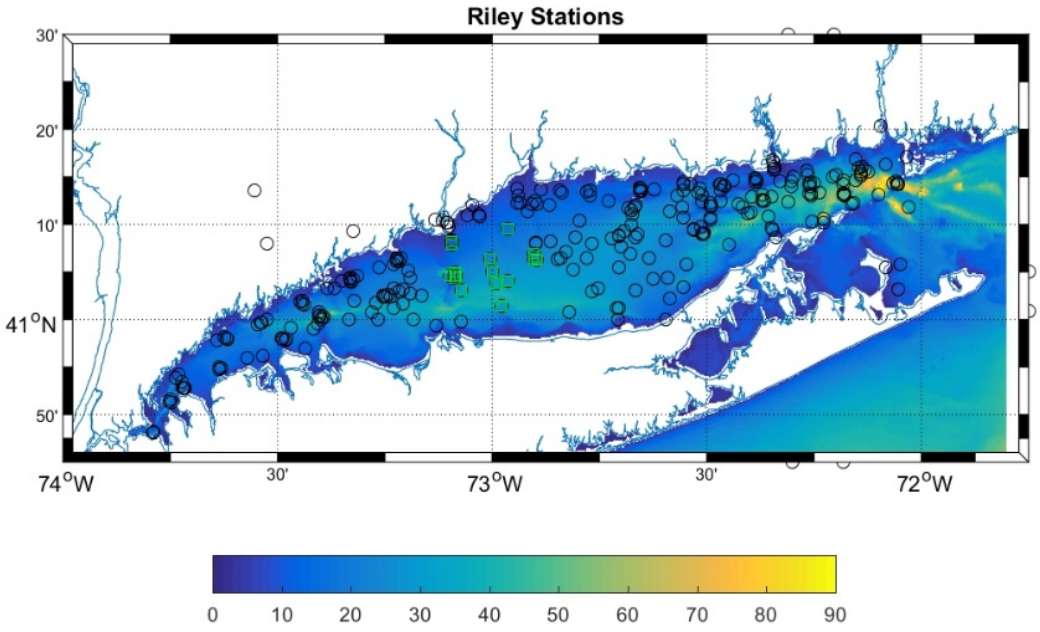

Figure 1.10. Map of Long Island Sound showing the bathymetry by the color shading (scale is in meters) and the location of all the samples in the Riley data set. (Note that the stations over land are obviously transcription errors). The stations with the green squares in the central Sound have the longest data record. The temperature at the surface (above 5 m) and at depth (below 10 m) at these stations in shown in Figure 1.11. Though the record is relatively short, there are few high quality measurements in in this time frame.

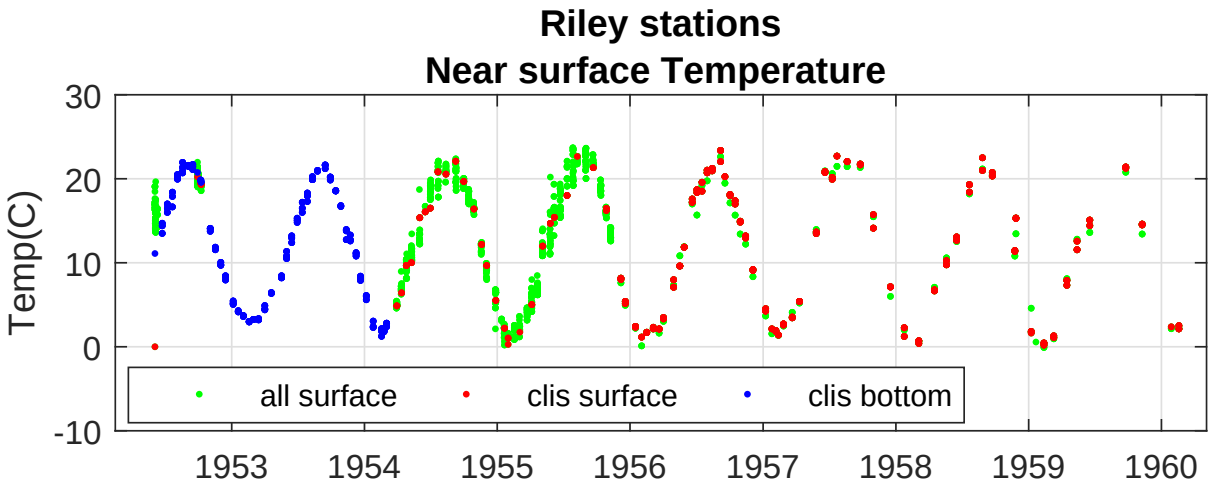

Figure 1.11. Near surface (red) and near bottom (blue) temperature for the stations reported by Riley and shown in Figure 1.10 by the green squares.

1.3.5 New York City DEP Measurements

The New York City Department of Envoronmental Protection has been operating a monitoring program for water quality in the East River during the summer (June-August) since 1909 and data is available from the New York-New Jersey Harbor Estuary Program (http://www.harborestuary.org/) from 1914. The data are in a simple ASCII format and have been quality checked. The stations in the western end of the Sound at the entrance to the East River, E8 (Throgs Neck), E9 (Stepping Stones), and E10 (Hart Island) are discussed here and their locations are shown in Figure 1.1. Wilson et al. (2008) analyzed these data and showed that bottom water temperatures in July and August had declined (cooling) almost 2 ºC between 1940 and 2005. The earlier data is shown in Figure 1.12.

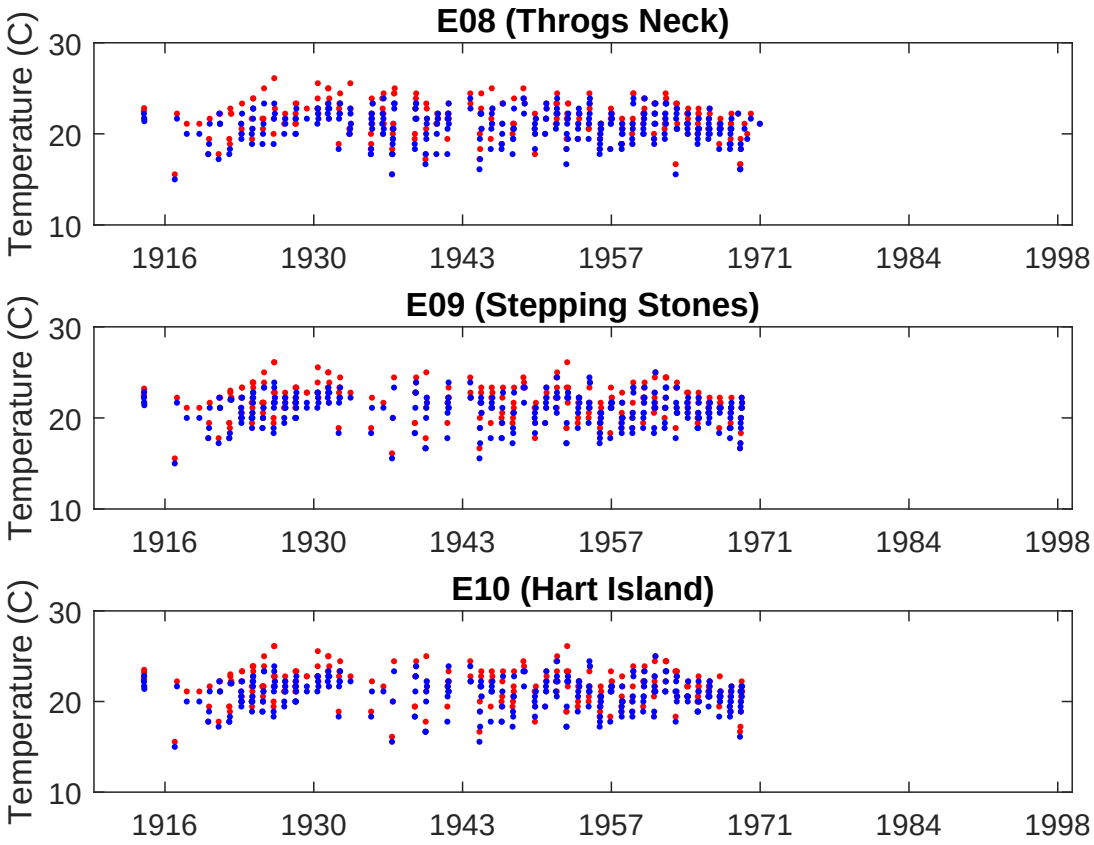

Figure 1.12. Time series of surface (red) and bottom (blue) water temperatures at three NYC DEP sampling stations in Western Long Island Sound.

1.3.6 Proxy Estimates 1 – Woods Hole Water Temperatures.

Since the data record for coastal water temperatures is short and exhibits frequent data gaps, it is valuable to use physics-based empirical relationships with other variables to interpolate between observations and, when appropriate, extend the record. There are two records that we wish to discuss here, temperature from other coastal sites in the New England and atmospheric temperature records.

One of the longest records of water temperatures in the coastal ocean was published by Nixon et al. (2004). They aggregated measurements made in Woods Hole Harbor, MA, for over 100 years. Bumpus (1957) made the early measurements with a bucket and thermometer. Later measurements used more modern technology. Nixon et al. (2004) discuss the data quality assessment. The data record was made available by S. Granger at http://dlaweb.whoi.edu/DIGRES/water temp.php (though it appears this site is inactive as of November 2015). The record demonstrated the existence of large amplitude variation in seasonal mean temperature. They also suggest that the warming has occurred in both summer and winter seasons.

Since the data sources were diverse, the Nixon et al. (2004) data file format is awkward. However, we streamlined it for this analysis and Figure 1.13 shows the entire monthly average record.

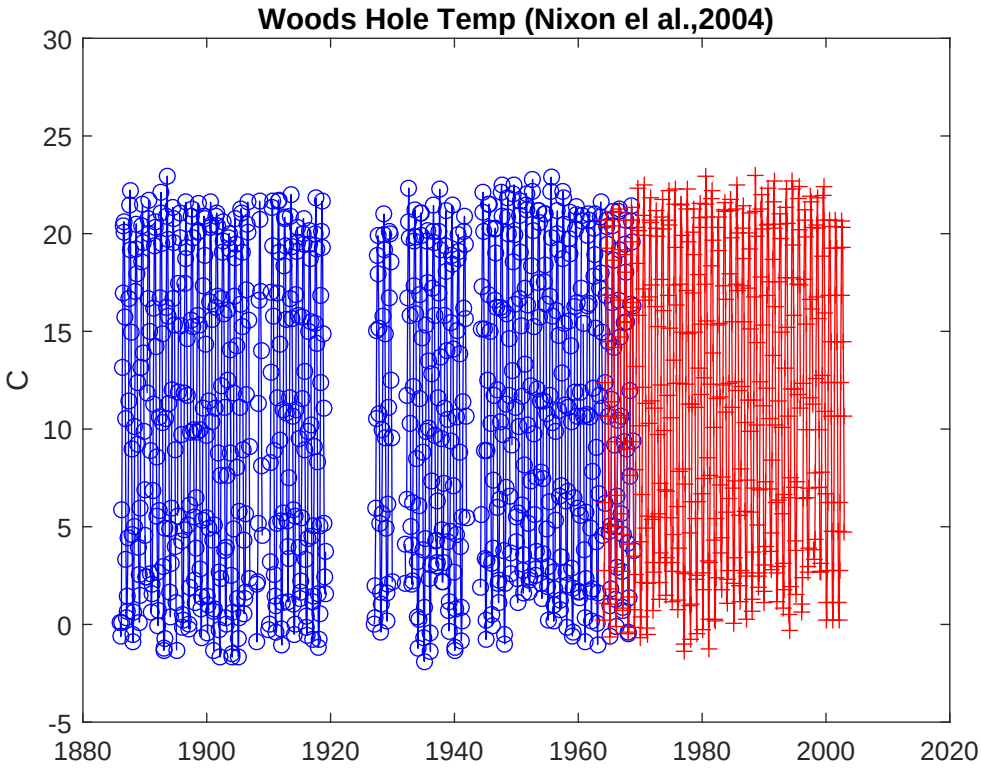

Figure 1.13. Monthly average temperature in Woods Hole, MA, harbor. Data from Nixon et al. (2004).

The data set has recently been exploited by Bell et al. (2014) who augmented it for their application with recent measurements at NOAA water level sensor (Station 8454000) to study summer and winter flounder population changes. The data show a warming in winter mean temperatures. We also acquired the data from the NOAA Center for Operational Oceanographic Products and Services (COOPS) data base (http://tidesandcurrents.noaa.gov/). The data is hourly from 1996, though there are data gaps. More recent years have data at five minute intervals but we averaged these to an hourly value before the data screening procedures. *Figure 1.14* shows the raw data. The samples shown by the red symbols were eliminated as obvious instrument malfunctions. The variance about the monthly average is substantially greater prior to 2000, so following the approach of Bell et al. (2014), we rejected samples greater than three standard deviations from the mean prior to computing the mean. This produced the record shown in *Figure 1.15*. The two standard deviation (post rejection) interval is indicated by the red dashed lines surrounding the mean.

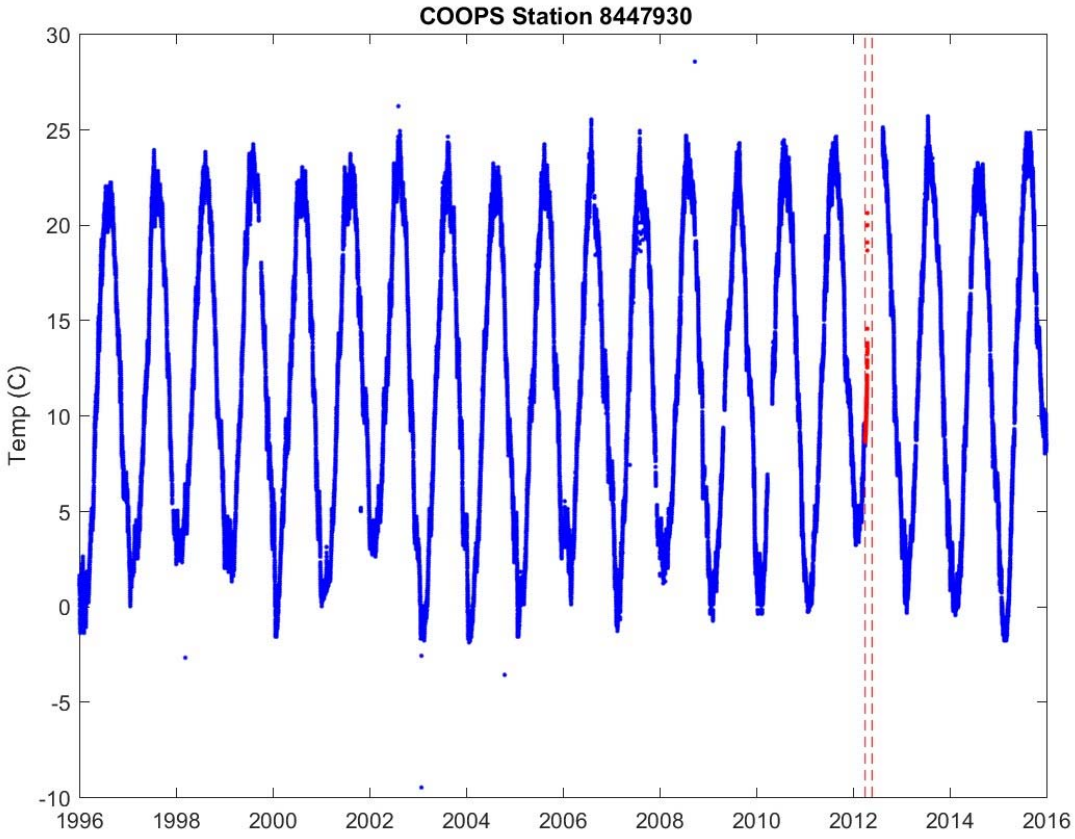

Figure 1.14. The hourly data acquired from the NOAA COOPS temperature sensor (8454000) at Woods Hole Harbor is shown in blue. The red lines show intervals were the instrumentation performance was suspect and the red dots show the sample that were acquired during these periods.

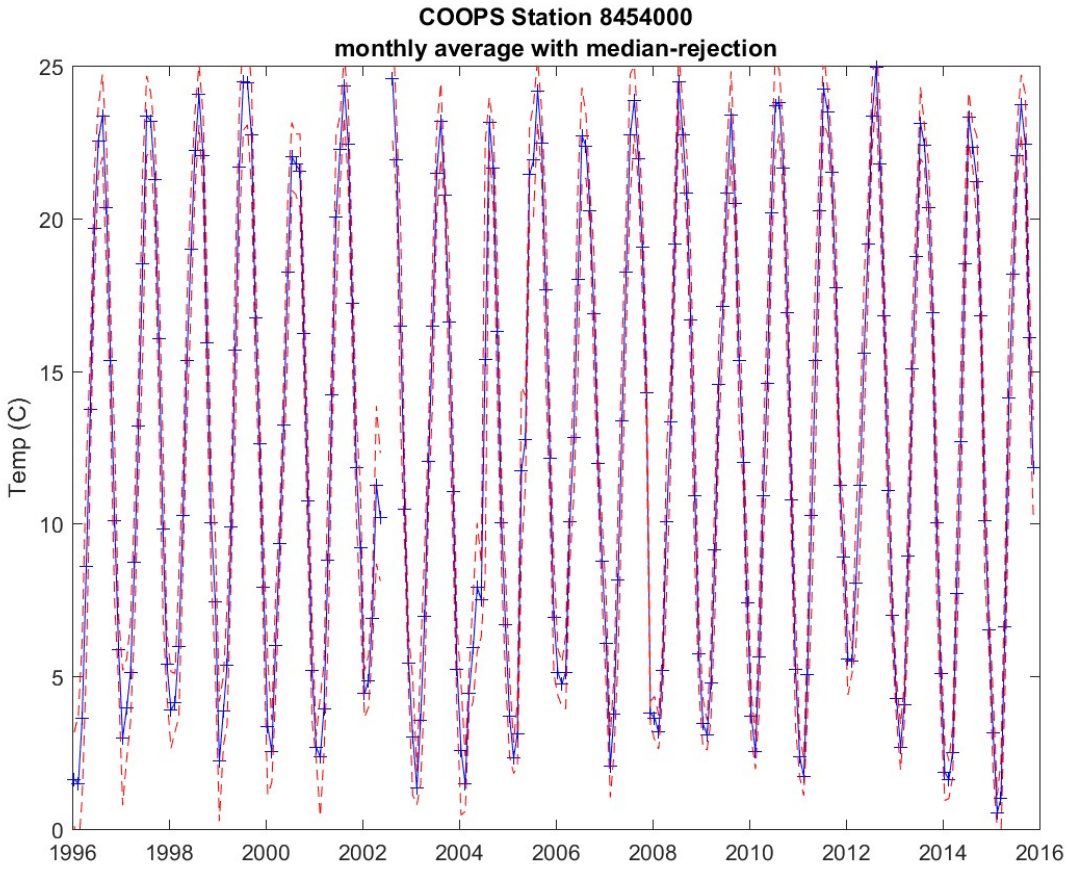

Figure 1.15. The monthly average of the hourly data from Woods Hole Harbor (see Figure 1.13) after the samples that were more than three standard deviations from the median were eliminated is shown by the blue '+' symbols. The red dashed line shows the two standard deviation interval about the mean.

To construct a long series we must ensure that there is no systematic bias associated with the type or location of the instruments. Figure 1.16(a) shows the monthly mean temperatures at Woods Hole constructed by Nixon et al. (2004) and our averages of the NOAA COOPS station data. The red '+' symbols show the data acquired by Nixon et al. (2004) from the Woods Hole Oceanographic Institution, and the green samples show the values they transcribed from log books. The blue samples are from the thermistor maintained by NOAA COOPS program. The vertical black dashed lines show the overlap in the first two records. The means are compared in Figure 1.16(b). The correlation is 99%. The mean difference is 0.01 ºC and the standard deviation is 0.1 ºC. These records are clearly consistent.

The overlapping period of the Nixon and COOPS data is identified in Figure 1.16(a) by the solid lines. A comparison of the monthly averages is illustrated in Figure 1.16(c). The scatter is slightly larger. The standard deviation of the differences is 1.0 ºC and the mean difference is 0.54 ºC and the slope of a regression by least-squares is 0.99. Subtraction of 0.54 ºC from the COOPS means will remove the bias.

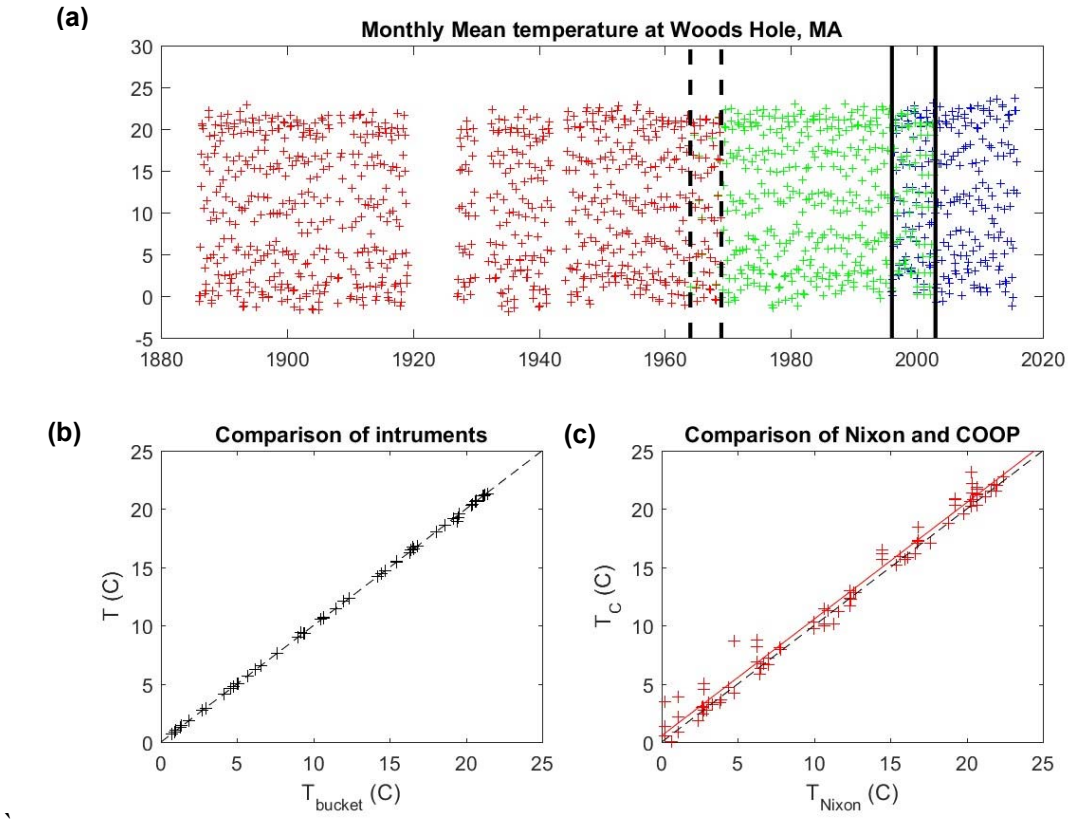

Figure 1.16. (a) The green and red symbols show the time series of Nixon et al. (2004) after monthly averaging; the blue symbols show the NOAA COOPS data. The duration of the overlaps between the data transferred to computer formats by WHOI and those digitized by Nixon et al. (2004) is bounded by the black dashed lines. A comparison between the two series in this interval is shown in (b). The overlap between the NOAA and the Nixon data is identified by the solid vertical lines and the comparison of the measurements is shown in (c).

1.3.7 Proxy Estimates II – Coastal Air Temperatures.

Another well-established correlation is between the temperature of the atmosphere near the coast and near shore water temperatures. This is particularly high in the winter. The longest records near LIS are at Bridgeport, Sikorsky Airport and Tweed-New Haven Airport. The raw data hourly observations are available from the National Climatic Data Center (NCDC) from the site ftp://ftp.ncdc.noaa.gov/pub/data/noaa. The data is stored by year and various station codes: Bridgeport is 725040 and Tweed-New Haven is 725045. The raw measurements shown in Figure 1.17(a) and (b), and the monthly averaged values are shown in Figure 1.17(c). Both records begin in 1973 and are continuing; however, the New Haven site has several gaps. The monthly averaged trends (Figure 1.17c) are very similar, with a correlation of 0.99. A linear regression shows that the New Haven record is 0.47 ºC warmer than the Bridgeport measurements and the slope is 0.97. The summer peaks and winter troughs display inter-annual variations of several degrees. These will be discussed further in the next section.

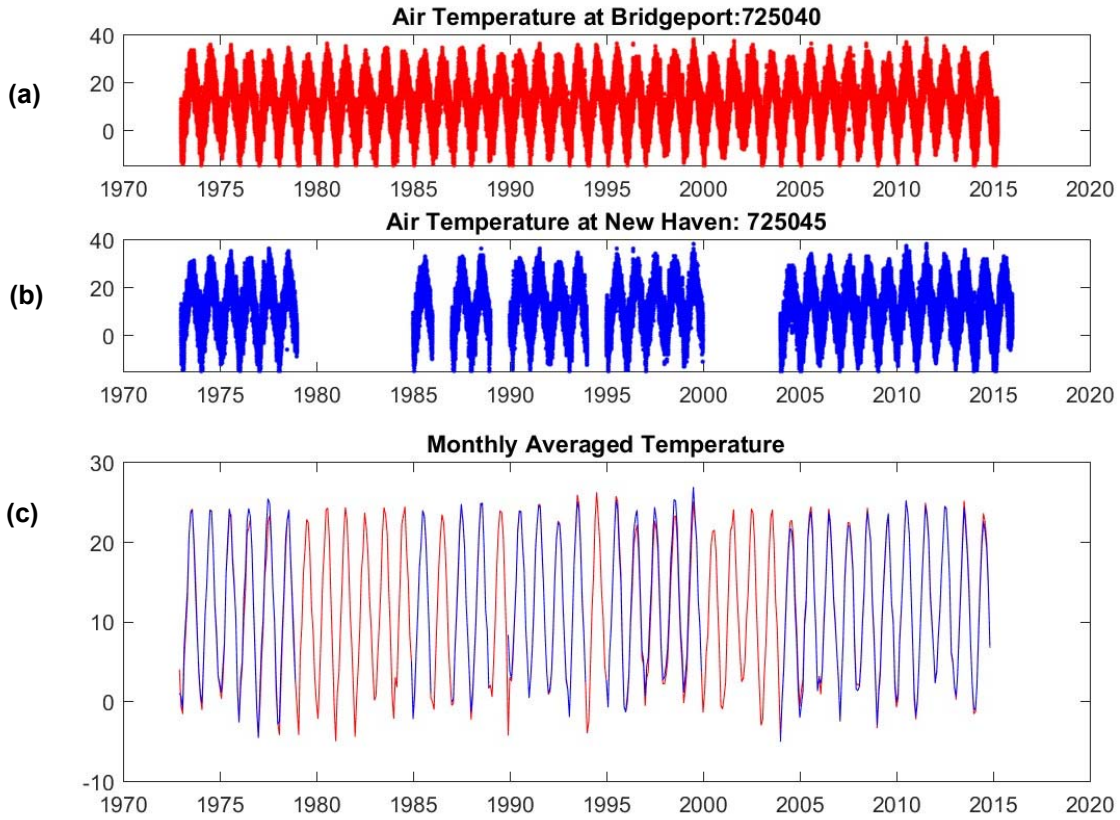

Figure 1.17 (a) and (b) show the hourly temperature measurements at the Bridgeport and New Haven, respectively. The monthly means of the records are shown in (c).

There are many other old records of meteorological observations. Unfortunately, they are not continuous at any single location for very long. The Berkeley Earth Project (http://berkeleyearth.org/) undertook a comprehensive program to evaluate and reconcile, as far as possible, such measurements around the world to assess the magnitude of climate change. The approach exploits spatial and temporal correlation of the monthly average temperatures between stations that are closely located, and then adjustments are introduced to reduce inconsistencies and biases. The methods are documented in Rohde et al. (2013). Data can be conveniently downloaded from http://berkeleyearth.lbl.gov/station-list/. These files contain the raw data, identification of all the stations and records contributing to the analysis product, and the "adjusted" temperature record. The analyses for the area of Bridgeport and New Haven are therefore closely linked. The Bridgeport analysis is shown in Figure 1.18(a). Since there is a long history of uncoordinated measurements, the integration effort leads to a long record. Figure 1.18(b) illustrates the difference between the raw records and the "adjusted" values.

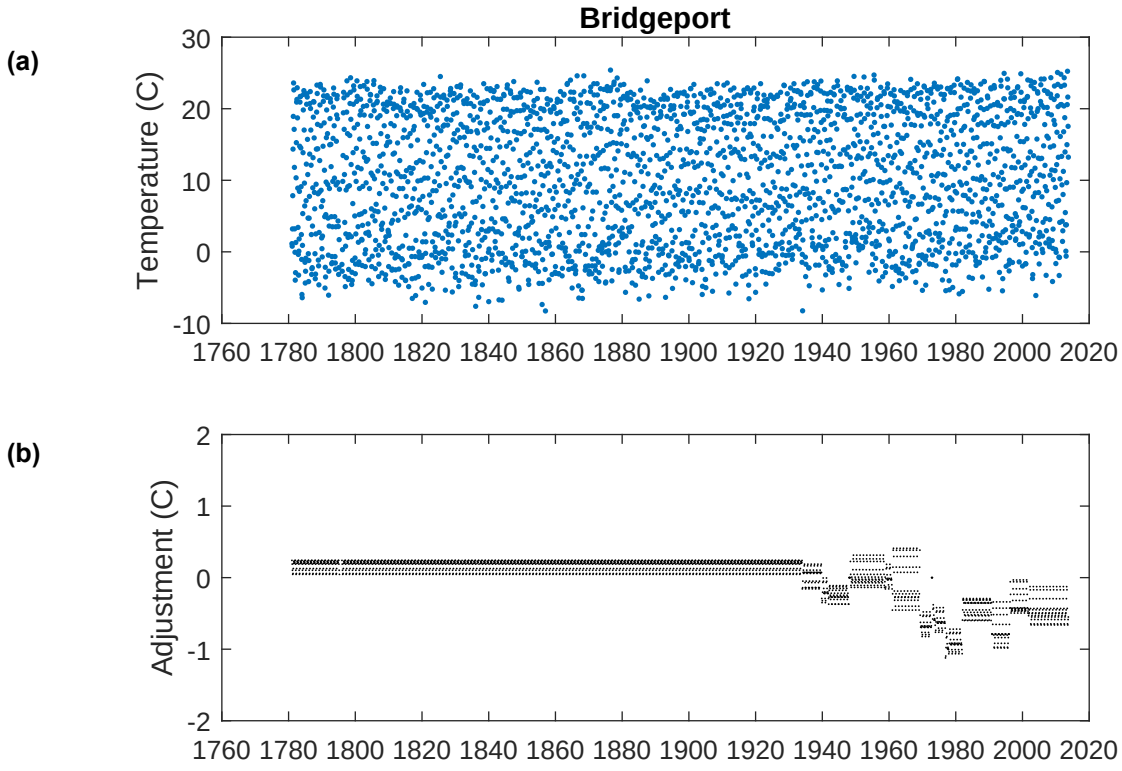

Figure 1.18. (a) The adjusted monthly mean temperature at Bridgeport produced by the Berkeley Earth project. (b) The adjustments made to the raw data. Note the differences in the scales.

1.4 Coastal Water Temperature Trends

The annual cycle in water temperature in LIS is very large. Minimum temperature in winter reaches 0 ºC and in the summer it can reach 25 ºC. The geometric and bathymetric constrictions at both the east and west ends of the Sound cause strong tidal currents and large rates of vertical mixing which limit the interaction with the waters of the shelf. This means the seasonal cycle of heating and cooling is only partially moderated by the inflow from the ocean. To detect subtle longer term changes in the temperature the annual cycle has to be removed. Options for this include averaging over the years or examining trends in the mean temperature of a particular month of season. A third option arises when daily data at a single site is available for a long period of time. Trends in the day of the year when the temperature first passes a particular temperature threshold (either rising or falling) can also be used.

The mean annual cycle of temperature variations in the nearshore water of Long Island as observed at the Millstone Power plant is shown in Figure 1.19. The blue line shows the mean calculated on a weekly basis and the red lines show the two standard deviation interval. Clearly, the maximum occurs in August and the minimum in February. The black dashed lines surrounding the February minimum extend from January 1st to April 1st because the difference between the mean values in that interval and the annual minimum are less than the standard deviation in February. So, the weekly mean temperatures during this interval are not very different. Similarly, the means in the interval July 1st to September 1st are not different from the maximum. This is a valuable insight since it implies that data gaps in these intervals will not

seriously bias the estimate of the mean. Since the rate of change of temperature in higher in the transition months, missing data will have a much larger effect.

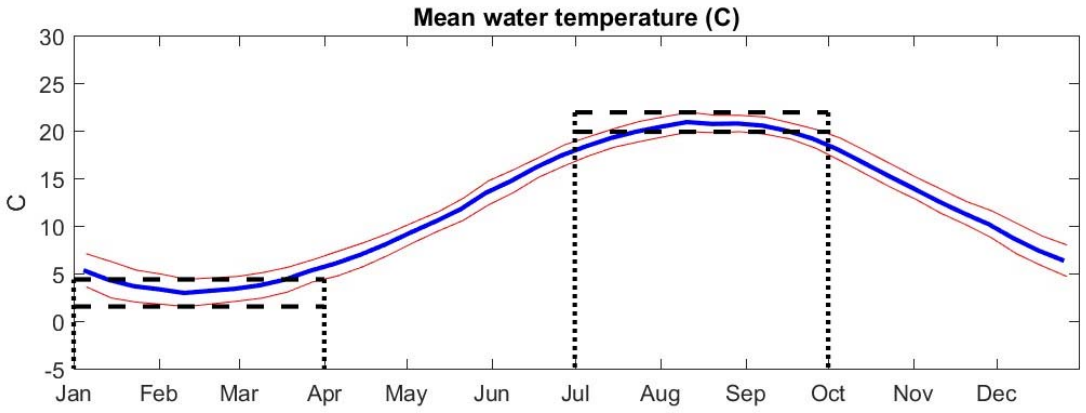

Figure 1.19. The means cycle of water temperature at Millstone Point is shown by the blue line. The red lines show the standard deviation of weekly averages over the 40 year record. The dashed lines identify the interval when the temperature is not significantly different from the mean.

The winter (January, February and March) mean temperatures from the Milford Laboratory data ('+'), the Noank Laboratory data (squares), the Millstone Power Station (circles), and the surface samples in the Riley surveys (diamonds) are shown in Figure 1.20(a). The data span the years 1947-2013 and have a temperature range from -1 ºC to 6 ºC. The Milford data tend to be the lowest in all years. However, they are consistent with the Riley data in the latter half of the 1950s. The Millstone and Noank data are more consistent with each other and show higher values.

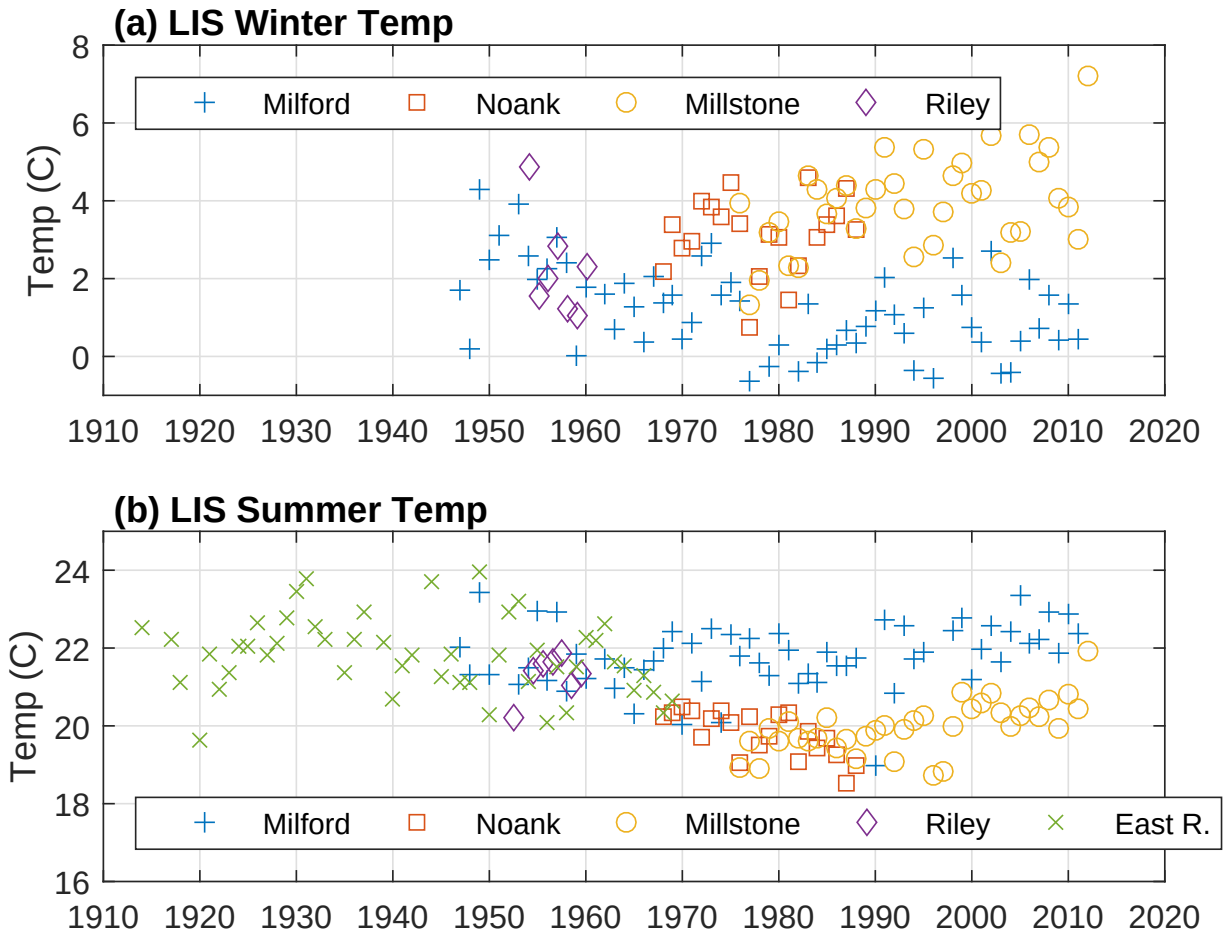

Figure 1.20. (a) Time series of the winter (Jan-March) mean temperature from Milford ('+'), Noank (square), Millstone (circle) and the surface samples in the Riley surveys (diamond). (b) Time series of the summer (July-September) means from the same sources, with the addition of the surface samples from the NYC DEP stations E8-10 ('x').

There is evident time correlation between the series. This is largely due to the fact that the rate of heating of the water has scales of variation that are greater than the scale of the Sound. Differences in the temperature arise from the water depth and differences in the rate of exchange with water of much greater depth. In the winter, the eastern stations are warmer, and in the summer, they are cooler because the deep waters of the shelf do not vary in temperature as much.

To characterize the regional temperature trends, we create an LIS "temperature index" by adjusting the data to represent the temperature at the Millstone Power Plant by computing the mean difference between segments of the series that overlap in time. This is similar to the approach developed by the Berkeley Earth Project (see Rohde et al., 2013) to align air temperature measurements from different sources and station locations. The Millstone data is used as the benchmark since it has high data quality and has the most overlap with the other series. The Milford and Noank Laboratory data may also have small biases associated with the lag between the withdrawal from the ocean and the measurement. The correlations, r^2, and mean differences, b, between the Millstone record and the others are listed in Table 1.1. The third

column from the left shows the Milford and Riley record are 3.26 ºC and 3.04 ºC lower than the Millstone record, but the Noank data are only 0.34 ºC lower. The root mean square residual differences, ϵ, between the adjusted series are listed in the fourth column of Table 1.1. The Noank and Milford labs have errors of 0.40 and 0.56. The correlation between the Millstone record and the Riley ship data is much lower, though statistically significant, and the residual error larger in much lower. This is partly due to the short duration of the record.

Table 1.1. Adjustments to the time series of the winter means to create temperature index.

	r^2=correlation	b= Mean difference (ºC)	ϵ =r.m.s. difference (ºC)
Noank Laboratory	0.93	-0.34	0.40
Milford Laboratory	0.86	-3.26	0.56
Riley Cruises	0.56	-3.04	1.19

The summer (July, August and September) means are shown in Figure 1.20(b). The availability of the measurements in the East River allows the data record to extend almost 100 years. Note that in this season the Milford Laboratory data show the highest temperatures. Though the water temperatures are much warmer, 18-24 ºC, the magnitude of the range of temperatures is similar (~6 ºC). However, the variation within any single series is smaller. The series are significantly correlated and the r^2 values are listed in Table 1.2 together with the mean difference and the residual error.

Table 1.2. Adjustments to the time series of the summer means to create temperature index.

	r^2=correlation	b= Mean difference (ºC)	ϵ =r.m.s. difference (ºC)
Noank Laboratory	0.41	-0.04	0.53
Milford Laboratory	0.43	1.92	0.74
Riley Cruises	0.53	1.51	0.31
East River Stations	0.28	1.82	1.06

Once these seven empirical constants (the b values in Table 1.1 and Table 1.2) are applied to the data, the variation in temperature is substantially reduced as is shown in Figure 1.21. The winter temperatures (Figure 1.21a) were clearly highest, over 6 ºC, around 1950. There was a subsequent drop to below 3 ºC over the following 25 years. Since 1975 the average winter temperatures appear to be increasing with a very warm year in 2012, bringing the adjusted temperature up to similar levels as 1950. To make the temporal evolution clearer, Figure 1.22(a) shows the same data overlain by a trend line. This was computed as the mean of all

measurements in three year bins. The dashed lines show plus and minus a standard deviation about the mean. The 1975 low temperature (2.5 ºC) is more than a standard deviation (0.8 ºC) below the long term average value of 4.4 ºC.

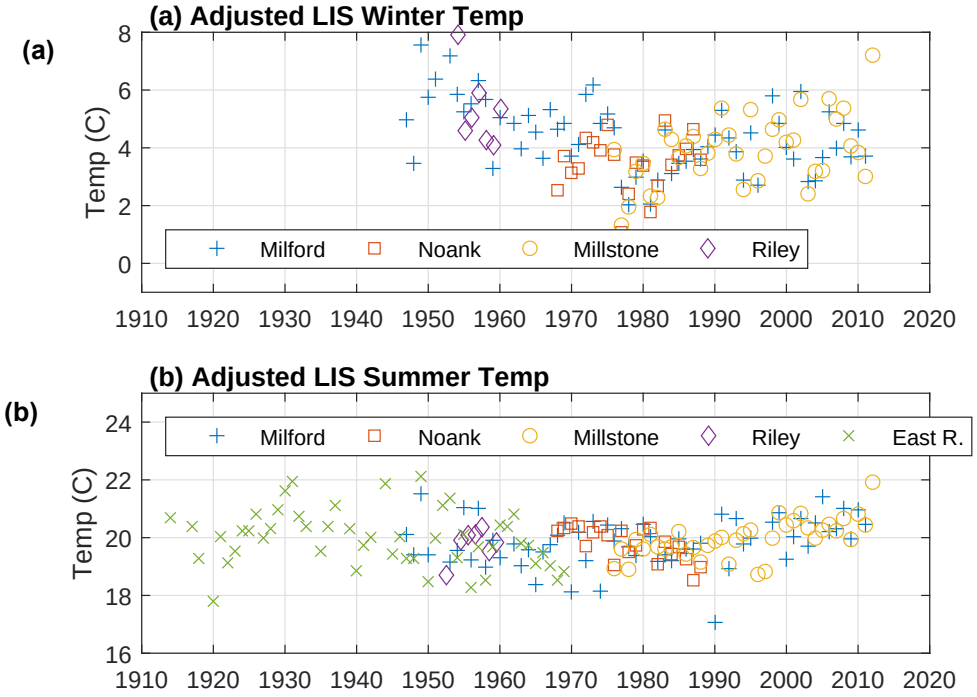

Figure 1.21. Time series of the adjusted winter (a) and summer (b) mean temperatures. Symbols are as in Figure 1.20.

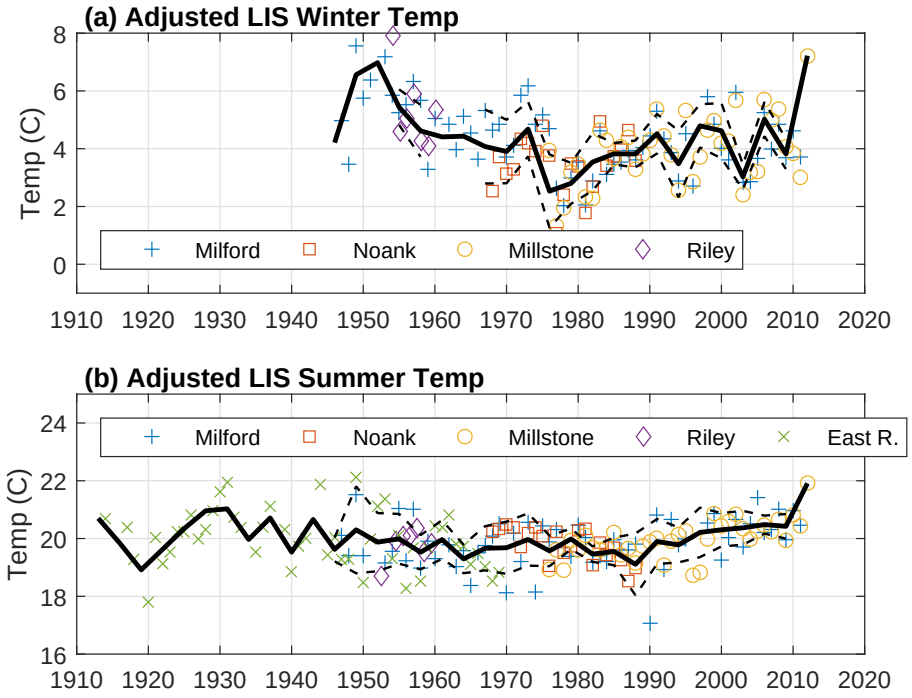

Figure 1.22. Same as Figure 1.21, but with the solid black lines showing the average across the different adjusted data sources in 3-year bins. The dashed lines show the standard deviations where more than four estimates are in a 3-year interval.

Once the temperature data are adjusted to the Millstone series, the summer variations about the long term mean (20.0 5 ºC) (see Figure 1.21b) are much smaller amplitude. The trend line in Figure 1.22(b) is helpful in showing that there has been a slight cooling from the 1930s to1990 and then a warming has occurred since then. The most significant anomaly in the record is the recent high temperatures of 2012.

To assess the value of this index of LIS water temperature trends we compare it to the long record of water temperature constructed by Nixon (2004), as augmented by the NOAA COOPS observations following Bell et al. (2014) and described in Section 1.3.6. We also compare it to the analysis of air temperature record at Bridgeport, CT, constructed by Rohde et al. (2013). Figure 1.23(a) shows the bin averaged winter mean adjusted LIS temperatures in black with the upper and lower bound of the two standard deviation interval shown by the dashed lines. The green and blue lines show the Woods Hole and Bridgeport records averaged in the same way. To facilitate the assessment of the temporal relationships between the series, the mean difference between each and the LIS temperature index has been subtracted. The adjustments are listed in Table 1.3. The high correlation between all three winter series is clearly evident. Almost every dip and peak in the LIS series aligns with one in the other series. This not the case in the summer as is clear in Figure 1.23(b). The weak variations in the summer series, together with the noise imposed by wind and tide induced motions of the seasonal thermocline and data processing, tend to obscure the detection of correlation in the summer if it existed. The estimate of r^2 for the summer Woods Hole and LIS series is low and insignificant. The value of $r^2 = 0.38$ between the Bridgeport record and the temperature index is, however, significant. The longer term trends noted in the summer LIS temperature index are replicated in the Woods Hole and Bridgeport series – a slight cooling between 1930 and 1990 and a slight warming since then.

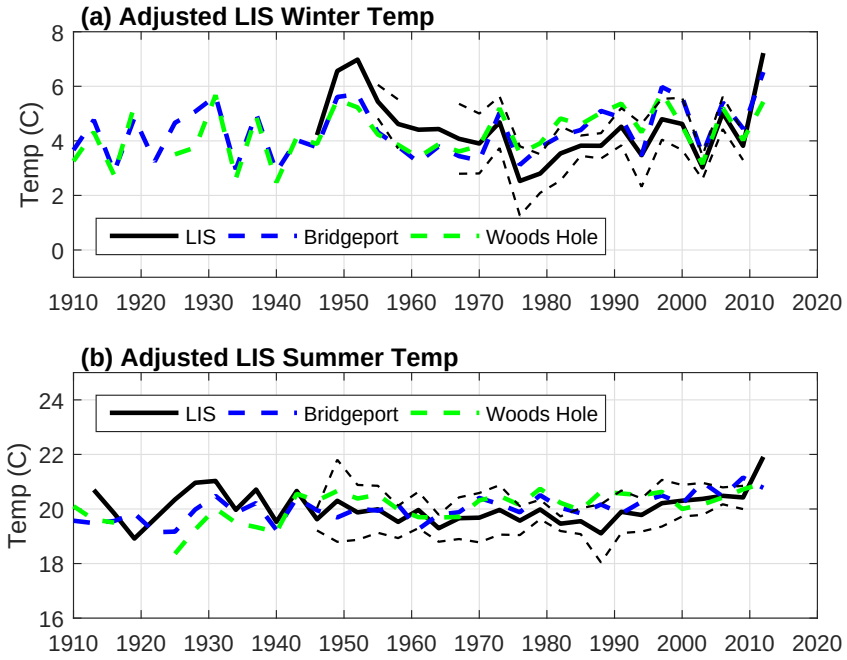

Figure 1.23. The summer (a) and winter (b) bin averaged LIS temperature index (black) series with the Woods Hole water (green) and Bridgeport air (blue) temperatures averaged in the same manner. Note that the Woods Hole and Bridgeport temperature series have been off-set by the amounts shown in Table 1.3.

Table 1.3. Correlation and offsets between the bin-averaged LIS temperature index and the water temperature series from Woods Hole and the air temperature from Bridgeport in winter and summer.

	r^2=correlation	b= Mean difference (°C)
Woods Hole Winter	0.62	-2.7
Bridgeport Winter	0.74	-3.9
Woods Hole Summer	0.04*	0.5
Bridgeport Summer	0.38	1.0

Table 1.3 lists the correlation values computed from the intervals of data overlap. In the winter the r^2 values are 0.62 and 0.74 for Woods Hole and Bridgeport series, respectively. It is clear that the atmospheric processes that control weather in southern New England (as measured by the air temperature at Bridgeport) dictate the coastal water temperatures. That the mean air temperatures are the lowest of the three series indicates that heat is being transferred to the atmosphere. This cooling at the surface tends to cause the coastal waters to be well mixed and

shallow and isolated areas to be colder. That the Woods Hole harbor series is colder than the LIS temperature index suggests that LIS has more exchange with the deeper waters.

One of the advantages of the high winter correlation between the LIS temperature index and the longer series is that that information about the past winter temperatures can be inferred. Figure 1.24 shows the same information as Figure 1.23 but the axis has been extended back to 1880 so that the more recent variations can be viewed in a broader context. The long term upward trend in both the winter (Figure 1.24a) and summer (Figure 1.24b) temperatures are immediately obvious. The red lines show the linear regression through the Bridgeport data. The slopes are 0.5 and 0.8 ºC/century for the summer and winter respectively and are consistent with the rate of change of global average temperatures.

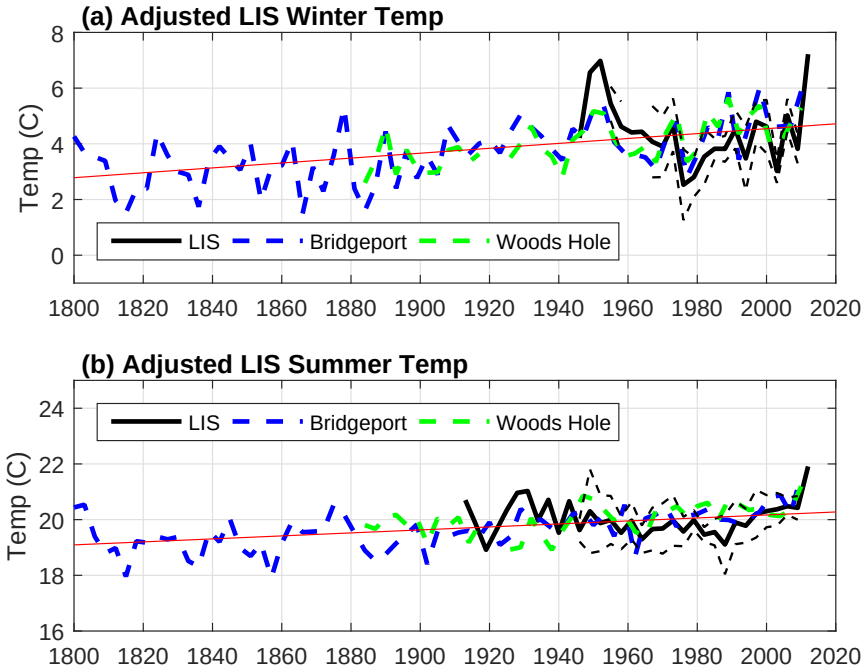

Figure 1.24. Same as Figure 1.23 but with a longer time range. The red lines show linear regression results for the Bridgeport air temperature series.

Of more interest, however, are the very long time scale oscillations. It is clear that during the interval 1960-2000 both the winter and summer series were at, or below, the long term trend line. In contrast, most of the interval 1910-1960 showed a positive anomaly. The winter data between 1860 and 1910 also show a tendency to be below the long term trend though decadal period oscillations dominate the variability.

The recent "rapid" warming since 1965 (at rate that is an order of magnitude larger than the trend in the global average), has been noted by several authors (Stachowicz et al., 2002; Bell et al., 2014; and Oczkowski et al., 2015) and is most clearly evident in Figure 1.24(a). A three degree increase over 30 years is large, but the Woods Hole and Bridgeport records suggest that between 1885 and 1925 there was a similar increase. More broadly, the amplitude of the decadal scale oscillations is approximately 2 ºC so rates of change of order 1 ºC/decade (of both signs) are to be expected.

1.5 Summary and Conclusions

We have assembled and quality checked a large and diverse array of observations of temperature in Long Island Sound. We have included the data from the both the eastern and western extremities of the estuary. Our analysis of the seasonal cycle at the Millstone Power Plant record showed that the rate of change of temperature was smallest in January-March and July to September, so we chose these times to examine longer term trends since they would be less prone to bias by irregular sampling. Four records were assembled for the winter and five for the summer. An index of the summer and winter temperatures was created by computing the mean difference between contemporaneous segments of the observation records. Three empirical constants were used in the summer and four in the winter. The data were then bin averaged in three year intervals to create records that span 1930 to 2012 in the winter and 1915 to 2012 in the summer.

The aggregated data series, a LIS temperature index, showed that water temperatures in the interval 1960-2010 were anomalously cool in both the winter and the summer, whereas the winters between 1945 and 1955 were anomalously warm. Since 1965 temperatures in both the summer and the winter have been rising. The summer and winter of 2012 were both anomalously warm.

The winter temperature index was then shown to be very highly correlated with the water temperatures series created at Woods Hole Harbor by Nixon et al. (2004), and the air temperature record assembled by Rohde et al, (2013) for a coastal station in Bridgeport, CT. The correlation with the Bridgeport record was also significant in the summer. Accepting the assumption that the correlation has not changed, the LIS temperature index can be extrapolated backwards in time to assess whether recent changes in temperature are unusual.

1.6 References

Bell, R. J.; Hare, J.A.; Manderson, J.P.; and Richardson, D.E. (2014). Externally driven changes in the abundance of summer and winter flounder. ICES Journal of Marine Science, doi:10.1093/icesjms/fsu069.

Bumpus, D.F. (1957). Surface water temperatures along Atlantic and Gulf Coasts of the United States. Special Scientific Report Fisheries No. 214. U.S. Department of the Interior, Fish and Wildlife, Washington, D.C.

Camacho, J., S.A. Qadri, H. Wang and M.K. Worden (2006). Temperature acclimation alters cardiac performance in the lobster *Homarus americanus.* J Comp Physiol. A., doi:10.1007/s00359-006-0162-1.

Crowley, H.A. (2005). The seasonal evolution of thermohaline circulation in Long Island Sound, PhD thesis, Stony Brook Univ., Stony Brook, N. Y.

Gay, P. S., J. O'Donnell and C.A. Edwards (2004). Exchange between Long Island Sound and adjacent waters, J. Geophys. Res., 109, C06017, doi:10.1029/2004JC002319.

Hansen, J., R. Ruedy, M. Sato and R. Reynolds (1996). Global surface air temperature in 1995: Return to pre-Pinatubo level. *Geophys. Res. Lett.*, **23**, 1665-1668, doi:10.1029/96GL01040.

Hansen, J., R. Ruedy. M. Sato and K. Lo (2010). Global surface temperature change. Reviews of Geophysics. Rev. Geophys., 48, RG4004, doi:10.1029/2010RG000345.

Hao, Y. (2008). Tidal and residual circulation in Long Island Sound. Ph.D. Dissertation, Marine Sciences Research Center, Stony Brook University, Stony Brook, NY, 70 pp.

Hare, J. A. and Able, K.W. (2007). Mechanistic links between climate and fisheries along the east coast of the United States: explaining population outbursts of Atlantic croaker (*Micropogonias undulatus*). Fisheries Oceanography, 16:31–45. doi:10.1111/j.1365-2419.2006.00407.x.

Howell, P., J. Benway, C. Giannini, and K. McKown (2005). Long-term population trends in American lobster (Homarus americanus) and their relation to temperature in Long Island Sound. Journal of Shellfish Research 24(3):849-857. doi:10.2983/0730-8000(2005)24[849:LPTIAL]2.0.CO;2.

Howell, P. and P.J. Auster (2012). Regime shift in the finfish community of a Northwest Atlantic estuary associated with changes in thermal regime. Coastal and Marine Fisheries: Dynamics, Management, and Ecosystem Science 4:481-495.

Kaputa N.P. and Olsen, C.B. (2000). State of Connecticut Department of Environmental Protection, Long Island Sound Ambient Water Quality Monitoring Program: Summer Hypoxia Monitoring Survey '91-'98 Data Review. CTDEEP, Water Management Bureau, 79 Elm St, Hartford, CT 06106. 45 pp.

Keser, M., J.T. Swenarton, J.M. Vozarick, and J.F. Foertch (2003). Decline in eelgrass (Zostera marina L.) in Long Island Sound near Millstone Point, Connecticut (USA) unrelated to thermal input. Journal of Sea Research 49:11-26.

Lee, Y.J., (2009). Mechanisms Controlling Variability in Long Island Sound. Ph.D. thesis, School of Marine and Atmospheric Sciences, Stony Brook University, New York.

Lee, Y.J. and K.M.M. Lwiza. (2008). Characteristics of bottom dissolved oxygen in Long Island Sound, New York, Estuar.Coast. Shelf Sci., 76:187-200. doi:10.1016/j.ecss.2007.07.001.

McCardell, G.M. and J. O'Donnell (2009). A novel method for estimating vertical eddy diffusivities using diurnal signals with application to Western Long Island Sound. J. Mar. Systems. 77 (2009) 397–408.

Nixon S.W., S. Granger, B.A. Buckley, M. Lamont, and B. Rowell (2004). A one hundred and seventeen year coastal water temperature record from Woods Hole, Massachusetts. Estuaries 27: 397–404.

Northeast Utilities Environmental Laboratory (2001). Monitoring the Marine Environment of Long Island Sound at Millstone Nuclear Power Station (Northeast Utilities System, Waterford, CT).

Northeast Utilities Environmental Laboratory (1987). Summary of Studies Prior to Unit 3 Operations (Northeast Utilities System, Waterford, CT).

O'Donnell, J., R.E. Wilson, K. Lwiza, M. Whitney, W.F. Bohlen, D. Codiga, T. Fake, D. Fribance, M. Bowman, and J. Varekamp (2014). The Physical Oceanography of Long Island Sound. In Long Island Sound: Prospects for the Urban Sea. Latimer, J.S., Tedesco, M., Swanson, R.L., Yarish, C., Stacey, P., Garza, C. (Eds.), ISBN-13: 978-1461461258.

Oczkowski A.; R. McKinney, S. Ayvazian, A. Hanson, C. Wigand, and E. Markham (2015). Preliminary Evidence for the Amplification of Global Warming in Shallow, Intertidal Estuarine Waters. PLoS ONE. 10(10): e0141529. doi:10.1371/journal.pone.0141529.

Riley, G.A. (1952). Hydrography of the Long Island and Block Island Sounds, Bull. Bingham Oceanogr. Collect., 13, article 3.

Riley, G.A. (1956). Oceanography of Long Island Sound: 1952-1954. II. Physical Oceanography Bulletin of the Bingham Oceanographic Collection, V.15, Peabody Museum of Natural History, Yale University, New Haven, Connecticut, USA.

Rohde, R., R.A. Muller, R. Jacobsen, S. Perlmutter, A. Rosenfeld, J. Wurtele, J. Curry, C. Wickham and S. Mosher (2013). Berkeley Earth Temperature Averaging Process. Geoinfor Geostat: An Overview 1:2. doi:10.4172/gigs.1000103.

Stachowicz, J.J., J.R. Terwin, R.B. Whitlatch, and R.W. Osman (2002). Linking climate change and biological invasions: Ocean warming facilitates nonindigenous species invasions. *Proc. Natl. Acad. Sci. U.S.A.* 99, 15497.

Wilson, R.E., R.L. Swanson and H.A. Crowley (2008). Perspectives on long-term variations in hypoxic conditions in western Long Island Sound, J. Geophys. Res., 113, C12011, doi:10.1029/2007JC004693.

Chapter 2 - Precipitation

Table of Contents

List of Figures

List of Tables

2. Ecological Driver: Precipitation

2.1 Introduction

Precipitation occurs directly on to the surface of Long Island Sound (LIS) and its watershed as rain and snow. It can impact ecosystems in a variety of ways. The over-land precipitation leads to runoff to streams, ground water, and marshes where it can impact the turbidity, the nutrient level and the salinity. The mechanisms though which precipitation acts as an ecological driver can be complex. For example, high flow rates in streams that arise during high precipitation rate events can increase sediment concentration through bank erosion and stream migration. In addition, atmospheric deposition of particulate nitrogen to the earth and surface of LIS is rapid when rain begins. On an annual basis, the total fluxes are likely influenced by the number of rain events or days with rain.

An increase in the frequency of extreme rainfall events in northeastern United States has been suggested by the analysis of DeGaetano (2009) and USGCRP (2009). These studies focused on the probability of the occurrence of very large (e.g., 2 inch/day) events and showed that in New England these were more frequent now than in 1960. The predictions of climate models for the effect of recent warming on large storms of 2013 were less clear (Knutson et al., 2014). The intrinsic variability of the climate systems could account for much of the current observations. The analysis on future changes predicted by models reported in Walsh et al. (2014) and Horton et al. (2014) concluded that though the magnitude of the change of mean annual precipitation amounts was very uncertain, there was high confidence that the magnitude of annual daily maximums would increase.

In this chapter we describe trends in observations of precipitation rates in the coastal areas surrounding LIS so that ecologists seeking understanding of variability in communities can readily assess the potential effects of precipitation. We also provide access to the quality-controlled measurements in a convenient format to facilitate additional work. In the following Section 2.2, we summarize existing reports on the character of precipitation in the region. In Section 2.3 we describe the available observations and the processing steps that we used to create the data files that are analyzed and archived. The characteristics of the trends and variability are presented in Section 2.4, and a summary of results and recommendations for future work are provided in 2.5.

2.2 Precipitation Patterns

There have not been any focused studies of precipitation in the LIS watershed since Miller et al. (2002). They examined daily precipitation totals archived by the National Oceanic and Atmospheric Administration (NOAA) at the National Climate Data Center (NCDC) at 70 stations in Connecticut, Rhode Island and southern Massachusetts up to 1994. They found that the average of all data was 44.8 inches/year but that the annual means had an increasing trend at approximately 0.1 inch per year between 1895 and 1994. They did not analyze snow since they judged it to be a minor contribution to the precipitation. They also showed that there was not a significant seasonal cycle, the variability within a month being much greater than the differences between monthly means. However, the occurrence of high rainfall events was clustered in late summer due to tropical cyclones.

2.3 Precipitation Observations

Measurements of precipitation are archived at the National Oceanographic Data Center (NODC) and can be accessed through the "Climate Data Online" web site https://www.ncdc.noaa.gov/cdo-web. The site supports searching by state, county or station name, and data can be downloaded, though there are limits on the size of each data request. A variety of options for data format is provided. They are referred to as "Custom GHCN-Daily CSV" format. The data are described comprehensively by Menne et al. (2012a and b). The data have a sophisticated quality assurance protocol that is documented by Durre et al. (2010).

Since the focus of this study is on the effects on LIS ecosystems, we identified stations with records spanning at least 50 years within 20 km of the shoreline. Table 2.1 lists the station names, ID number, latitude, longitude and elevation, and Figure 2.1 shows the locations relative to the shoreline of the Sound.

Table 2.1. Summary of station information. (Note that shaded stations did not pass the data quality evaluation.)

	Station Name	Elevation (m)	Latitude (deg)	Longitude (deg)
USW00054790	SHIRLEY BROOKHAVEN AIRPORT	25	40.822	-72.869
USC00307134	RIVERHEAD RES FARM	30.5	40.962	-72.716
USC00307633	SETAUKET STRONG NY	12.2	40.959	-73.105
USC00300889	BRIDGEHAMPTON NY US	18.3	40.946	-72.307
USC00305377	MINEOLA NY US	39.9	40.733	-73.633
US1NYNS0007	FLORAL PARK 0.4	24.1	40.723	-73.711
USC00063207	GROTON CT US	12.2	41.351	-72.039
USW00014707	GROTON NEW LONDON	3	41.328	-72.049
USC00065266	NEW HAVEN CT	7.3	41.3	-72.933
USW00014758	NEW HAVEN TWEED	1.8	41.267	-72.883
USC00060801	BRIDGEPORT CT US	43	41.2	-73.2
USW00094702	BRIDGEPORT SIKORSKY MEMORIAL	7.9	41.167	-73.133
USC00065910	NORWICH PUB UTIL	6.1	41.533	-72.067
USC00060128	ANSONIA 1 NE	42.7	41.35	-73.067
USC00060120	ANSONIA CT US	6.1	41.333	-73.083
USC00065077	MOUNT CARMEL CT	54.9	41.4	-72.9
USC00061762	DANBURY CT US	123.4	41.4	-73.417
USW00054734	DANBURY MUNICIPAL AIRPORT	139.3	41.367	-73.483
USC00066655	PUTNAM LAKE CT	91.4	41.083	-73.633
USC00067002	ROUND POND CT	243.8	41.3	-73.533
USC00067157	SAUGATUCK RESERVOIR CT	92	41.25	-73.35
USC00067970	STAMFORD 5 N	57.9	41.133	-73.55
USC00064767	MIDDLETOWN 4 W	112.5	41.55	-72.717
US1CTMD0005	WESTBROOK CENTER 1.1	10.7	41.297	-72.441
USC00069067	WESTBROOK CT US	11.9	41.3	-72.433

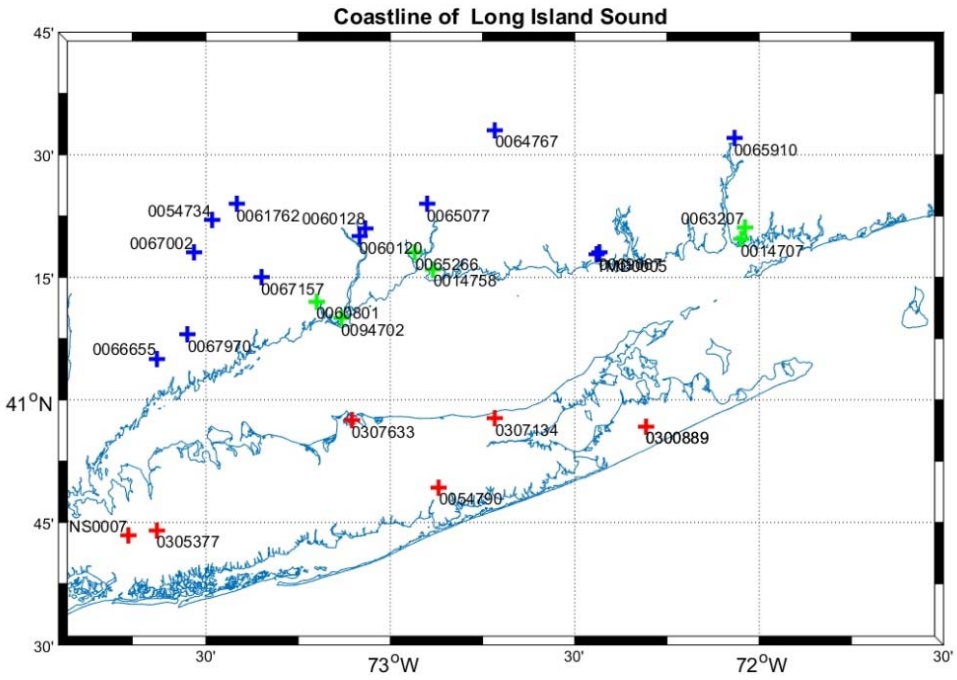

Figure 2.1. Map of the coastline of Long Island Sound showing the locations of the meteorological stations used in the analysis of precipitation variations. See Table 2.1 for locations and station names. Note that the green stations will be referred to as "upland CT", the blue stations as "coastal CT" and the red stations as "LI".

The data were downloaded in the "Custom GHCN-Daily CSV- Output format" and the variables DATE (year, month and day), PRCP (daily rainfall total in 1/10 mm) and SNOW (mm of snow accumulated) and their data source and quality flags were extracted**.** Baxter et al. (2005) reported an extensive analysis of the ratio of snow depth to the equivalent water precipitation. The ratio showed significant variation across the United States, and partially explained the observations. In the southern New England area the long-established estimates of 1 cm of snow to 1 mm of equivalent rainfall was not inconsistent with their results. Note that Kunkel et al. (2007) advised caution on the reliability of the snow estimates in the NCDC database. We included snow in our analysis using the factor 1/10 to convert snow depth to rainfall. But as noted by Miller et al. (2002) it is not a major contributor to total precipitation in the region and small biases in the estimates are not likely to be significant.

The data for each station were examined for consistency. All the daily accumulated rainfall data are plotted in the upper frames of the figures in the Appendix. Selected stations are shown in Figure 2.2. The color of the points indicates the data source to track the source of inconsistencies. The legend of each figure has code that is linked to the NCDC's data source as defined in Table 2.2. Most of the data is from the "COOP SoD" source. This refers to the summaries of daily land surface observations that are from stations in the National Weather Service (NWS) cooperative station network. The NCDC's data also includes many other sources such as stations supported by the Federal Aviation Administration (FAA), National Park Service

(NPS), Bureau of Land Management (BLM), U.S. Forest Service (USFC), and U.S. Geological Survey (USGS). The NCDC also aggregates data from international sources.

(a) Westbrook, CT.

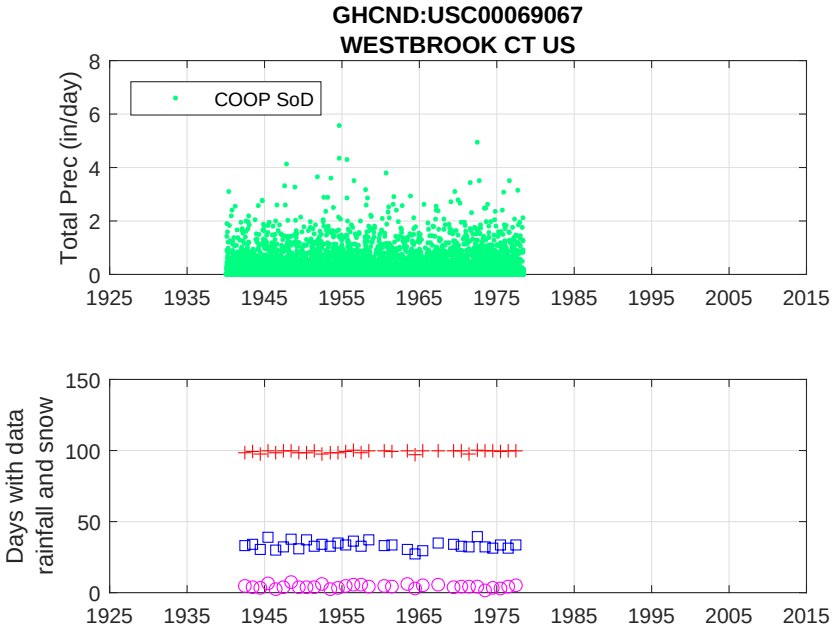

(b) Floral Park, NY.

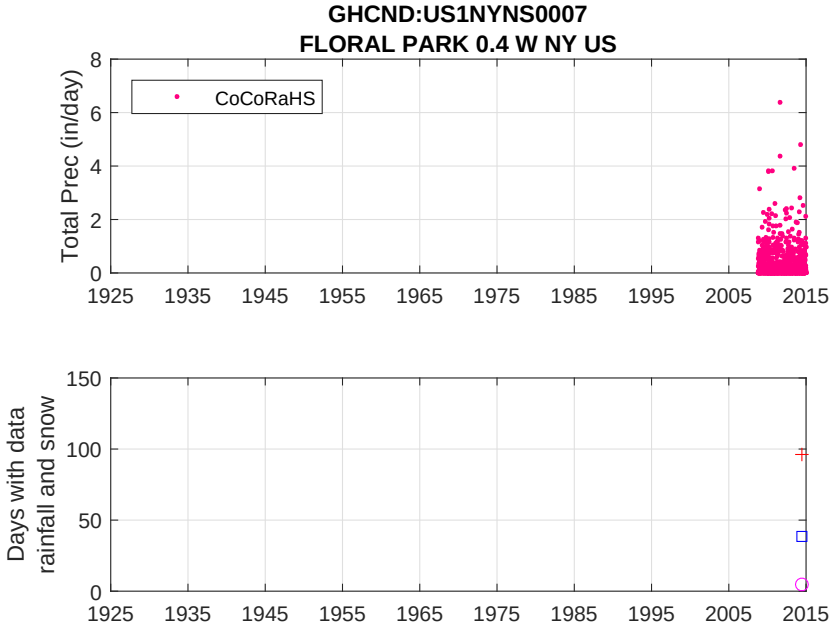

(c) Saugatuck Reservoir, CT.

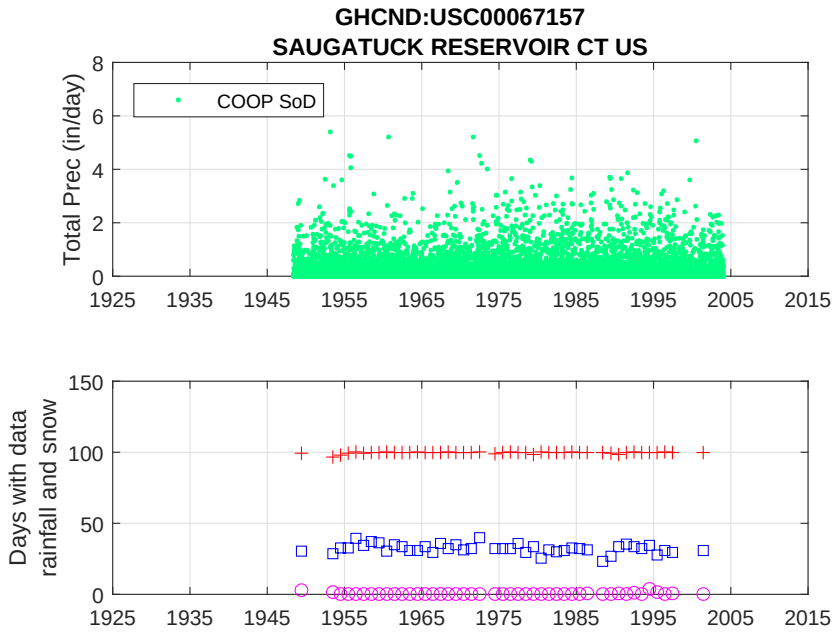

(d) Groton-New London Airport, Groton, CT.

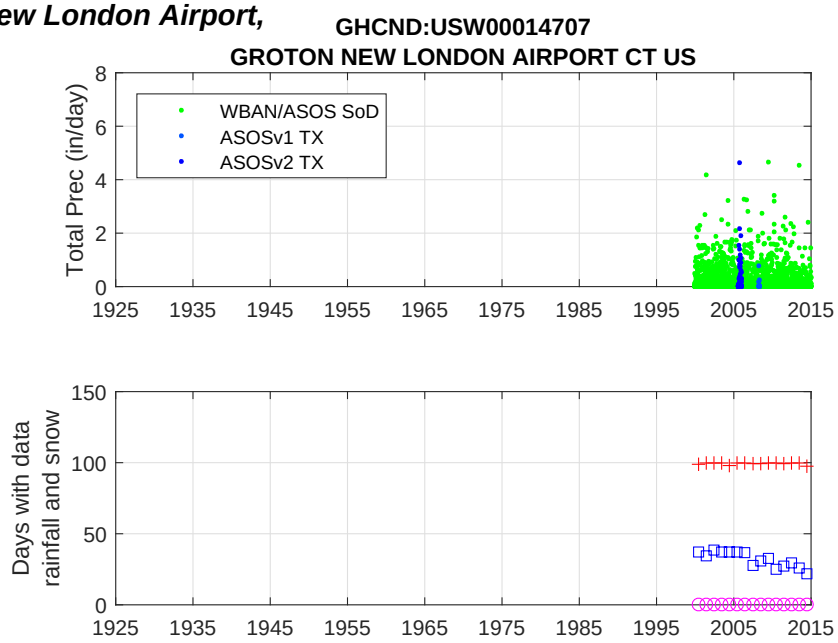

Figure 2.2. The points in the upper graph of each sub-figure show the total daily precipitation data available at (a) Westbrook, CT, Station; (b) Floral Park, NY, Station; (c) Saugatuck Reservoir, CT, Station and (d) Groton-New London Airport Station. The color indicates the source. The code is explained in Table 2.2. Years when the rainfall data was reported (including zero values) on at least 95% of the days were identified. To show the interval of useful data the red '+' symbols in the lower graph of each station show the fraction (percentage) of the year in which rainfall measurements were recorded. The number of days with measureable rain is shown by the blue squares, and days with measureable snow are shown by the magenta circles.

Table 2.2. Data source codes from "SFLAG1" in the document
http://www1.ncdc.noaa.gov/pub/data/ghcn/daily/readme.txt

Code	Figure Code	Source
0	COOP SoD	U.S. Cooperative Summary of the Day (NCDC DSI-3200)
6	CDMP	CDMP Cooperative Summary of the Day (NCDC DSI-3206)
7	COOP SoD TX	U.S. Cooperative Summary of the Day -Transmitted (NCDC DSI-3207)
A	ASOSv1 TX	U.S. Automated Surface Observing System (ASOS)
B	ASOSv2 TX	U.S. ASOS data (NCDC DSI-3211)
F	FortData	U.S. Fort data
H	HPRCC TX	High Plains Regional Climate Center real-time data
K	COOP SoD DG	U.S. Cooperative Summary of the Day (digitized)
N	CoCoRaHS	Community Collaborative Rain, Hail, and Snow (CoCoRaHS)
W	WBAN/ASOS SoD	WBAN/ASOS Summary of the Day from NCDC's Integrated Surface Data (ISD).
X	FirstOrderSOD	U.S. First-Order Summary of the Day (NCDC DSI-3210)
Z	DatzillaRep	Datzilla official additions or replacements

Our review of the data in Figure 2.2(a) and (b) showed that the Westbrook Center (US1CTMD0005) and Floral Park, NY (US1NYNS0007) stations had many data gaps and no years satisfied the 95% data return threshold. Figure 2.2(c) shows that though the Saugatuck Reservoir (USC00067157) station had persistent reports of rain and snow between 1950 and 2004, the number of days of measureable snowfall was mainly zero. This is inconsistent with other stations so this station was regarded as unreliable. Similarly, Putnam Lake (USC00066655), Round Pond (USC00067002), Danbury Airport (USW00054734), both Ansonia stations (USC00060128 and USC00060120), New Haven -Tweed Airport (USW00014758), and Shirley-Brookhaven Airport (USW00054790) had inconsistent delivery of snow measurements. It appears that the airports did not emphasize measurement of snow. These stations were also classified as unreliable.

Figure 2.2(d) shows that no snow was recorded at the Groton-New London Airport station (USW00014707). It also shows a declining number of days of rain, a feature that is inconsistent with other regional stations. This station was also classified as unreliable. Unfortunately the reliability of measurements at the nearby Groton (USC00063207) station dropped in the last decade (see Figure 2A.17) and only two years delivered measurements more than 95% of the time. The color codes in the lower frame of Figure 2A.17 show that the drop in reliability coincided with a change in the mode of data transfer to digitized paper forms and then to NCDC DSI-3207 (a web-based data input approach). However, most of the record is reliable.

2.4 Trend and Variability Analysis

Figure 2.3 shows the mean and ± a standard error of the total precipitation at each of the stations with reliable data. Note that the standard error was computed without correction for serial correlation, and therefore might be slightly underestimated. The red symbols show the statistics for the stations on Long Island while the blue and green show the data for coastal and upland Connecticut, respectively. It is immediately obvious that the values are appreciably higher than the estimate of Miller et al. (2002) of 44.8 inches. In part, this is a consequence of the fact that they included many more stations to the north and none from Long Island, and they omitted the contributions from snow. These data are most relevant to the coastal habitats of Long Island Sound.

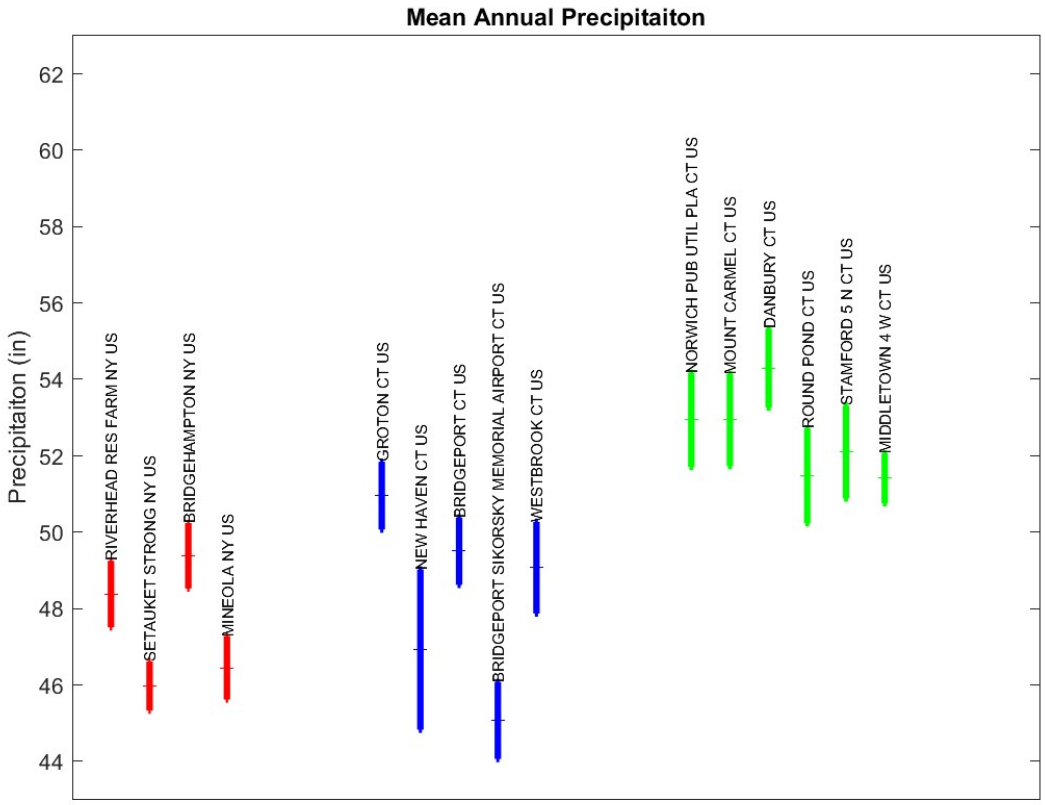

Figure 2.3. Comparison of the long term mean annual precipitation (inches) at the stations listed in Table 2.1. The colors correspond to those in Figure 2.1 and represent the geographic location. Those in red are located on Long Island, NY. The blue stations are in Connecticut and close to the shoreline, while the stations represented by green are in more upland locations in Connecticut.

It is also clear that the Long Island (red) and coastal Connecticut (blue) means are largely consistent. This is somewhat surprising considering the differences in the observation intervals and that the spatial separation is in excess of 100 km (compare Riverhead, New Haven and Mineola, for example). The upland stations (in green) have significantly higher annual

precipitation but also show similar magnitudes despite the fact that Norwich is almost 160 km east of Danbury. The higher precipitation at the inland stations can be attributed to the higher altitude. That the Norwich station (USC00065910) is only at 6 meters yet has almost identical mean annual precipitation as Danbury (USW00054734) and Middletown (USC00064767) suggests that the distance from the coast is a significant effect.

The temporal variability of the annual precipitation data is shown in Figure 2.4. The colors identify the geographic location of the reporting stations. As in Figure 2.1 and Figure 2.3 the red points show the LI stations, the blue show coastal CT and green show the more inland stations. The scatter in the data due to inter-annual and spatial variations is substantial. The drought of the mid 1960s is clearly evident and there is evidence of an upward trend since then. The differences between regions and the longer term trends are unclear due to the large variance.

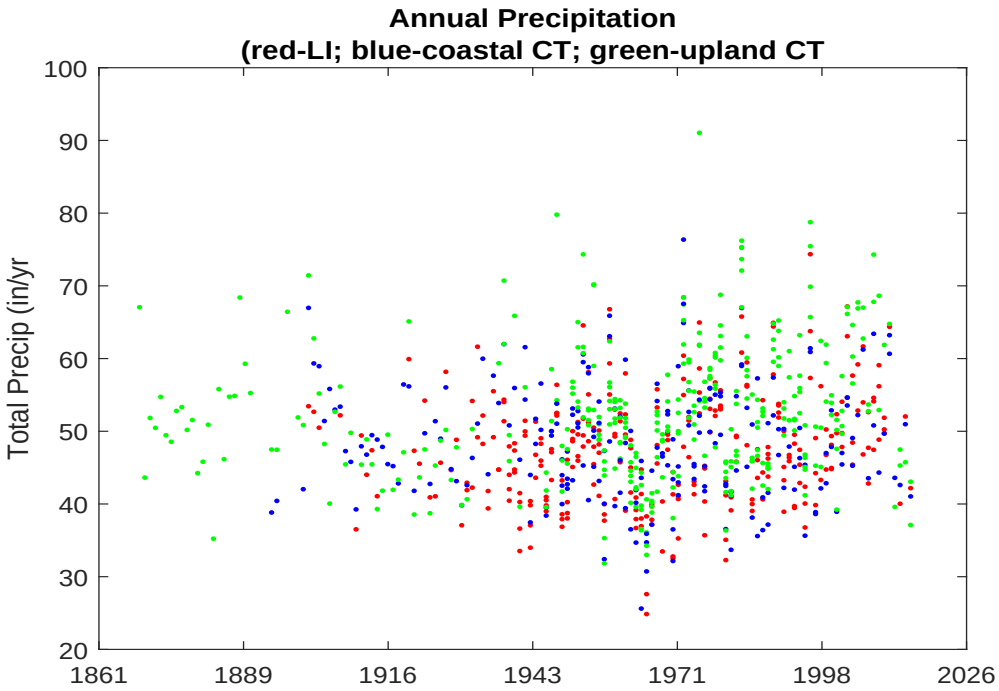

Figure 2.4. The time series of the annual precipitation at the stations listed in Table 2.1 that meet the reliability criteria. Data in red are located on Long Island, NY. The blue points are from coastal Connecticut and green from more upland locations in Connecticut.

To reduce the inter-annual variability in the data, spatial averages across the three geographical areas are computed and shown in Figure 2.5 using the same color convention in which red shows the annual average across the Long Island stations, and blue and green show the average in coastal and inland Connecticut, respectively. The mean across all stations is also shown in black but is obscured by the other series. All three records are very highly correlated with variations about the long term mean that have peak amplitudes in the range of 10 to 20 inches. This is much larger than the regional differences. The temporal standard deviation of the average across all

stations is shown in Table 2.3 to be 7 inches, while that of each of the regional averages is approximately 3 inches. In conclusion, only 20% of the variation about the spatially averaged series is due to the temporal change. The spatial structure is therefore much more significant.

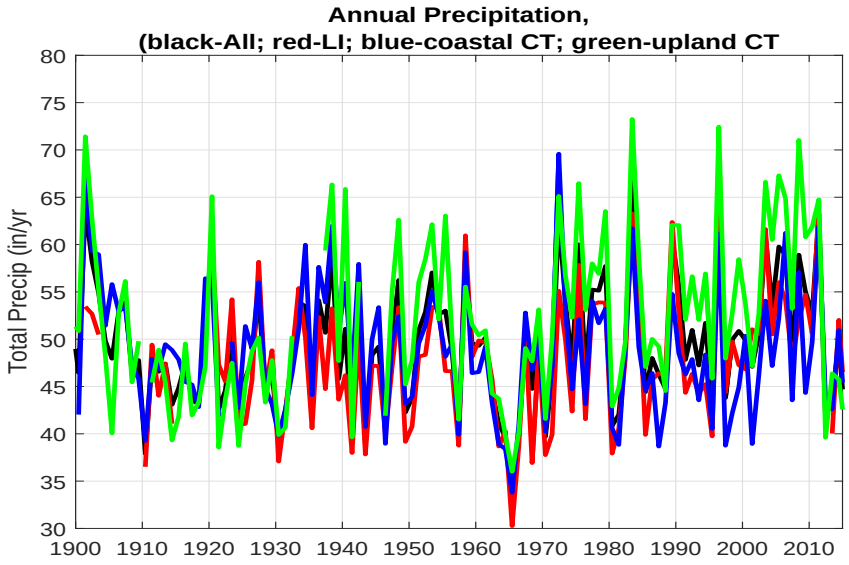

Figure 2.5. Average by year of all annual precipitation estimates across the three geographic areas. The blue points are from coastal Connecticut and green from more upland locations in Connecticut.

Table 2.3. Standard deviation of the regionally averaged annual precipitation (inches).

All Stations	Long Island	Coastal CT	Upland CT
7.0	2.7	3.6	3.4

To reveal the long term spatial structure more clearly, we applied a seven year box car filter to the mean of all the stations and the three regional series. The black line in Figure 2.6 shows the evolution of the mean at all stations. There is evidently a large positive anomaly at the beginning of the 20th and 21st centuries and three negative anomalies in between, including the drought in the mid 60s. Whether there is a long term trend is ambiguous. Using all the data we find a slope of 0.5 inches per century increase, much less than the Miller et al. (2002) estimate. Since their analysis preceded the high precipitation years after 2000, we repeated the regression calculation using only data from 1916 to 1994 and found 5.1 inches per century as the slope. However, we conclude that there is no unequivocal evidence of change in the regional mean annual precipitation.

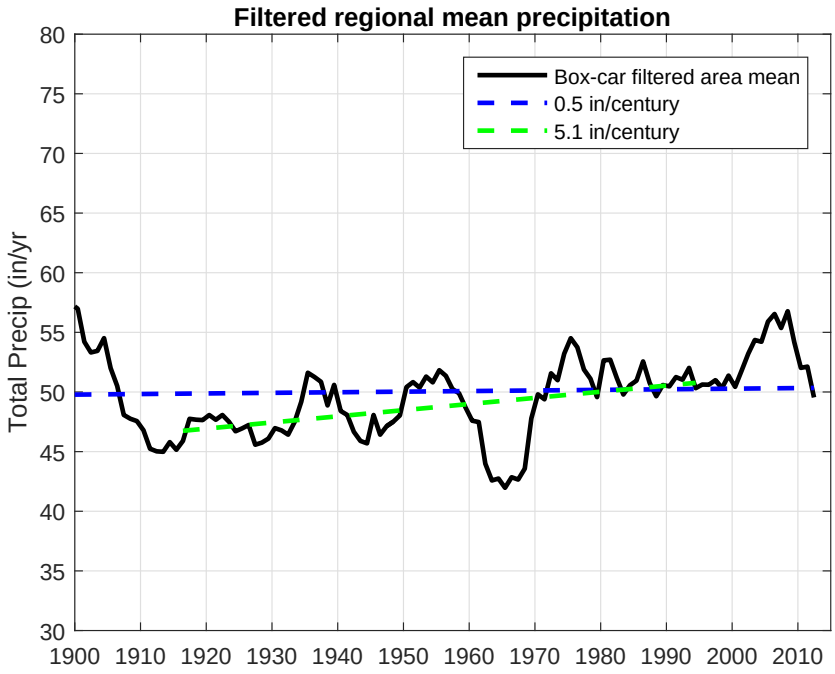

Figure 2.6. The black line shows the regional mean precipitation filtered with a box-car moving average. The blue dashed line shows the long term trend estimated using un-weighted linear regression and all the data. The slope shows an increase of 0.5 inches per century. The green dashed line also shows a regression based on data between 1915 and 1994. The rate of increase is more rapid at 5.1 inches per century. The differences between the trends in the three sub-regions are computed by subtracting the mean of all the stations (Figure 2.6) from the mean of each of the other three series.

Figure 2.7 shows the results after a 7-year running-mean filter has been applied to each series. The green line shows that the annual precipitation anomaly in the inland areas since 1935 is generally higher than the others in keeping with the results in Figure 2.3. The coastal Connecticut stations (blue) and Long Island Stations (red) show a generally decreasing trend. The decadal-scale variability in the upland CT (green line) is negatively correlated with the variations on Long Island and of approximately equal magnitude (about 5 inches). A significant peak in the cross correlation of these series occurs at zero lag with a magnitude of -0.5. This is consistent with the conclusion that the regional mean is not changing very much but the Long Island and coastal area have experienced a reduction in the annual precipitation while the inland areas have experienced a slight increase.

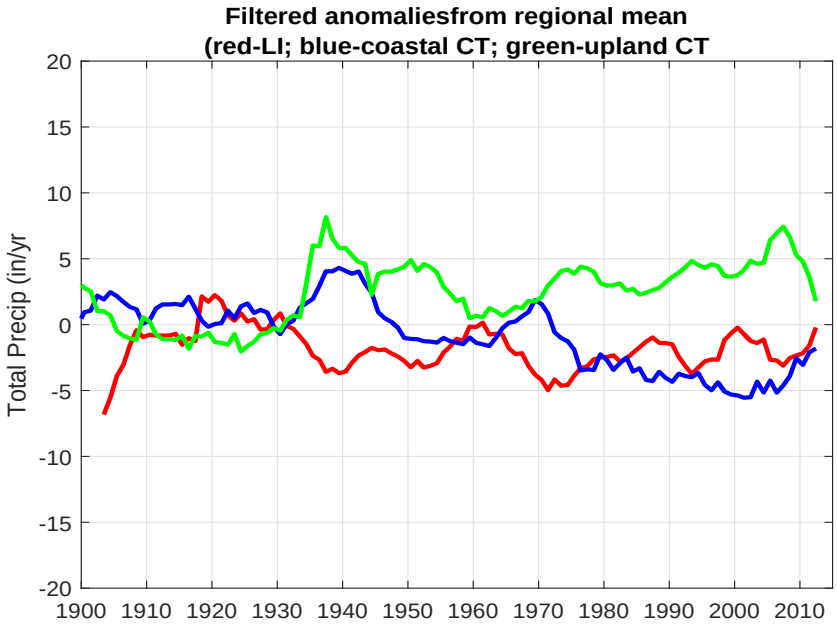

Figure 2.7. Difference between the box-car filtered average precipitation across the entire region and the filtered average in the three sub-areas. The blue and red lines show the anomaly in coastal Connecticut and Long Island, and the green line shows the upland locations in Connecticut.

The total annual rainfall is not the only important influence on coastal ecology. The number of days of rain and snow may also be significant. Figure 2.8 displays the variation in the number of days on which greater than zero rainfall and snow were reported at the stations listed in Table 2.1. The red line in the upper and lower graphs show the average rain and snow days at the Long Island stations after a 7 year long box-car filter has been applied to remove the year-to-year fluctuations. The analysis reveals that in most years it rains approximately 10 fewer days on Long Island (mean of 100 days) than in coastal Connecticut (120 days). The area wide mean over the whole record, and in inland Connecticut, is 115 days with a standard deviation of 13 days. Coastal Connecticut endured more rain days in the period 1925-35 but there was a decline until 1960 and since then the variation has been less. Long Island also endures fewer days of snow (11) than Connecticut (14) in most years. However, the number of snow days has been declining throughout the 20th century across the region. This is particularly apparent on Long Island where the mean of the last 30 years shows three days less snow than the earlier period.

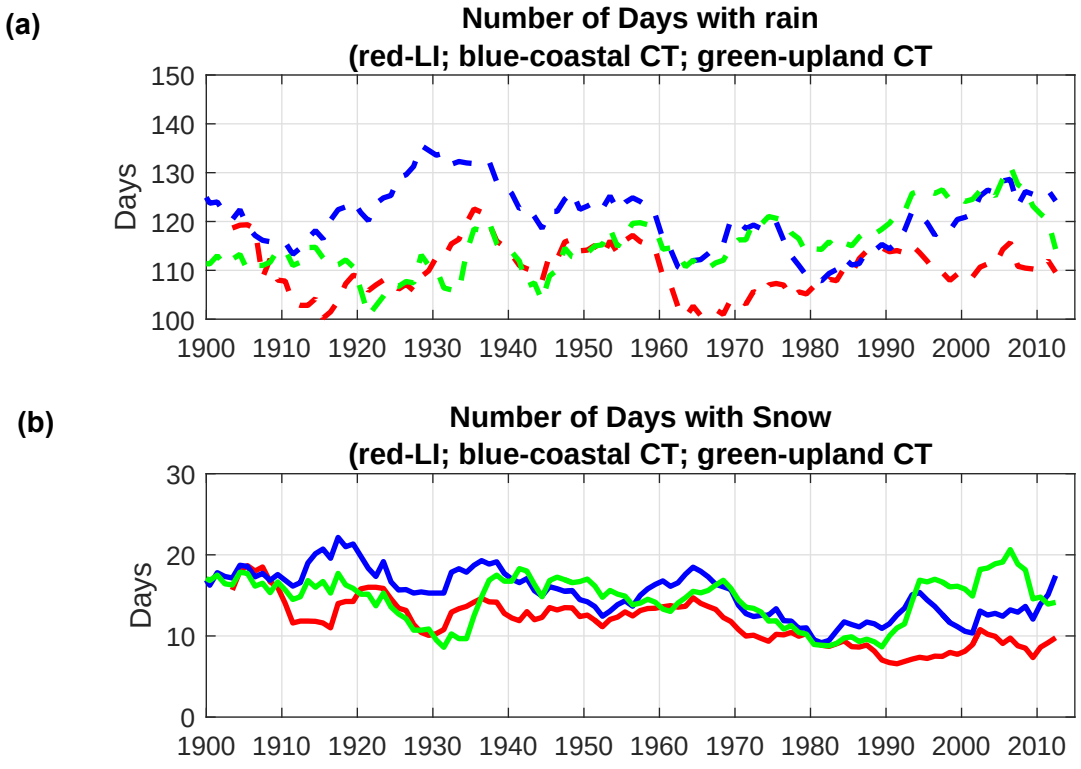

Figure 2.8. (a) Evolution of the average across the three region of the number of days in which rain was measured. A seven-year box-car filter has been applied to the records. (b) Corresponding data for snowfall. The red lines show the Long Island station data and the blue and green show the coastal and inland Connecticut stations.

The work of DeGaetano (2009) and USGCRP (2009) suggested that the frequency of high precipitation events had increased across New England. To investigate whether this is true in the LIS watershed, we examined the distribution of daily precipitation rates more closely. Figure 2.9 shows time series of the data from each of the three sub areas. Only years and stations when more than 95% of the days had data were included in the analysis and graphs. The gaps in the data are evident since the data density is high. These figures suggest that higher values are more frequent at the end of the 20th century.

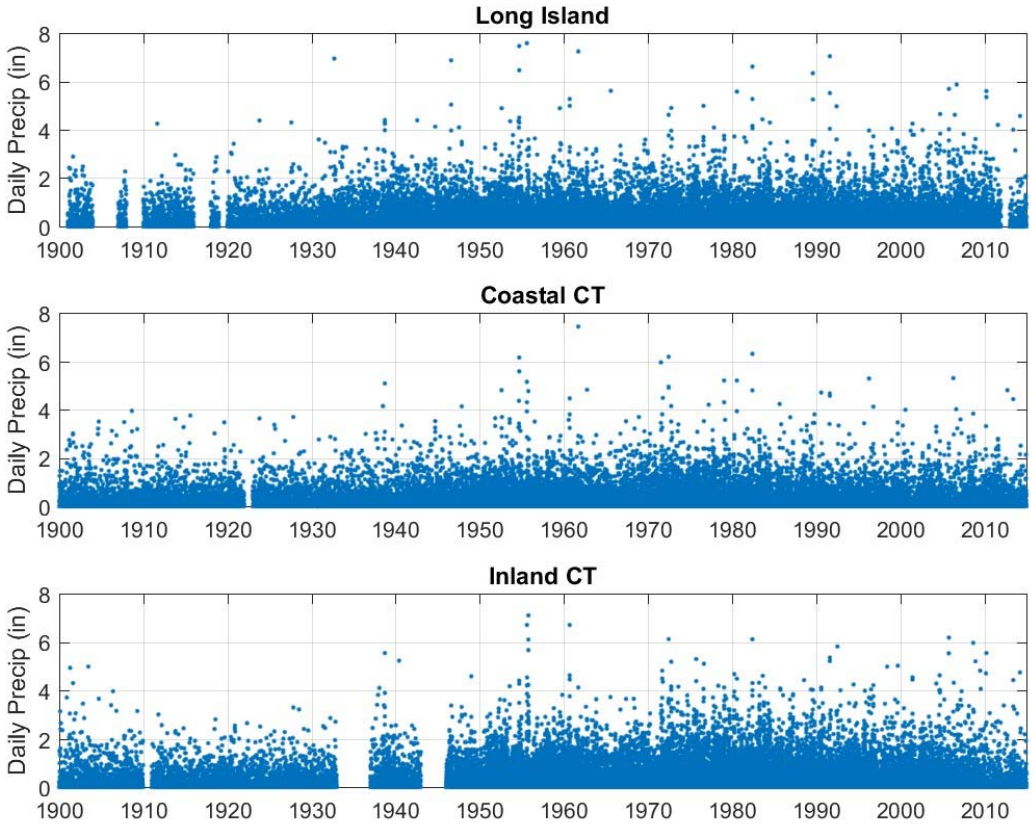

Figure 2.9. The daily observations of precipitation from all stations in the three regions.

Figure 2.10(a) shows the histograms of the distribution of the measurement grouped by station location. The red bars show the fraction of the measurements recorded at the Long Island stations in 0.25 inch bins. The blue and green bars show the corresponding values for the coastal and inland Connecticut stations. Note that the vertical axis is a log scale. If the 0-0.25 inches/day bin is eliminated, then much of the rest of the distribution is consistent with a negative exponential dependence of frequency on the precipitation rate. The three regions show similar distributions up to 3.5 inches/day though the inland Connecticut (green bars) is slightly higher.

The cumulative distribution of the frequency of observation is shown in Figure 2.10(b) using the same color code to clarify the character of the distribution at high precipitation rates. Note that values in excess of 2.0 inches/ day occur less than 0.05% of the time. The red and blue bars are slightly higher than the green bars in the range 0.5 to 3 inches per year. These small variations are largely explained by the slightly lower occurrence of 0-0.25 inch per day observations in upland Connecticut.

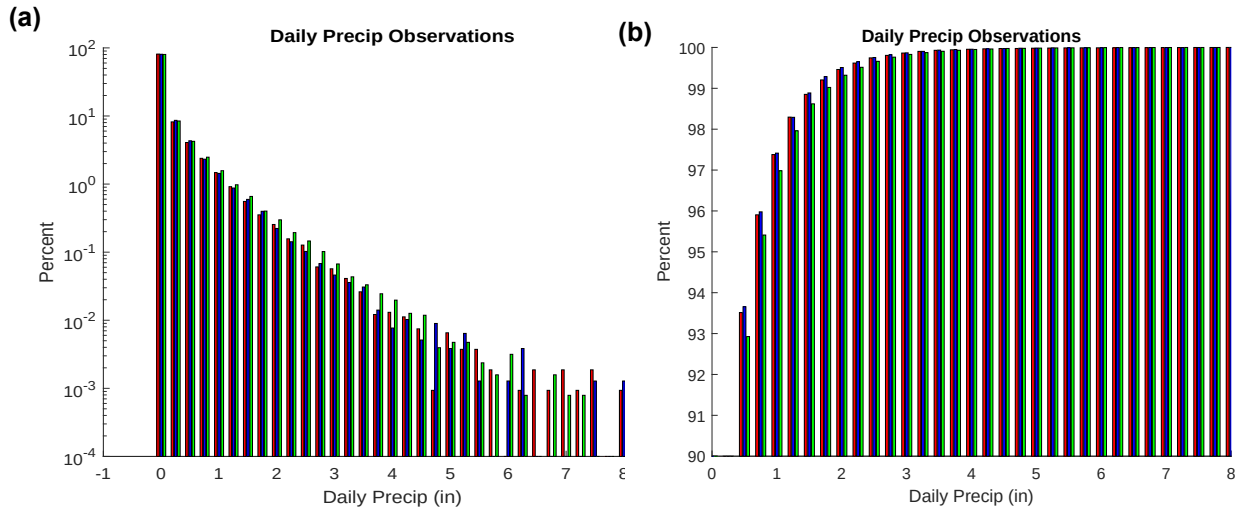

Figure 2.10. (a) Percentage of all observations in 0.25 inch/day bin. The red bars show the data from all stations on Long Island; blue and green show coastal and inland Connecticut data. (b) Cumulative distribution of observations.

Figure 2.11 shows how the fraction of observations greater than two inches per year varies with time. The percentage of observations in each sub area is plotted using the same color code and added to the other sub areas. Note that five-year intervals were used to stabilize the estimates but the percentage of observations per year is presented. The distribution in the three areas is highly correlated and of comparable magnitude. There appears to have been a large increase in the occurrence of high rainfall days after 1940 and then a dip in the mid-1960s. Between 1975 and 2000, the frequency of high precipitation reached a maximum and then declined. This is not completely inconsistent with the analysis of DeGaetano (2009). His conclusion applies to a much larger region and based on extreme value statistics using only data before 2007. Our results show no evidence of an increase in extreme precipitation events in the coastal areas surrounding Long Island Sound.

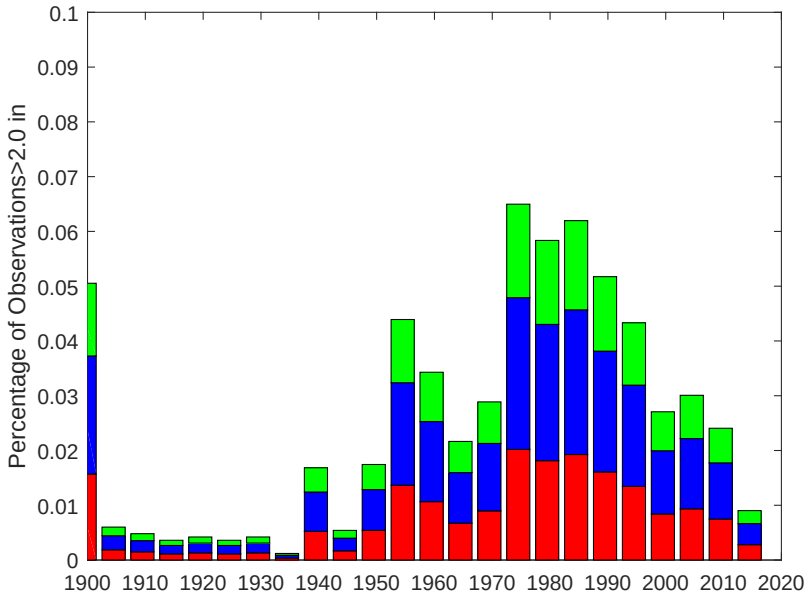

Figure 2.11. Percentage of all observations in excess of 2 inches per day in 0.25 in bins. Red shows Long Island, and blue and green show coastal and inland Connecticut.

2.5 Summary

We have identified a subset of the NODC weather observation stations that span the area surrounding LIS and evaluated the data quality for the estimation of Total Precipitation (rain and snow). The station data was analyzed to discriminate differences from coastal Connecticut, inland Connecticut and Long Island. We find that the mean annual precipitation at the inland stations is significantly higher than in the coastal areas and Long Island (Figure 2.3). The records show substantial year to year variability (Figure 2.5) but that the area-wide average precipitation does not show a significant long term trend (Figure 2.6). There is, however, long term trends within the region with the annual precipitation in the coastal regions negatively correlated at decadal scales with those inland (Figure 2.7). The inland stations also show an increasing trend. The number of days of rain and snow was also examined and we show that there has been a slight decline in the number of snow days on Long Island over the last century. The number of days with rainfall exhibits decadal scale cycles but has not appreciably changed on Long Island or inland Connecticut, although there is evidence of fewer rain days in coastal Connecticut in the recent past relative to the 1930s. Finally, we examined the frequency of occurrence of rainfall events leading to more than two inches of rain in a day. We find no evidence of an increasing trend in the frequency of these events.

2.6 References

Baxter, M.A., C.E. Graves and J.T. Moore (2005). A climatology of snow-to-liquid ratio for the contiguous United States. Wea. Forecasting, 20, 729–744.

DeGaetano, A.T. (2009). Time-Dependent Changes in Extreme Precipitation Return-Period Amounts in the Continental United States. Journal of Applied Meteorology & Climatology, vol. 48, no. 10, pp. 2086–2099.

Durre, I., M.J. Menne, B.E. Gleason, T.G. Houston, and R.S. Vose (2010). Comprehensive automated quality assurance of daily surface observations. J. Appl. Meteor. Climatol., 49, 1615–1633.

Horton, R., G. Yohe, W. Easterling, R. Kates, M. Ruth, E. Sussman, A. Whelchel, D. Wolfe, and F. Lipschultz (2014). Ch. 16: Northeast Climate Change Impacts in the United States: The Third National Climate Assessment, J.M. Melillo, Terese (T.C.) Richmond, and G.W. Yohe, Eds., U.S. Global Change Research Program, 16-1-nn.

Knutson, T.R., F. Zeng and A.T. Wittenberg (2014). Seasonal and Annual Mean Precipitation Extremes Occurring During 2013: A U.S. Focused Analysis [in "Explaining Extremes of 2013 from a Climate Perspective"]. Bulletin of the American Meteorological Society, 95(9), S19-S23.

Kunkel, K.E., M.A. Palecki, K.G. Hubbard, D.A. Robinson, K.T. Redmond, and D.R. Easterling (2007). Trend Identification in Twentieth-Century U.S. Snowfall: The Challenges. J. Atmos. Oceanic Technol., 24, 64–73.

Menne, M.J., I. Durre, R.S. Vose, B.E. Gleason, and T.G. Houston (2012a). An overview of the Global Historical Climatology Network-Daily Database. Journal of Atmospheric and Oceanic Technology, 29, 897-910, doi:10.1175/JTECH-D-11-00103.1.

Menne, M.J., I. Durre, B. Korzeniewski, S. McNeal, K. Thomas, X. Yin, S. Anthony, R. Ray, R.S. Vose, B.E.Gleason, and T.G. Houston (2012b) Global Historical Climatology Network - Daily (GHCN-Daily), Version 3. NOAA National Climatic Data Center. http://doi.org/10.7289/V5D21VHZ.

Miller, D.R., G.S. Warner, F.L. Ogden, and A.T. DeGaetano (2002). Precipitation in Connecticut. CT. Inst. Water Resources, Special Report. (Available at http://www.ctiwr.uconn.edu/PrecipinCT/precip.pdf).

U.S. Global Change Research Program (USGCRP) (2009). Global Climate Change Impacts in the United States, T.R. Karl, J. M. Melillo, and T.C. Peterson, Eds. Cambridge University Press.

Walsh, J., D. Wuebbles, K. Hayhoe, J. Kossin, K. Kunkel, G. Stephens, P. Thorne, R. Vose, M. Wehner, J. Willis, D. Anderson, S. Doney, R. Feely, P. Hennon, V. Kharin, T. Knutson, F. Landerer, T. Lenton, J. Kennedy, and R. Somerville (2014). Ch. 2: Our Changing Climate. Climate Change Impacts in the United States: The Third National Climate Assessment, J.M. Melillo, Terese (T.C.) Richmond, and G.W. Yohe, Eds., U.S. Global Change Research Program, 19-67. doi:10.7930/J0KW5CXT.

Appendix 2

This Appendix displays the time series of daily precipitation and data consistency metrics at all the stations considered in the analyses reported in Chapter 2.

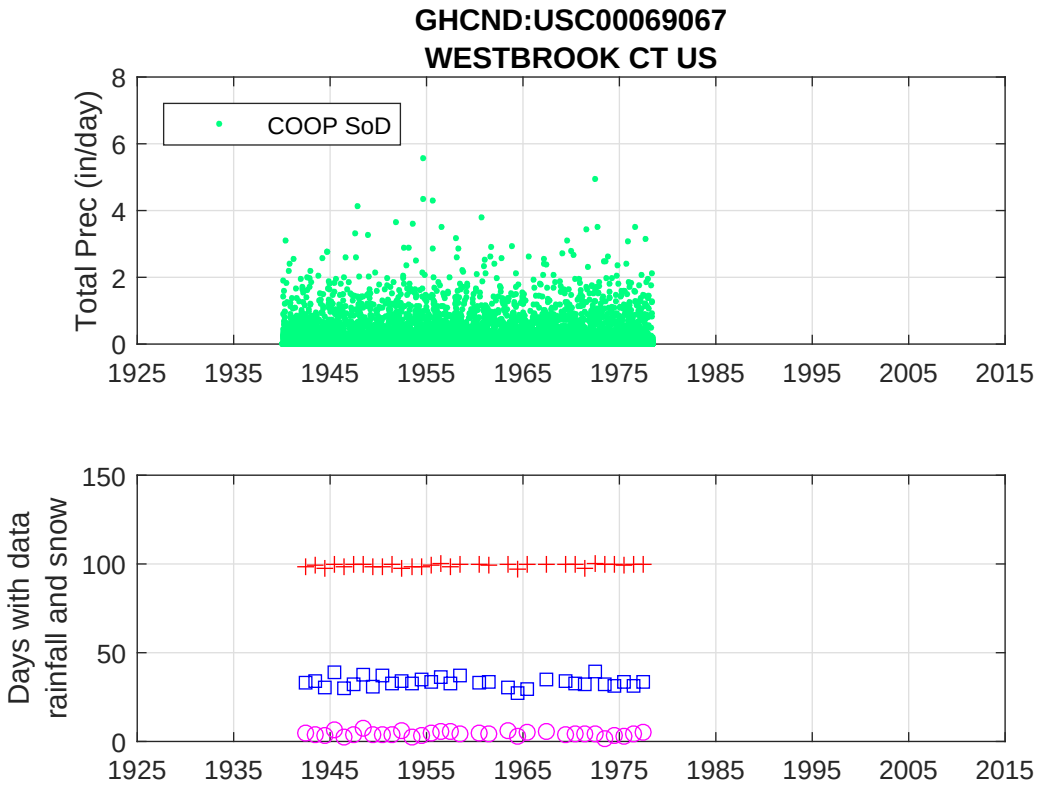

Figure 2A.1. The points in the upper frame show the total daily precipitation data available at the station indicated in the figure. The color indicates the source. The code is explained in Table 2.2. Years when the rainfall data was reported (including zero values) on at least 95% of the days were identified. To show the interval of useful data the red '+' symbols in the lower frame show the fraction (percentage) the year in which rainfall measurements were recorded. The number of days with measureable rain is shown by the blue squares, and days with measureable snow is shown by the magenta circles.

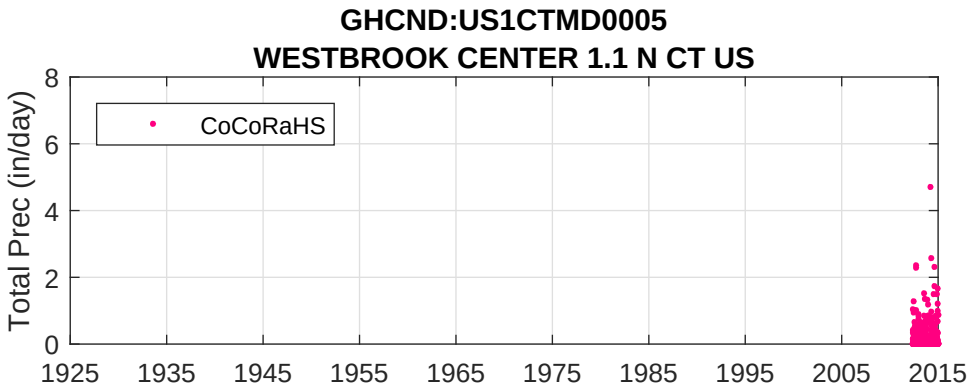

Figure 2A.2. The points in the upper frame show the total daily precipitation data available at the station indicated in the figure. The color indicates the source. The code is explained in Table 2.2. At this station there were no years when the rainfall data was reported (including zero values) on at least 95% of the days.

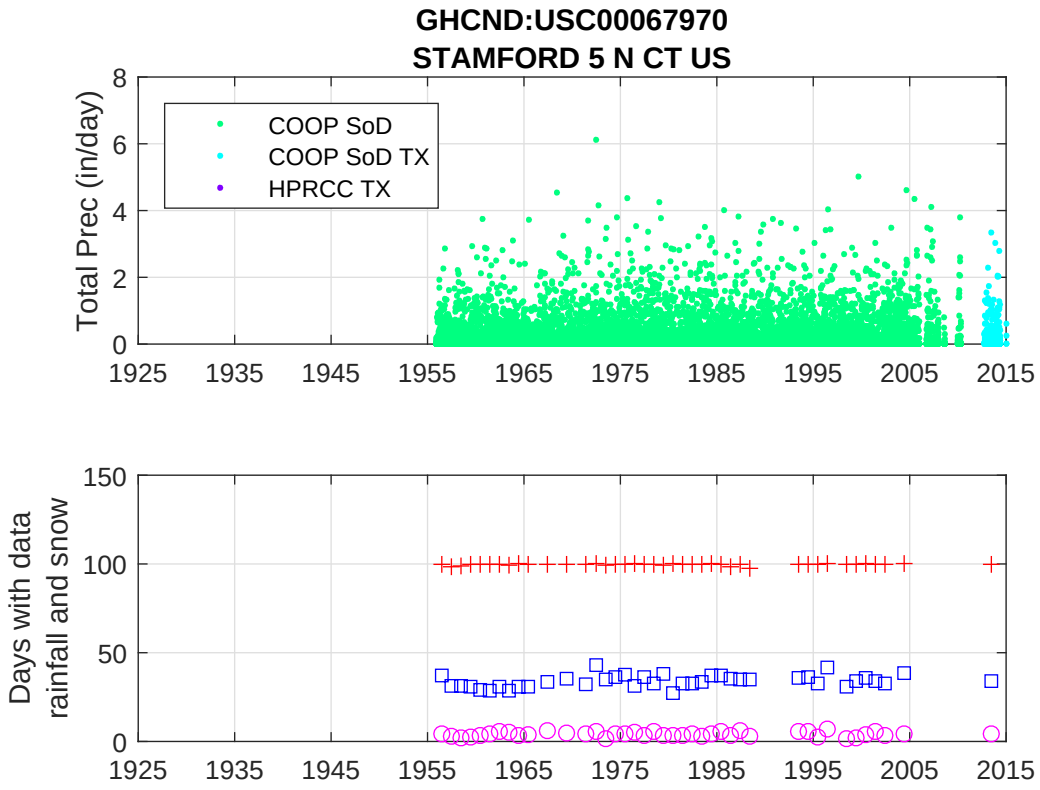

Figure 2A.3. The points in the upper frame show the total daily precipitation data available at the station indicated in the figure. The color indicates the source. The code is explained in Table 2.2. Years when the rainfall data was reported (including zero values) on at least 95% of the days were identified. To show the interval of useful data the red '+' symbols in the lower frame show the fraction (percentage) the year in which rainfall measurements were recorded. The number of days with measureable rain is shown by the blue squares, and days with measureable snow are shown by the magenta circles.

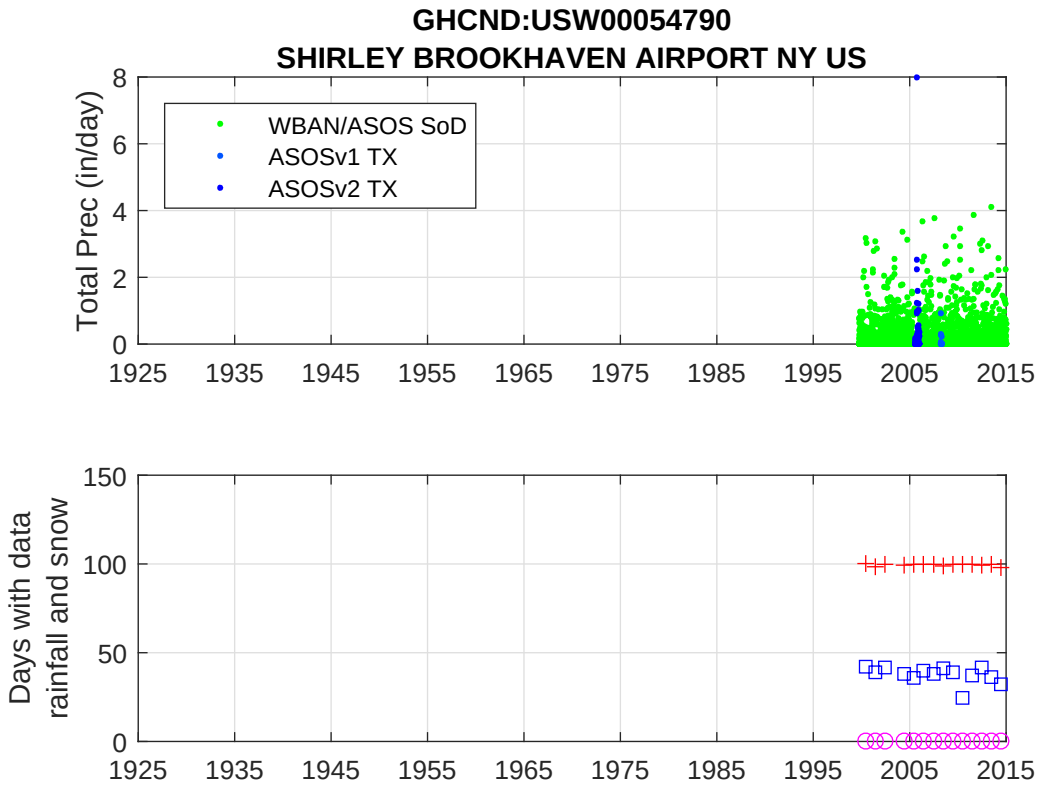

Figure 2A.4. The points in the upper frame show the total daily precipitation data available at the station indicated in the figure. The color indicates the source. The code is explained in Table 2.2. Years when the rainfall data was reported (including zero values) on at least 95% of the days were identified. To show the interval of useful data the red '+' symbols in the lower frame show the fraction (percentage) the year in which rainfall measurements were recorded. The number of days with measureable rain is shown by the blue squares, and days with measureable snow are shown by the magenta circles.

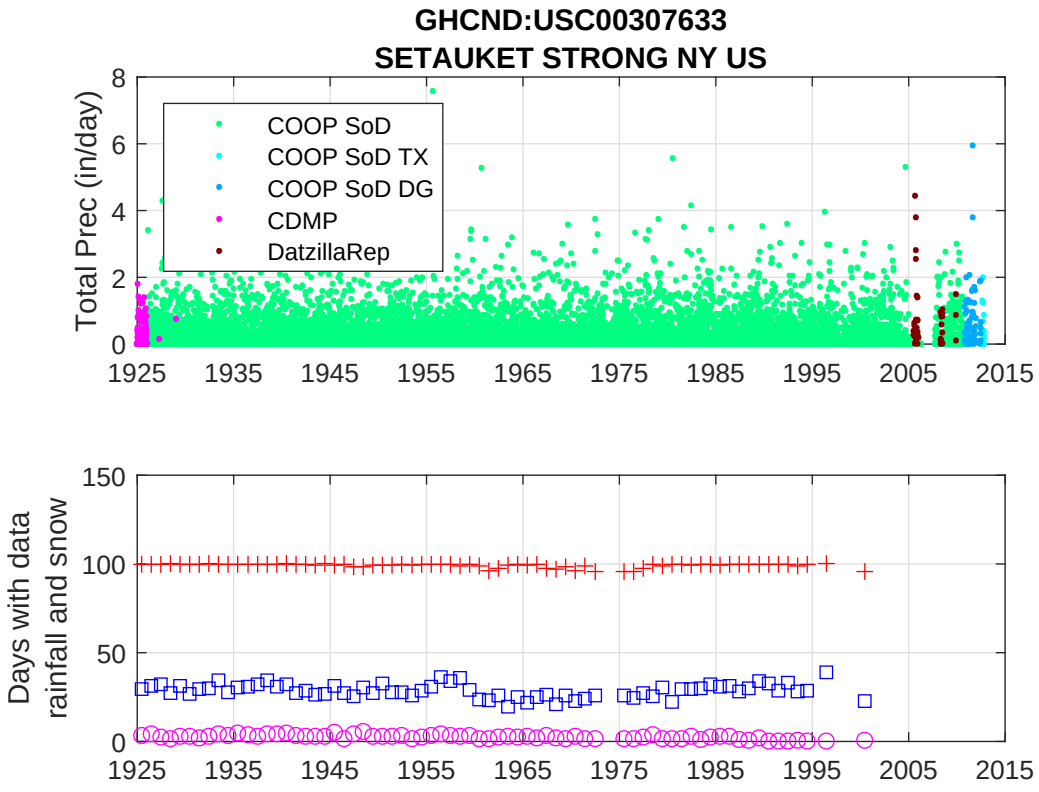

Figure 2A.5. The points in the upper frame show the total daily precipitation data available at the station indicated in the figure. The color indicates the source. The code is explained in Table 2.2. Years when the rainfall data was reported (including zero values) on at least 95% of the days were identified. To show the interval of useful data the red '+' symbols in the lower frame show the fraction (percentage) the year in which rainfall measurements were recorded. The number of days with measureable rain is shown by the blue squares, and days with measureable snow are shown by the magenta circles.

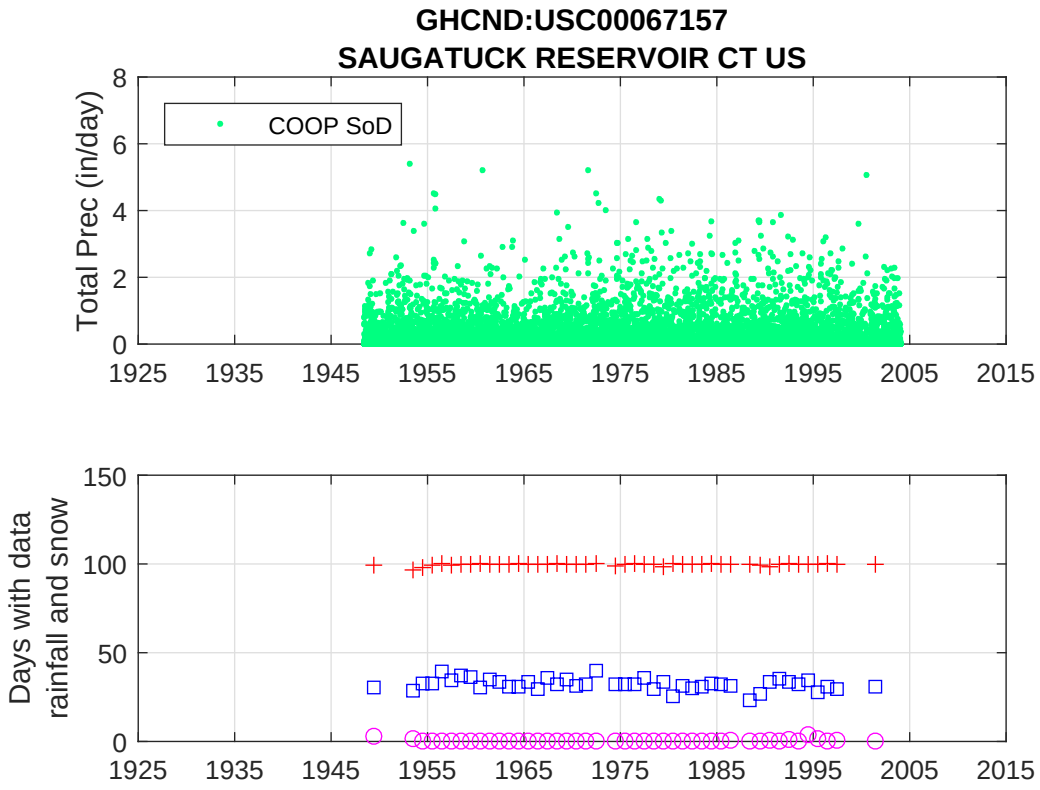

Figure 2A.6. The points in the upper frame show the total daily precipitation data available at the station indicated in the figure. The color indicates the source. The code is explained in Table 2.2. Years when the rainfall data was reported (including zero values) on at least 95% of the days were identified. To show the interval of useful data the red '+' symbols in the lower frame show the fraction (percentage) the year in which rainfall measurements were recorded. The number of days with measureable rain is shown by the blue squares, and days with measureable snow are shown by the magenta circles.

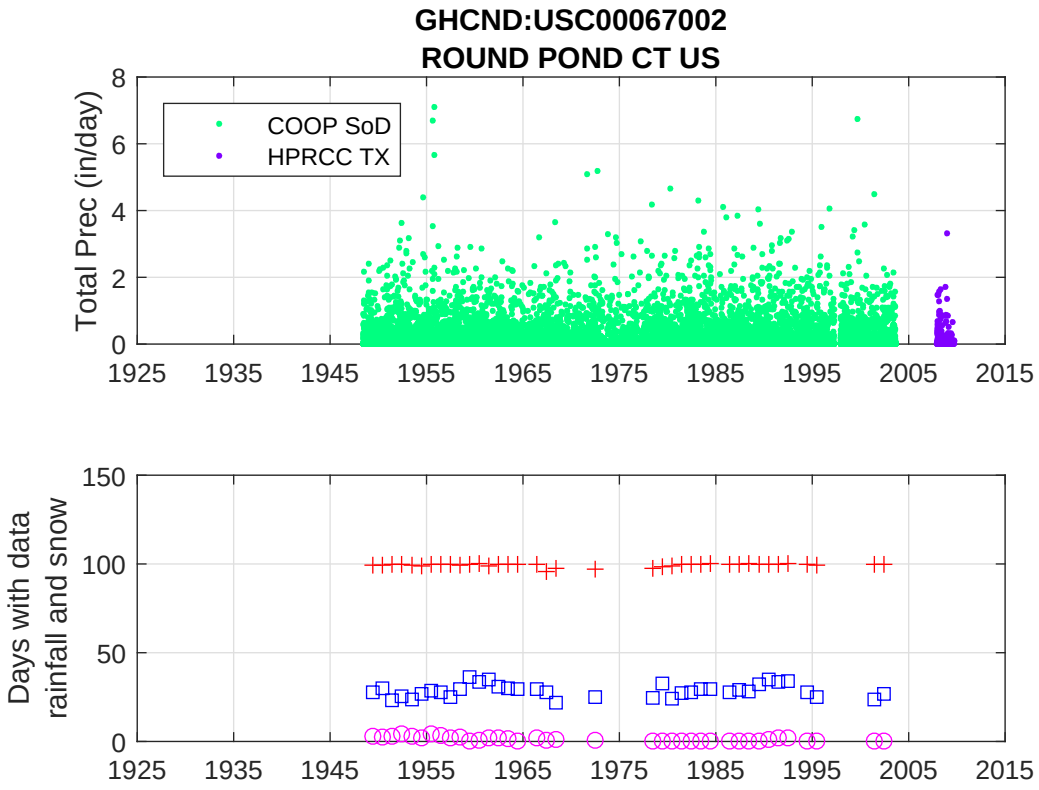

Figure 2A.7. The points in the upper frame show the total daily precipitation data available at the station indicated in the figure. The color indicates the source. The code is explained in Table 2.2. Years when the rainfall data was reported (including zero values) on at least 95% of the days were identified. To show the interval of useful data the red '+' symbols in the lower frame show the fraction (percentage) the year in which rainfall measurements were recorded. The number of days with measureable rain is shown by the blue squares, and days with measureable snow are shown by the magenta circles.

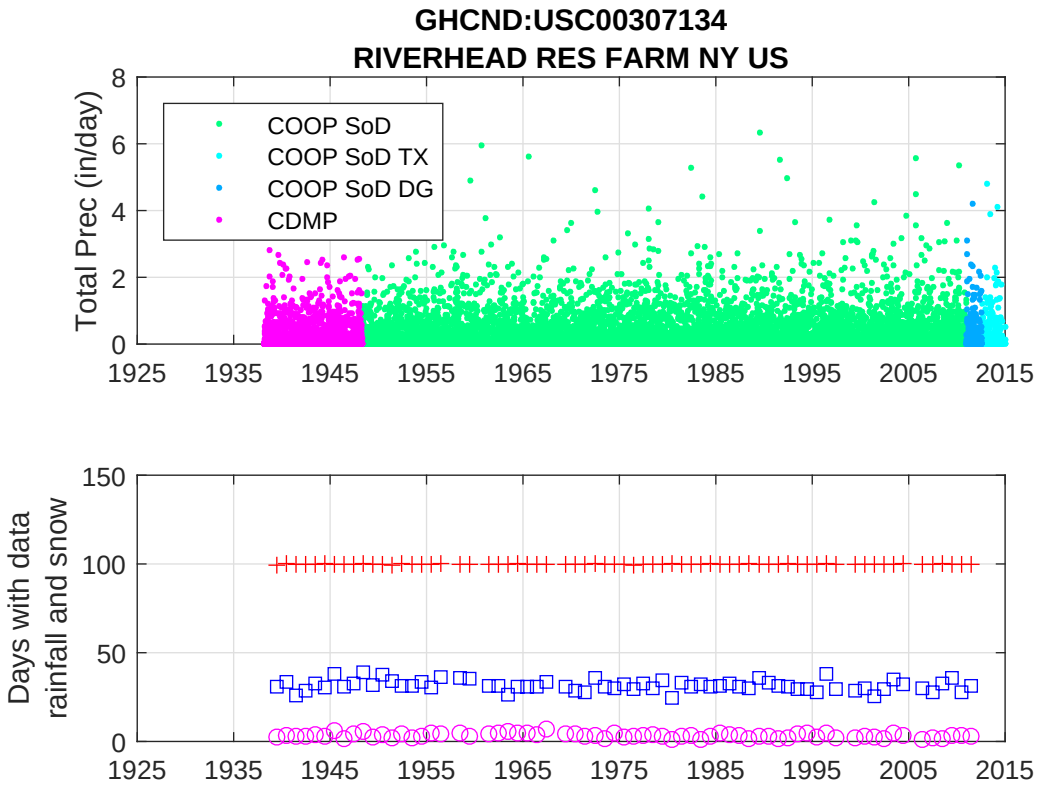

Figure 2A.8. The points in the upper frame show the total daily precipitation data available at the station indicated in the figure. The color indicates the source. The code is explained in Table 2.2. Years when the rainfall data was reported (including zero values) on at least 95% of the days were identified. To show the interval of useful data the red '+' symbols in the lower frame show the fraction (percentage) the year in which rainfall measurements were recorded. The number of days with measureable rain is shown by the blue squares, and days with measureable snow are shown by the magenta circles.

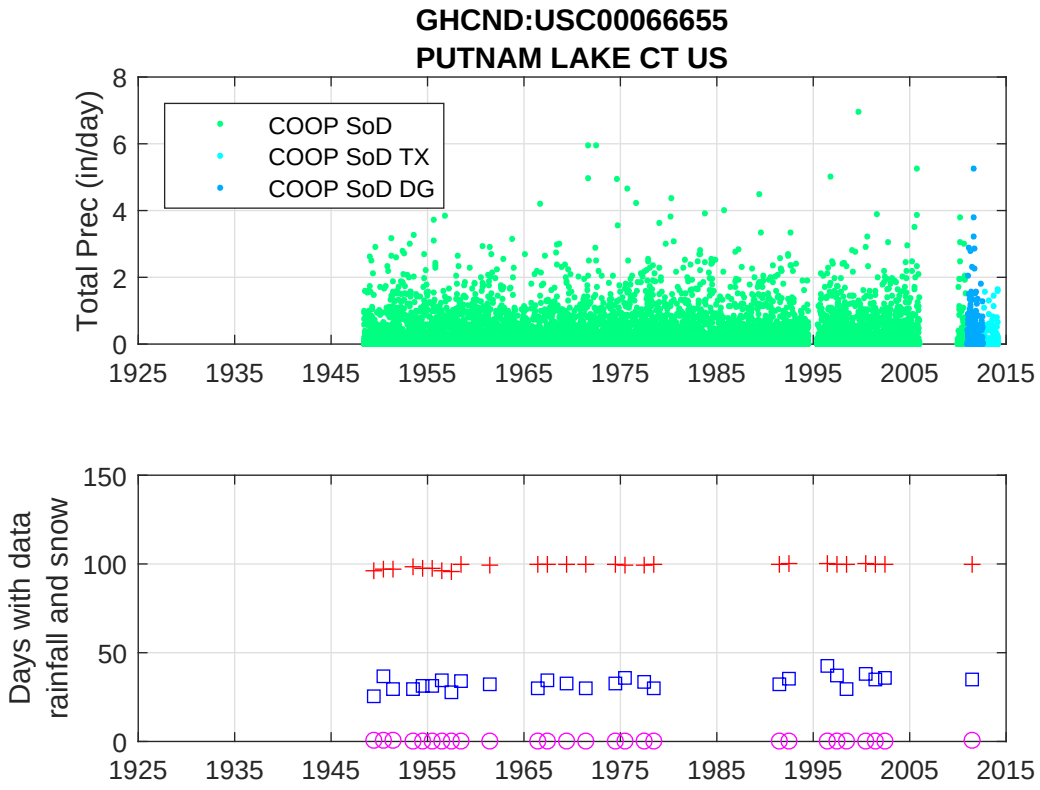

Figure 2A.9. The points in the upper frame show the total daily precipitation data available at the station indicated in the figure. The color indicates the source. The code is explained in Table 2.2. Years when the rainfall data was reported (including zero values) on at least 95% of the days were identified. To show the interval of useful data the red '+' symbols in the lower frame show the fraction (percentage) the year in which rainfall measurements were recorded. The number of days with measureable rain is shown by the blue squares, and days with measureable snow are shown by the magenta circles.

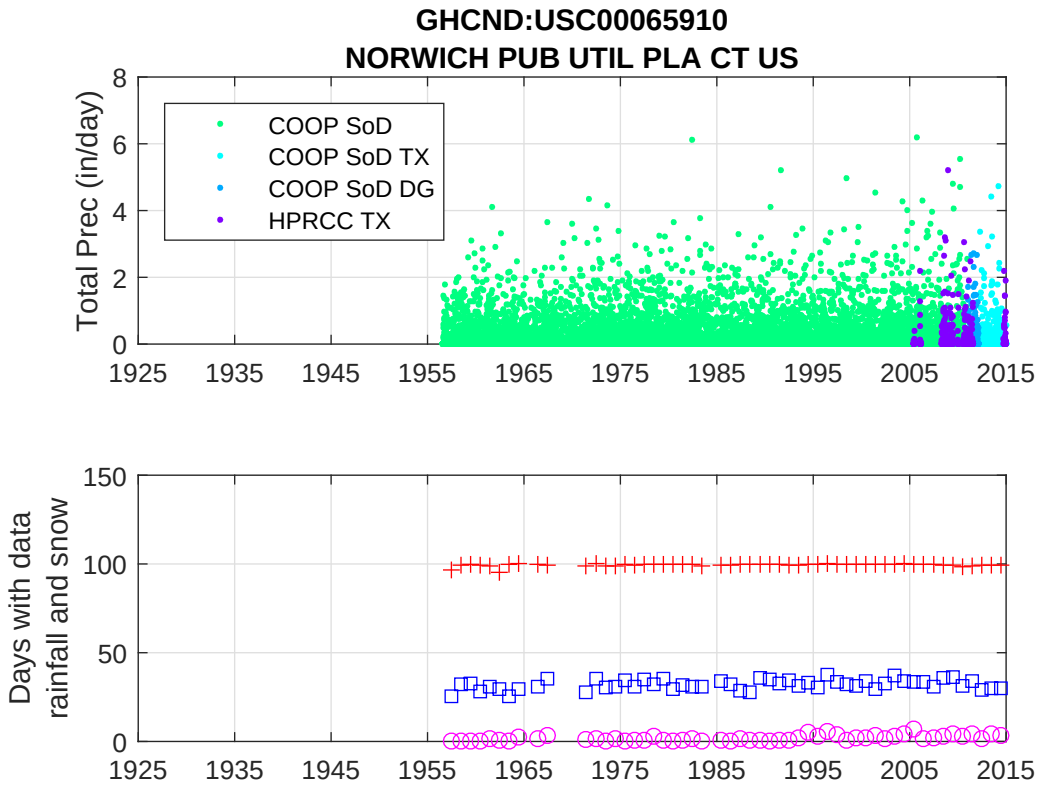

Figure 2A.10. The points in the upper frame show the total daily precipitation data available at the station indicated in the figure. The color indicates the source. The code is explained in Table 2.2. Years when the rainfall data was reported (including zero values) on at least 95% of the days were identified. To show the interval of useful data the red '+' symbols in the lower frame show the fraction (percentage) the year in which rainfall measurements were recorded. The number of days with measureable rain is shown by the blue squares, and days with measureable snow is shown by the magenta circles.

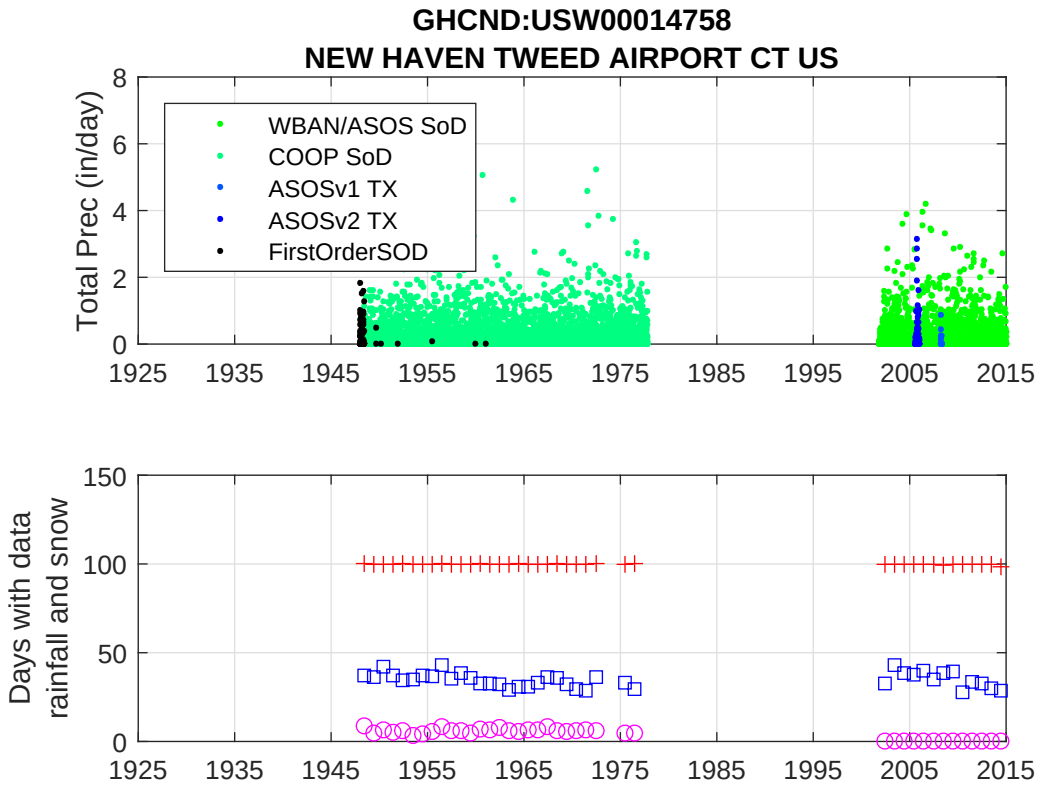

Figure 2A.11. The points in the upper frame show the total daily precipitation data available at the station indicated in the figure. The color indicates the source. The code is explained in Table 2.2. Years when the rainfall data was reported (including zero values) on at least 95% of the days were identified. To show the interval of useful data the red '+' symbols in the lower frame show the fraction (percentage) the year in which rainfall measurements were recorded. The number of days with measureable rain is shown by the blue squares, and days with measureable snow are shown by the magenta circles.

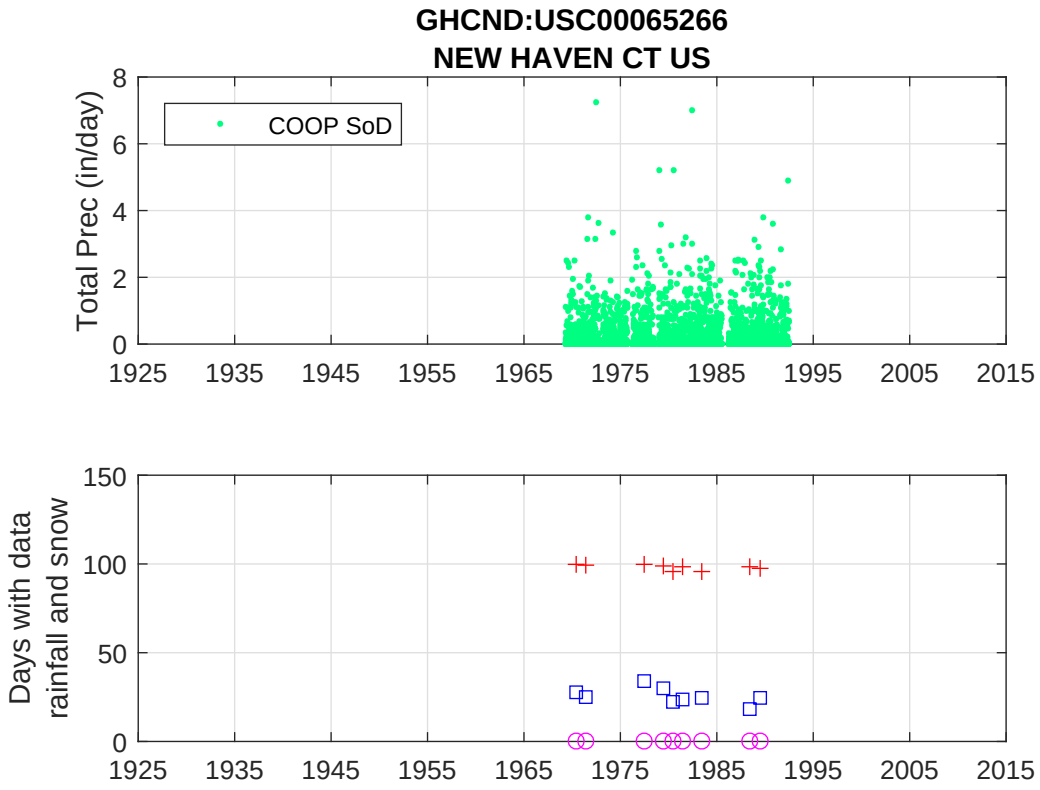

Figure 2A.12. The points in the upper frame show the total daily precipitation data available at the station indicated in the figure. The color indicates the source. The code is explained in Table 2.2. Years when the rainfall data was reported (including zero values) on at least 95% of the days were identified. To show the interval of useful data the red '+' symbols in the lower frame show the fraction (percentage) the year in which rainfall measurements were recorded. The number of days with measureable rain is shown by the blue squares, and days with measureable snow are shown by the magenta circles.

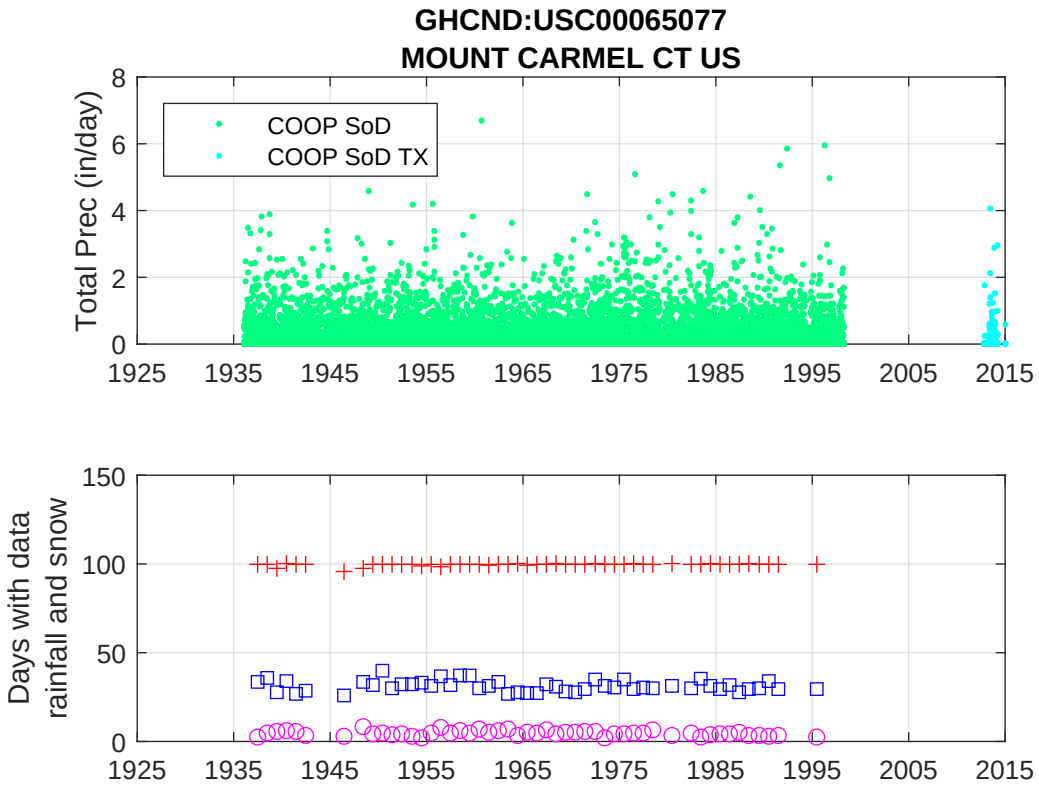

Figure 2A.13. The points in the upper frame show the total daily precipitation data available at the station indicated in the figure. The color indicates the source. The code is explained in Table 2.2. Years when the rainfall data was reported (including zero values) on at least 95% of the days were identified. To show the interval of useful data the red '+' symbols in the lower frame show the fraction (percentage) the year in which rainfall measurements were recorded. The number of days with measureable rain is shown by the blue squares, and days with measureable snow are shown by the magenta circles.

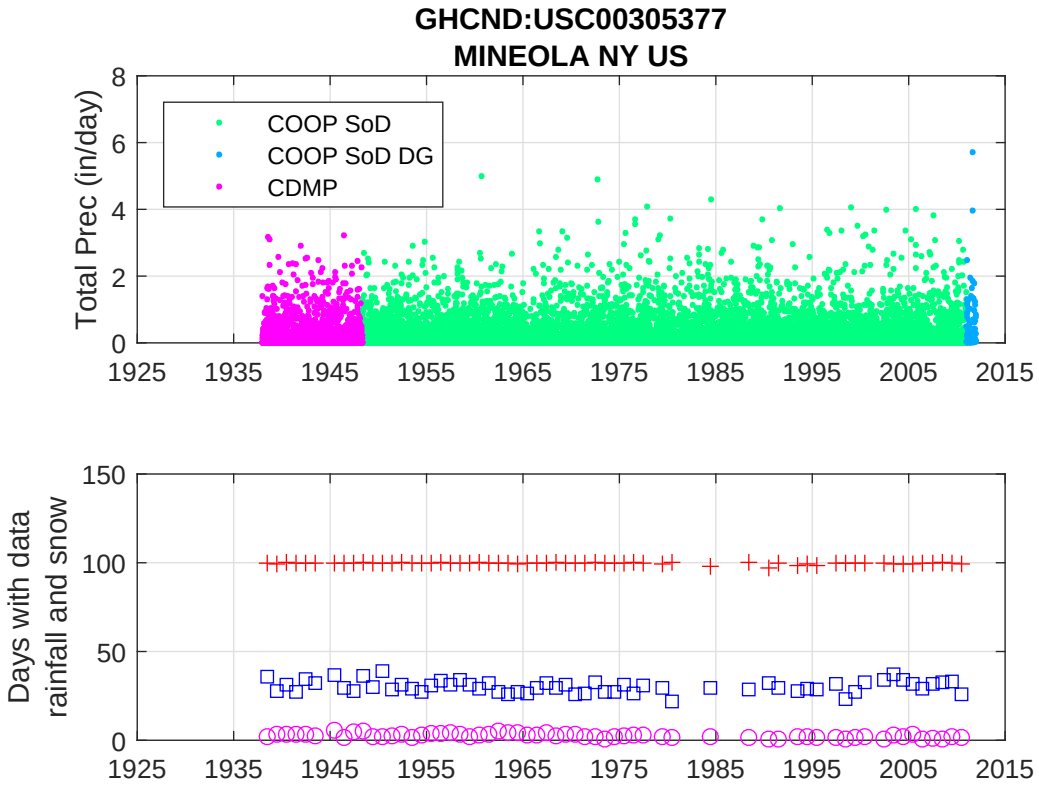

Figure 2A.14. The points in the upper frame show the total daily precipitation data available at the station indicated in the figure. The color indicates the source. The code is explained in Table 2.2. Years when the rainfall data was reported (including zero values) on at least 95% of the days were identified. To show the interval of useful data the red '+' symbols in the lower frame show the fraction (percentage) the year in which rainfall measurements were recorded. The number of days with measureable rain is shown by the blue squares, and days with measureable snow are shown by the magenta circles.

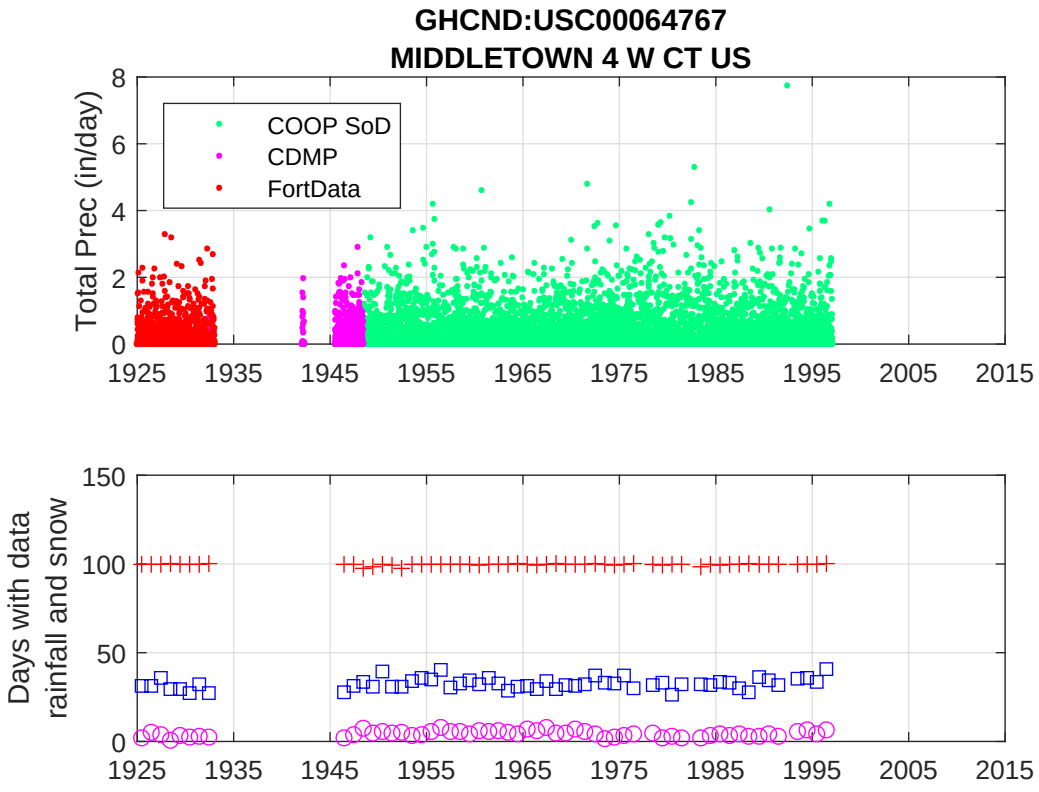

Figure 2A.15. The points in the upper frame show the total daily precipitation data available at the station indicated in the figure. The color indicates the source. The code is explained in Table 2.2. Years when the rainfall data was reported (including zero values) on at least 95% of the days were identified. To show the interval of useful data the red '+' symbols in the lower frame show the fraction (percentage) the year in which rainfall measurements were recorded. The number of days with measureable rain is shown by the blue squares, and days with measureable snow are shown by the magenta circles.

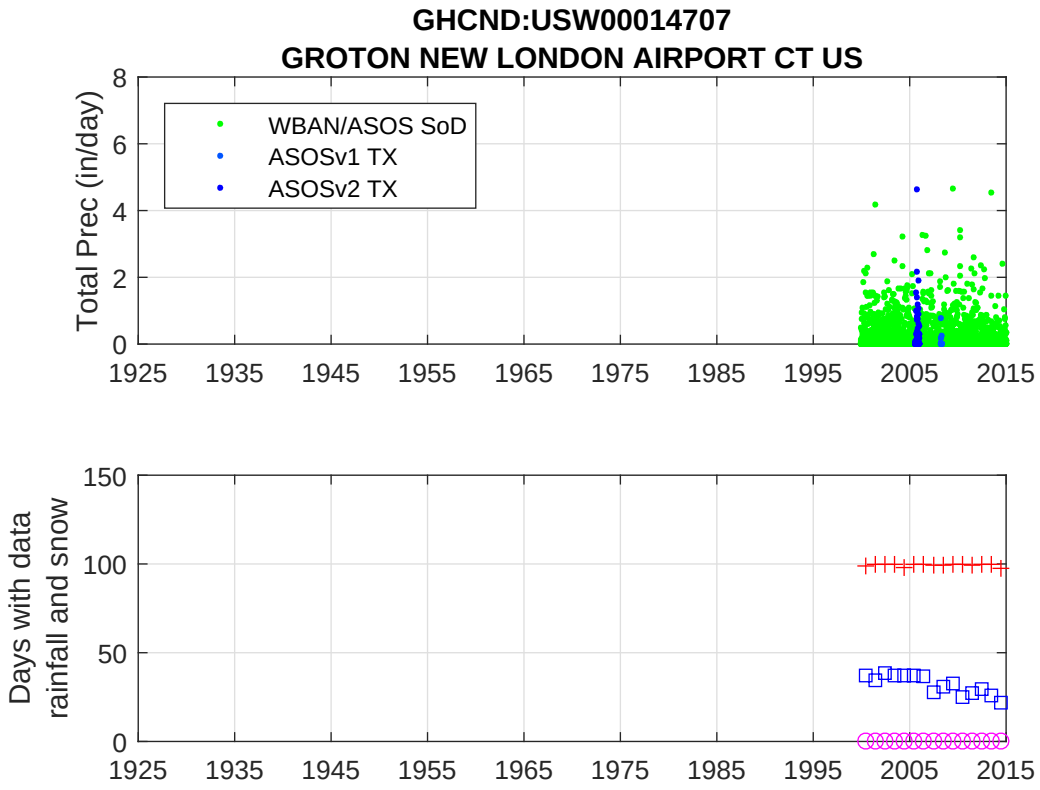

Figure 2A.16. The points in the upper frame show the total daily precipitation data available at the station indicated in the figure. The color indicates the source. The code is explained in Table 2.2. Years when the rainfall data was reported (including zero values) on at least 95% of the days were identified. To show the interval of useful data the red '+' symbols in the lower frame show the fraction (percentage) the year in which rainfall measurements were recorded. The number of days with measureable rain is shown by the blue squares, and days with measureable snow are shown by the magenta circles.

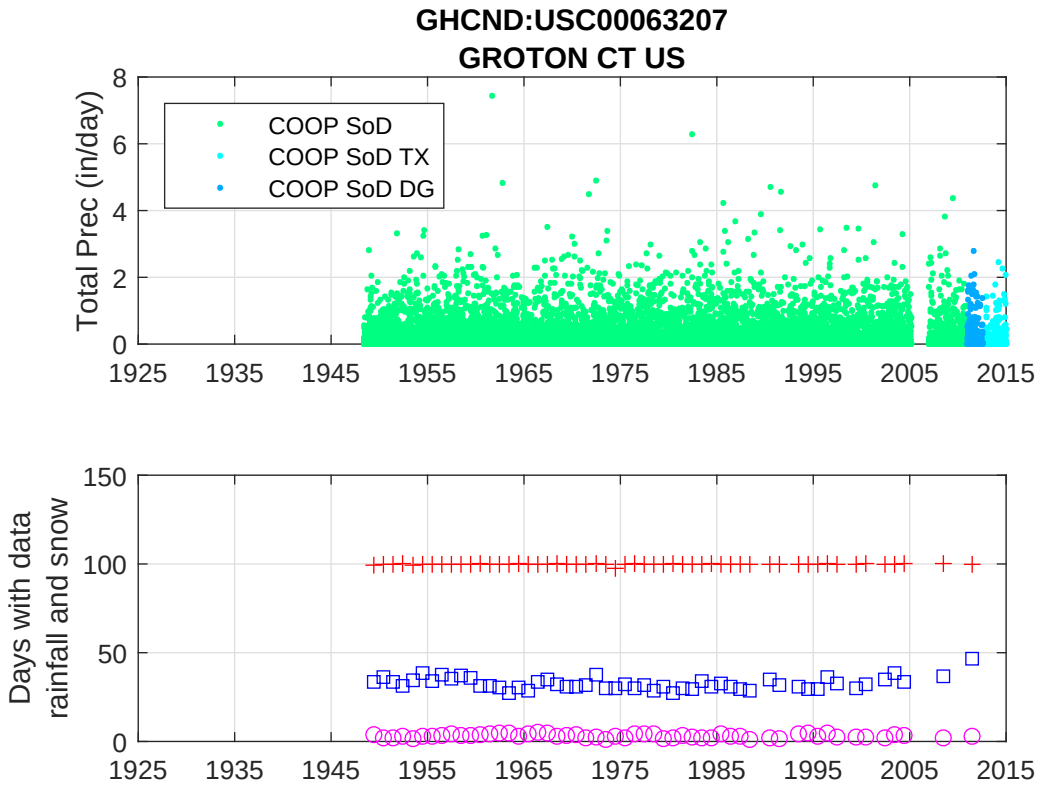

Figure 2A.17. The points in the upper frame show the total daily precipitation data available at the station indicated in the figure. The color indicates the source. The code is explained in Table 2.2. Years when the rainfall data was reported (including zero values) on at least 95% of the days were identified. To show the interval of useful data the red '+' symbols in the lower frame show the fraction (percentage) the year in which rainfall measurements were recorded. The number of days with measureable rain is shown by the blue squares, and days with measureable snow are shown by the magenta circles.

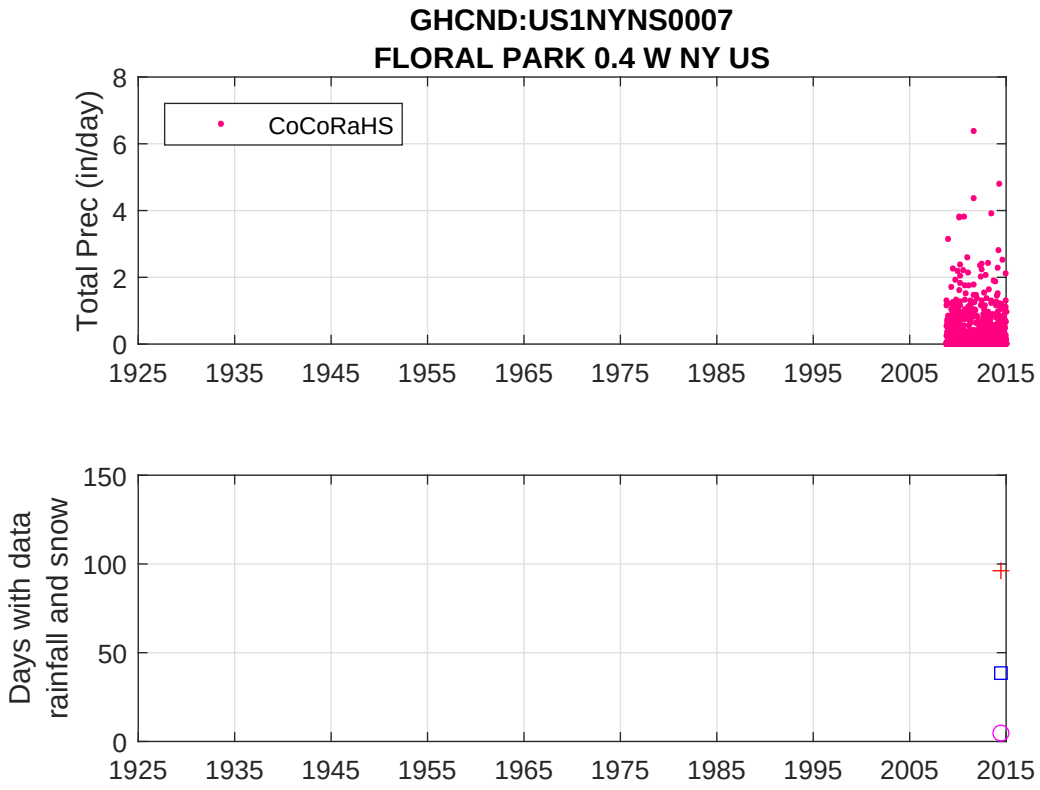

Figure 2A.18. The points in the upper frame show the total daily precipitation data available at the station indicated in the figure. The color indicates the source. The code is explained in Table 2.2. Years when the rainfall data was reported (including zero values) on at least 95% of the days were identified. To show the interval of useful data the red '+' symbols in the lower frame show the fraction (percentage) the year in which rainfall measurements were recorded. The number of days with measureable rain is shown by the blue squares, and days with measureable snow are shown by the magenta circles.

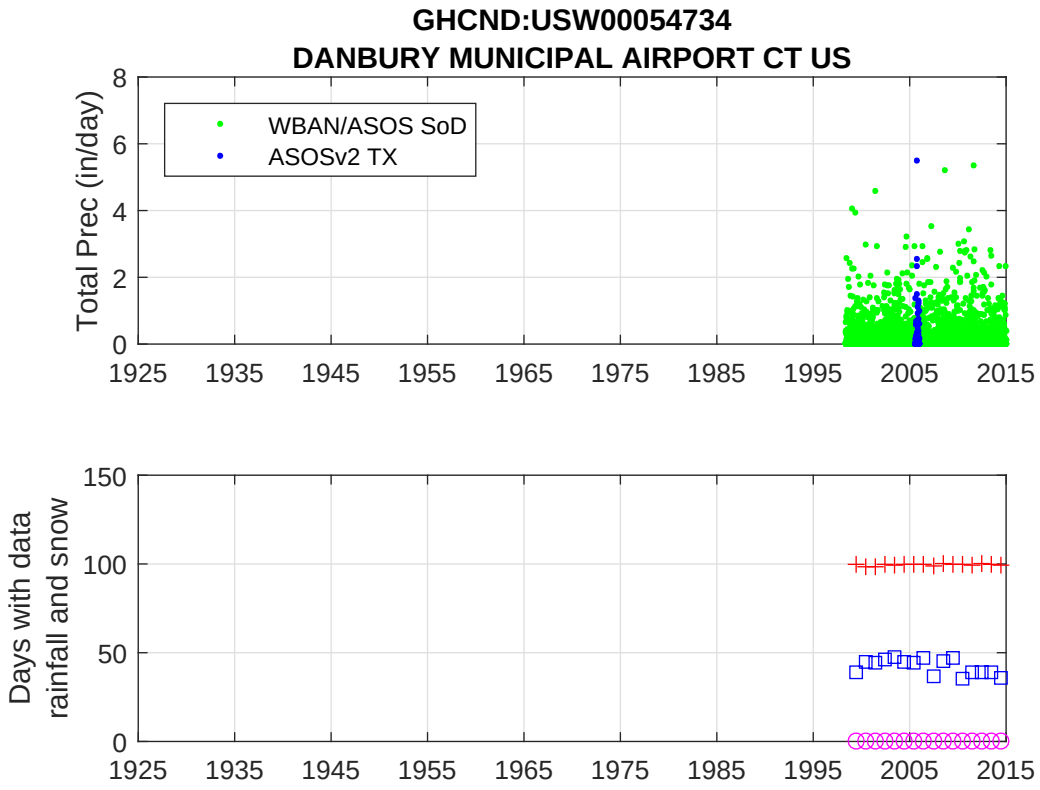

Figure 2A.19. The points in the upper frame show the total daily precipitation data available at the station indicated in the figure. The color indicates the source. The code is explained in Table 2.2. Years when the rainfall data was reported (including zero values) on at least 95% of the days were identified. To show the interval of useful data the red '+' symbols in the lower frame show the fraction (percentage) the year in which rainfall measurements were recorded. The number of days with measureable rain is shown by the blue squares, and days with measureable snow are shown by the magenta circles.

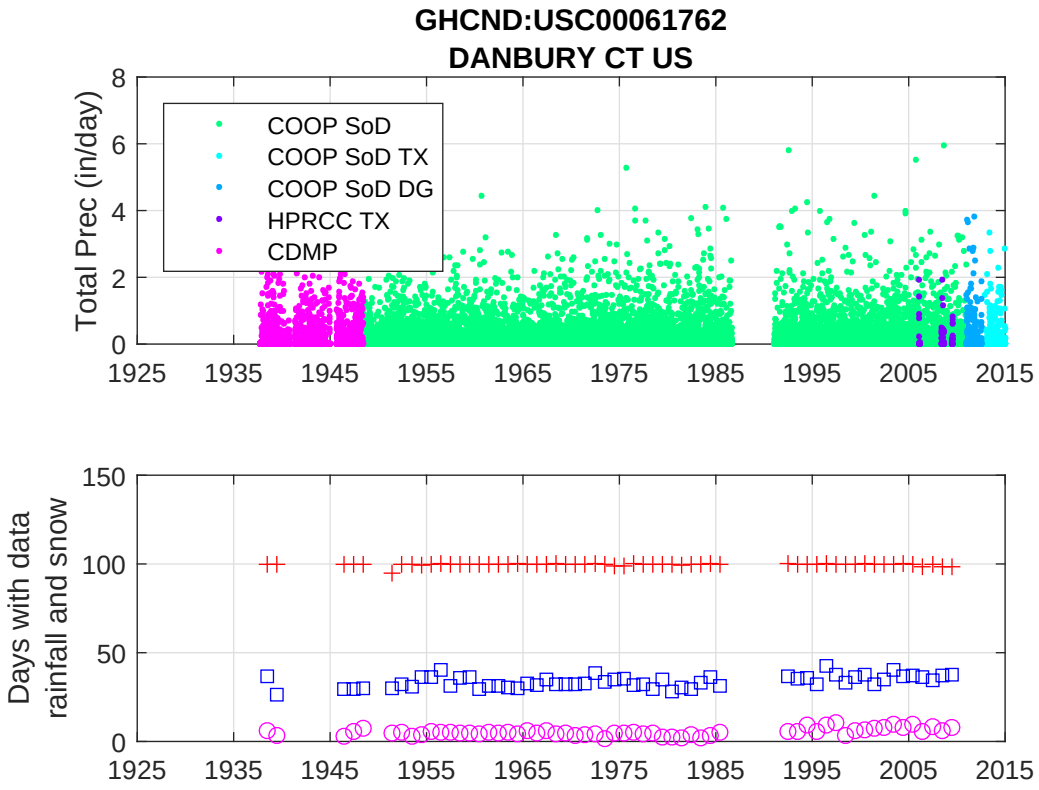

Figure 2A.20. The points in the upper frame show the total daily precipitation data available at the station indicated in the figure. The color indicates the source. The code is explained in Table 2.2. Years when the rainfall data was reported (including zero values) on at least 95% of the days were identified. To show the interval of useful data the red '+' symbols in the lower frame show the fraction (percentage) the year in which rainfall measurements were recorded. The number of days with measureable rain is shown by the blue squares, and days with measureable snow are shown by the magenta circles.

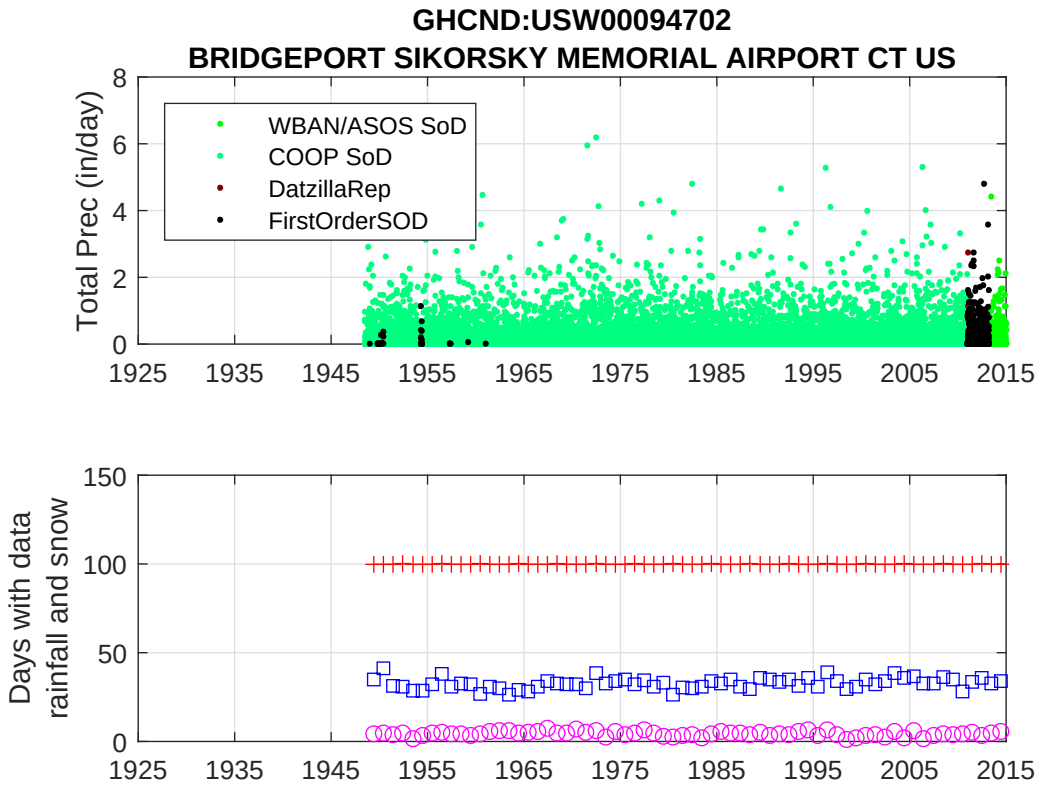

Figure 2A.21. The points in the upper frame show the total daily precipitation data available at the station indicated in the figure. The color indicates the source. The code is explained in Table 2.2. Years when the rainfall data was reported (including zero values) on at least 95% of the days were identified. To show the interval of useful data the red '+' symbols in the lower frame show the fraction (percentage) the year in which rainfall measurements were recorded. The number of days with measureable rain is shown by the blue squares, and days with measureable snow are shown by the magenta circles.

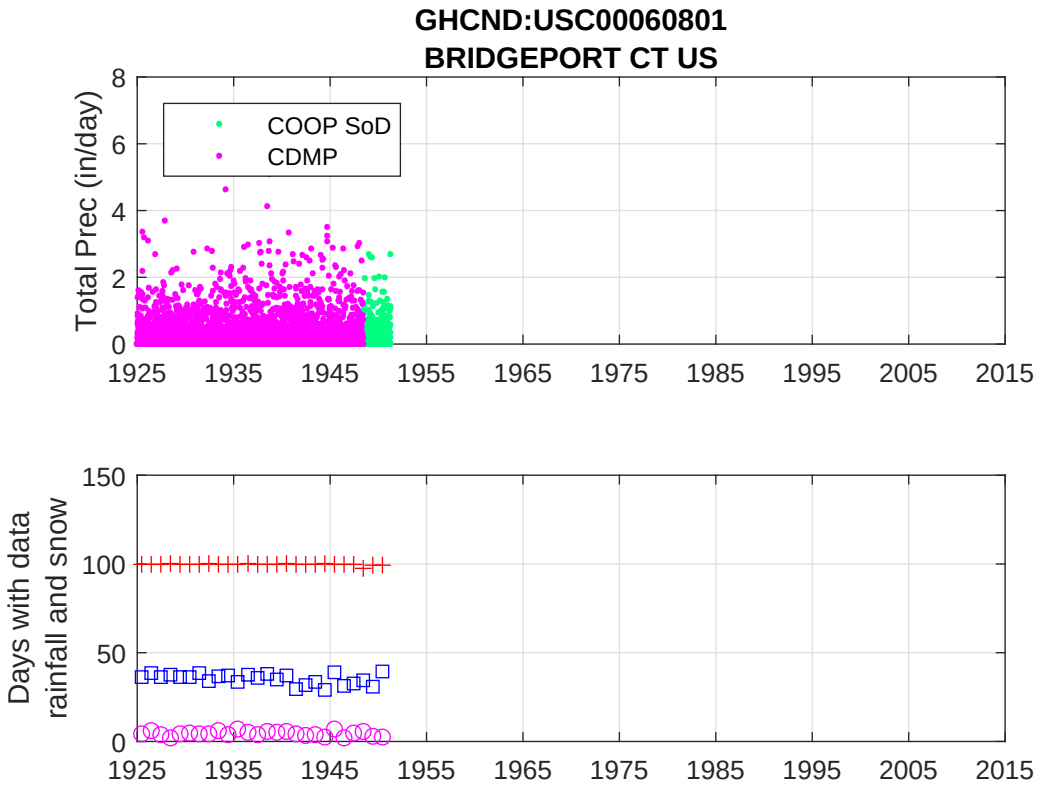

Figure 2A.22. The points in the upper frame show the total daily precipitation data available at the station indicated in the figure. The color indicates the source. The code is explained in Table 2.2. Years when the rainfall data was reported (including zero values) on at least 95% of the days were identified. To show the interval of useful data the red '+' symbols in the lower frame show the fraction (percentage) the year in which rainfall measurements were recorded. The number of days with measureable rain is shown by the blue squares, and days with measureable snow are shown by the magenta circles.

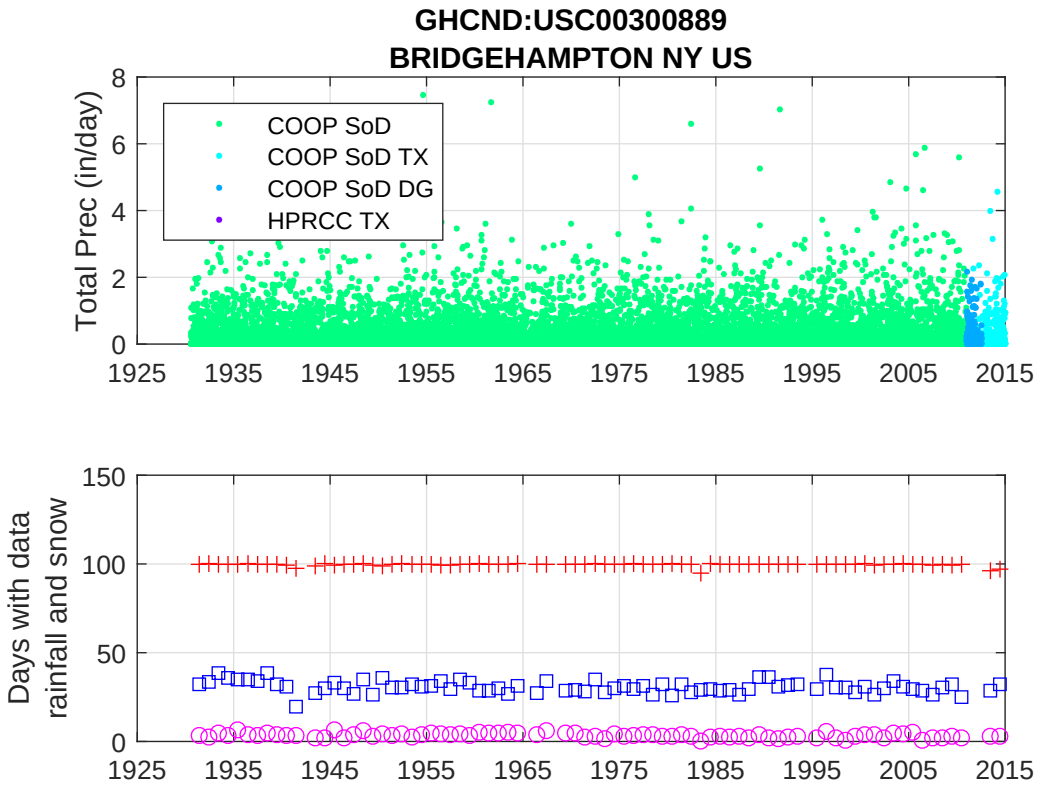

Figure 2A.23. The points in the upper frame show the total daily precipitation data available at the station indicated in the figure. The color indicates the source. The code is explained in Table 2.2. Years when the rainfall data was reported (including zero values) on at least 95% of the days were identified. To show the interval of useful data the red '+' symbols in the lower frame show the fraction (percentage) the year in which rainfall measurements were recorded. The number of days with measureable rain is shown by the blue squares, and days with measureable snow are shown by the magenta circles.

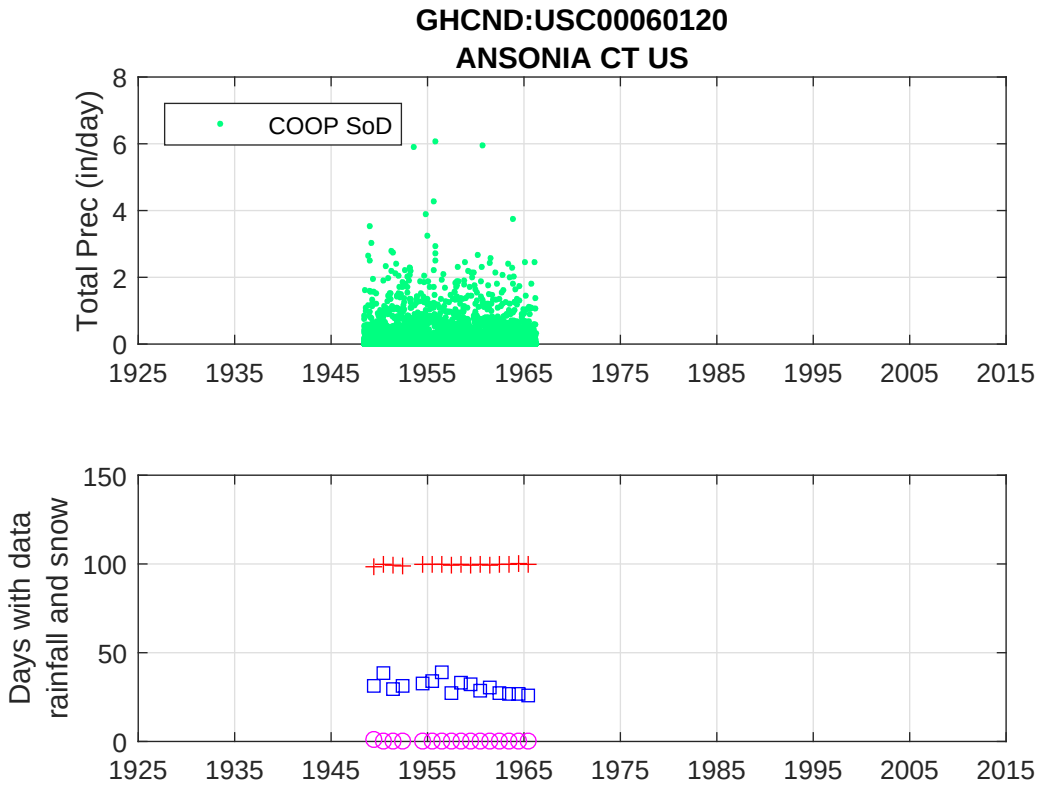

Figure 2A.24. The points in the upper frame show the total daily precipitation data available at the station indicated in the figure. The color indicates the source. The code is explained in Table 2.2. Years when the rainfall data was reported (including zero values) on at least 95% of the days were identified. To show the interval of useful data the red '+' symbols in the lower frame show the fraction (percentage) the year in which rainfall measurements were recorded. The number of days with measureable rain is shown by the blue squares, and days with measureable snow are shown by the magenta circles.

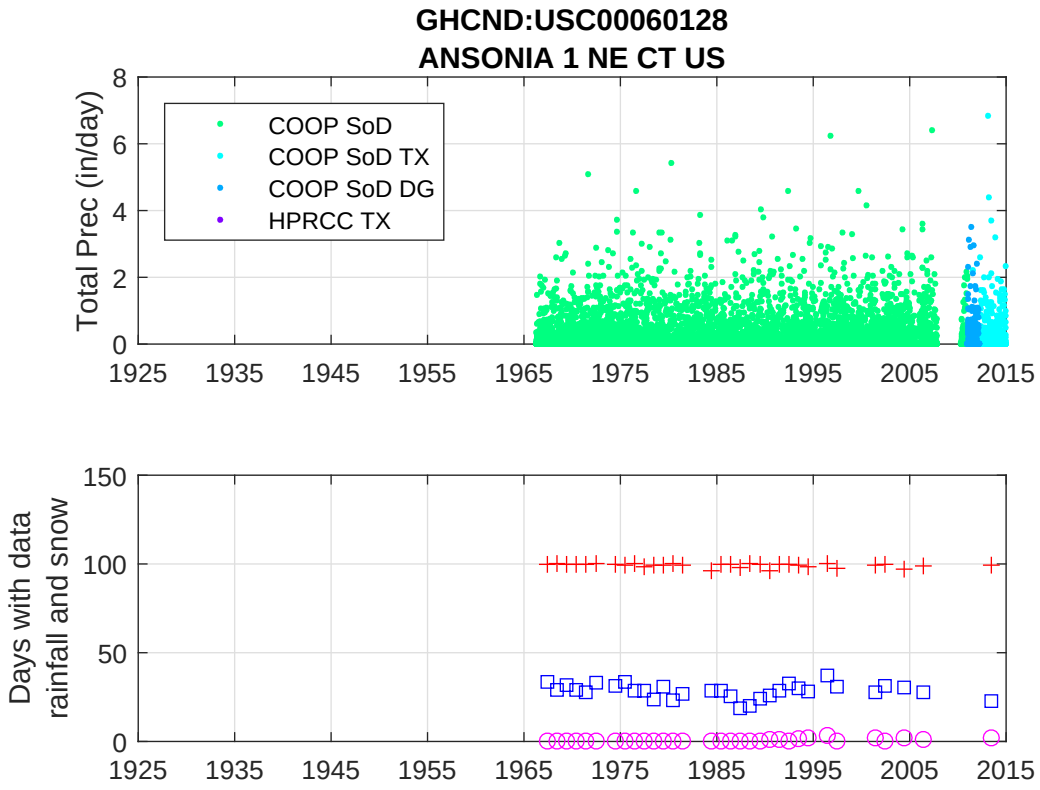

Figure 2A.25. The points in the upper frame show the total daily precipitation data available at the station indicated in the figure. The color indicates the source. The code is explained in Table 2.2. Years when the rainfall data was reported (including zero values) on at least 95% of the days were identified. To show the interval of useful data the red '+' symbols in the lower frame show the fraction (percentage) the year in which rainfall measurements were recorded. The number of days with measureable rain is shown by the blue squares, and days with measureable snow are shown by the magenta circles.

Chapter 3 - Coastal Air Temperature

Table of Contents

List of Figures

List of Tables

3. Ecological Driver: Coastal Air Temperature

3.1 Introduction

The air temperature has a direct effect on many coastal ecosystems. The flora and fauna of marshes and the rates of geochemical processes are all directly influenced. It is well established that the global average temperature has been increasing and is projected to increase more rapidly in the future (Kirtman et al., 2013). However, the mean temperature is not always the most important statistic of the environment in many ecological systems. For example, the time of the year that the temperature is above a threshold is important to insects and their predators, and many species of plants. We showed in Chapter 1 that the summer mean temperature at Bridgeport, Connecticut, has increased at a rate of 0.8 ºC/century; however, we uncovered a much earlier evaluation. The first assessment of the climate change in Connecticut was published in by Loomis and Newton (1866). They carefully examined the temperature measurements that had been recorded by numerous presidents and professors of Yale College in New Haven between 1779 and1865, and developed corrections to account for the time of day of the measurement. They then considered whether the annual, seasonal and monthly mean temperature had changed between the intervals 1779 to 1820, and 1820 to 1865. They also reported an analysis of the variation in the date of the last frost of spring and the first frost of fall. Since the records of direct observations of frost were unreliable, they used the occurrence of temperatures lower than 40 ºF (or 4.4 ºC) as a more convenient metric. They showed that this proxy was a reasonable predictor of frost when observations were available.

Since we now have access to the hourly observations of air temperature in New Haven, a comparison of 30 years of recent observations to those completed over 150 years ago is appropriate. In the next section, we describe the available data and then in section 3.3, we will evaluate the means and compare them to the Loomis and Newton (1866) results.

3.2 Data

The National Oceanic and Atmospheric Administration's (NOAA) National Centers for Environmental Information (NCEI) maintains and distributes meteorological measurements via anonymous file transfer from ftp://ftp.ncdc.noaa.gov/pub/data/noaa/. The site is straightforward to use though the amount of data that can be downloaded at one time is limited. The New Haven, Connecticut, site is referred to as station 725045. Data is available from 1973 to 2015 at hourly intervals. There are several substantial gaps, and several samples were obviously erroneous but had been overlooked by the NCEI data review process. Errors were detected by examining the deviations from a monthly trend. The interval August 4th, 2004 to August 9th, 2004 was eliminated since the temperature estimates fell rapidly to negative values. Another sample on June 29th, 1978 was also negative and was eliminated.

Figure 3.1 shows the air temperature data after removal of erroneous data. The periodic annual cycle is the dominant feature of the record. Summer maxima exceed 30 ºC every year and the winter lows fall to -15 ºC in most years. The data gaps between 1979 and 1985 and again from 2000 to 2003 are substantial; however, these will not be a serious obstacle in the analysis. There are a few shorter gaps in the winter between 1985 and 1992, as well.

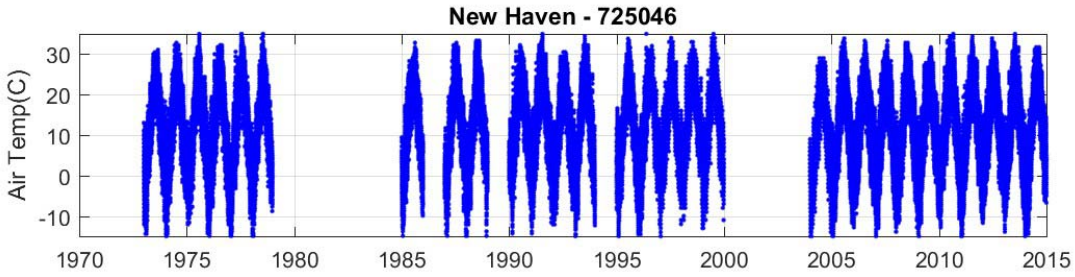

Figure 3.1. Time series of air temperature at Tweed New Haven Airport (725046) from 1973 to 2015.

3.3 Analysis

Loomis and Newton (1866) reported the monthly mean temperatures in New Haven at a variety of locations in the city in the vicinity of the Yale Campus. Some of the locations were not always recorded. The time of the samples were recorded, however, and a sophisticated correction scheme was developed to enable the unbiased estimation of the daily mean average from several samples per day. Table 3.1 shows the monthly means computed by Loomis and Newton (1866) for the period 1779-1820 and 1820-8165, together with the means computed from the data at Tweed-New Haven Airport between 1773 and 2015.

Table 3.1. Mean temperatures by month (col. 1) for the periods 1779-1820 (col. 2), and 1820-8165 (col. 3). The difference is in col. 4. The mean and standard deviation of the means estimated from the hourly data from Tweed-New Haven Airport between 1973 and 2015 are shown in columns 5 and 7. Column 6 shows the difference between the average from 1779-1865 and 1973-2015.

	1779-1820	1820-1865		1973- 2015		
Month	Mean	Mean	Difference	Mean	Difference	StD
1	-3.2	-2.9	0.2	0.0	3.0	5.3
2	-2.2	-2.1	0.0	0.8	3.0	4.8
3	2.1	2.4	0.3	4.7	2.5	4.8
4	8.4	8.1	-0.4	10.2	1.9	4.5
5	14.0	14.1	0.0	15.5	1.5	4.4
6	19.7	19.2	-0.5	20.7	1.2	3.9
7	22.1	22.0	0.0	24.0	2.0	3.5
8	21.6	21.0	-0.5	23.3	2.0	3.5
9	17.1	16.8	-0.4	19.5	2.5	4.3
10	10.7	10.5	-0.2	13.5	2.9	4.7
11	4.5	4.8	0.3	8.2	3.6	4.9
12	-0.8	-1.0	-0.2	3.1	4.0	4.9

As noted by Loomis and Newton (1866), the magnitude of the difference between the means in columns 2 and 3 is small, less than 0.5 ºC, and the signs show no pattern; half the values are positive and half are negative. Based on this evidence, they concluded that any change in

temperature over the 50 year interval between the centers of the two series was not significant. The mean temperature from Tweed-New Haven Airport is noticeably larger than in the earlier intervals. The difference between the 1973-2015 mean and the average of the two earlier estimates is shown in the 6th column of Table 3.1. The values are all positive and range from 1.2 to 4 ºC. The average difference is 2.5 ºC. Note that this consistent with a rate of 1ºC/century.

Figure 3.2 shows the annual cycle of the mean monthly temperature at New Haven. The solid line shows the estimates based on data from 1973-2015, and the red and green lines show the estimates of Loomis and Newton (1866). The dashed lines surrounding the solid black line shows plus and minus the standard error ($\sigma/\sqrt{N}$) where σ is the standard deviation of the means and N is the number of years of data contributing to the estimate of the monthly means. That the modern era is warmer is clear. Note that the warming in the winter is approximately double that in the summer.

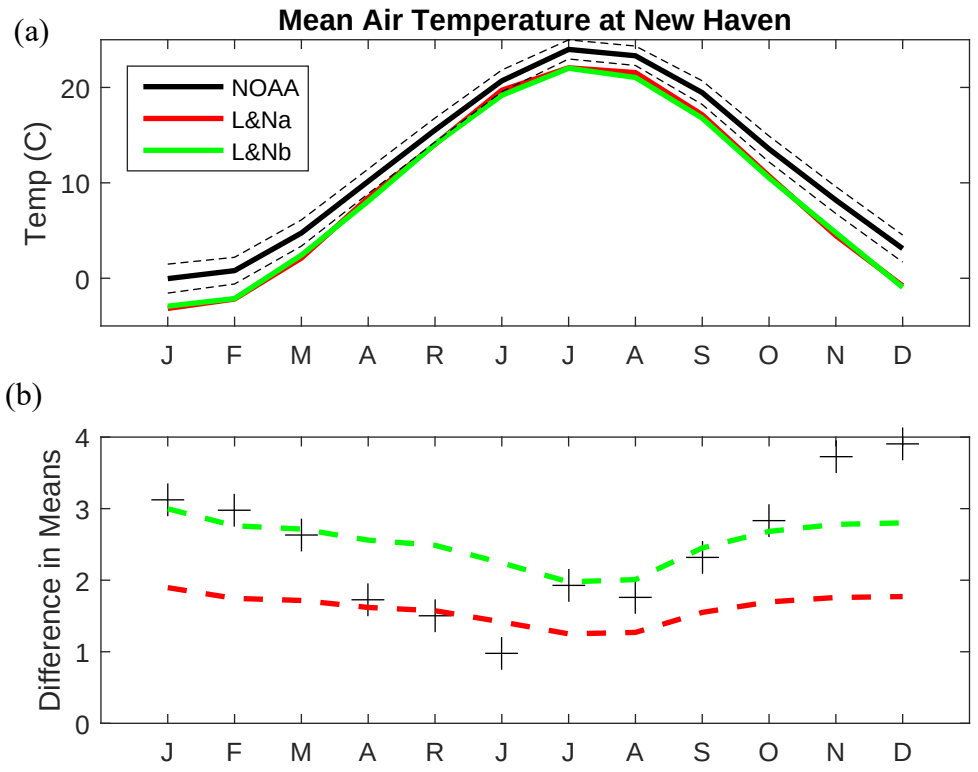

Figure 3.2. (a) shows the annual cycle of air temperature at New Haven, CT. The solid black line shows the monthly mean computed from the data from Tweed-New Haven Airport and the dashed lines above and below it show the standard error of the means. The green and red lines show the estimates from the analysis of Loomis and Newton (1866). They are almost identical. In (b) the difference between the black and the average of the green and red lines is represented by the '+' symbols. The red line shows value the difference would have to exceed to be different from 0 at the 95% confidence level assuming that all the estimates of the mean are independent. The green line shows the level if substantial autocorrelation is assumed.

The conventional test for the significance of the difference in two estimates of a mean is the Students' T test. Assuming that the standard deviation in the early record is the same as in our estimates (Loomis and Newton, 1866, didn't report it), then the difference would have to be greater than $t_{cr}\ \sigma\ \sqrt{(\frac{1}{N_1^2} + \frac{1}{N_2^2})}$ for it to be considered significantly different. Here N_1 and N_2 are the sample sizes of the data contributing to the mean. The red line in Figure 3.2(b) shows the significance threshold using $N_1 = 30$, $N_2 = 86$, and the values of σ listed in column 7 of Table 3.1. The differences in the means for each month are shown in Figure 3.2(b) by the '+' symbols. That they fall below the dashed red line in the spring (April-June) indicates that the differences are not significant. For the rest of the year, the hypothesis that the means are the same is rejected.

The critical assumption that underlies this test is that the $N_{1\&2}$ samples contributing to the estimate of the mean are independent. However, it is well established that there is serial correlation in the inter-annual variations in the atmosphere and ocean variables. An example is provided in Chapter 1 where it is clear that the summer and winter seasonal average temperatures in Long Island Sound exhibit long (3-10 year) period oscillations. To estimate the "equivalent sample size" the number of samples has to be reduced by approximately the ratio of the sample interval to the autocorrelation timescale.

The autocorrelation function can not be estimated conveniently from the data available at New Haven because the record has too many gaps. However, the Berkeley Earth Project (Rohde et al., 2013) synthesized an almost continuous record of monthly mean temperatures at Bridgeport (see Chapter 1). This record must be expected to have the same correlation structure as New Haven since it is close relative to the scale of weather systems. Using this data we computed the correlation function and found that it fell to the level of uncorrelated noise at 2.5-year lag. The green dashed line in Figure 3.2(b) shows an example of the effect of autocorrelation on the significance threshold. It was computed assuming that the autocorrelation duration was 2.5 years. We conclude that only the November-December means are significantly different.

Loomis and Newton (1866) also examined the data they assembled to assess whether there had been appreciable change in the date of the last frost of spring or the first frost of fall. Since the records of the occurrence of frost were unreliable, they instead examined trends in the last day in spring that 40 ºF (4.4 ºC) was recorded and the first day after the start of fall when the temperature fell below the threshold. They averaged the number of the day of the year from 1779-1820 and 1820-1865 and found that day 140.2 (May 19th) was the average last frost in the first series and 140.9 was the average in the later series. The first frost of fall occurred on average in day 266.2 (September 22nd) in the first series and 264.4 in the second series. These dates are represented in Figure 3.3 by the red (last frost) and blue (first frost) lines. The dashed lines show the means from the first range of years.

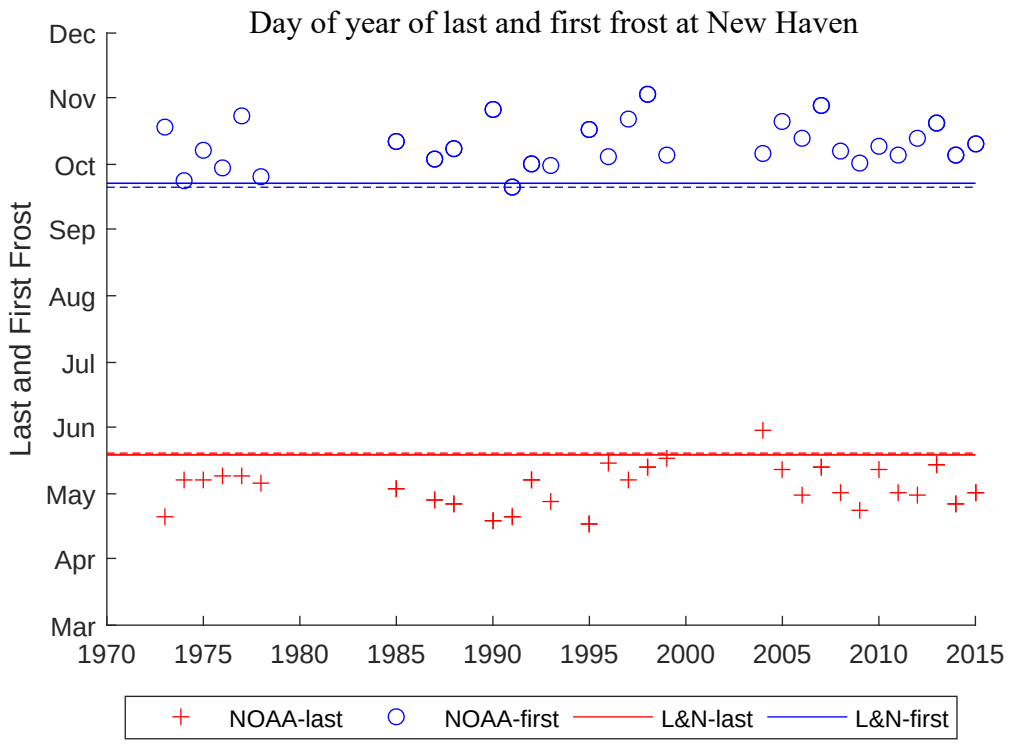

Figure 3.3. The day of the year when the last temperature value below 4.4 ºC (40 ºF) was observed in the data from Tweed-New Haven Airport is shown in by the red '+' symbols. The first day in the fall when the temperature falls below 4.4 ºC is shown by the blue circles. This threshold was chosen to represent condition suitable for frost. The red and blue lines show the mean date of these thresholds were crossed in the data records from 1779-1820 (red and blue solid lines) and 1820-8165 (red and blue dashed lines).

The time series of hourly temperatures from the Tweed-New Haven Airport were examined to assess whether these statistics of the annual temperature variations had changed in the last 200 years. A simple computer program automatically searched for all samples in a year before August that were less than 4.4 ºC and recorded the date and time of the last one. Similarly, all the samples below the threshold after August were sought and the date and time of the earliest recorded. We realized the hourly data might bias the detection allowing brief dips below the threshold to be detected that would not have been possible when five samples per day were being collected and interpolated. To assess the impact, we filtered (smoothed) the hourly data to remove fluctuations that had a four-hour period. This had no noticeable effect on the dates identified.

Figure 3.3 compares our results to those of Loomis and Newton (1866). The blue circles show the date of the first frost of fall (falling below 4.4 ºC) and the red '+' symbols show the last frost of spring (rising above 4.4 ºC). It is evident the last frost of spring is earlier and the first frost of fall is later. Only one sample in 30 was later than May 19th and the only one was earlier than September 20th. The distribution of these variable is not normal; however, for consistency with the earlier work we computed the mean days of the year to be 124.4 (May 3rd) and 285.0 (October 8th). In short, frosts now end16.2 days earlier than 200 years ago and they begin again 19.7 days later. The mean time between these transitions has lengthened by 35.9 days.

3.4 Summary and Discussion

We have presented an analysis of the air temperature fluctuations in a coastal area close to Long Island Sound. The data was extracted from a NOAA data base and then examined for inconsistencies. These were eliminated where possible. We then transcribed old observations from an obscure source that dated back to 1779. These data had been assiduously reviewed by the collators considering the era in which they worked. Comparison of the mean monthly temperature has revealed that there has been a warming of between 2 ºC and 4 ºC in the last 200 years. The larger values apply to the winter months (November-February) and the smaller values to April-August. The larger values are statistically significant.

We also examined the data for evidence of trends in the day of the year that frosts end in the spring, and start again in the fall. Loomis and Newton (1866) had published the mean for the period 1779-1865. We find that the frosts end earlier and begin again later by 16.1 and 19.7 days, effectively lengthening the warmer season by almost 36 days.

There have been global (Kirtman et al., 2013) and regional (Horton et al., 2014) analyses that have detected significant changes in air temperature. However, it is very difficult to detect changes at a single location. The availability of three decades of high quality air temperature data at Tweed-New Haven Airport, and the legacy of careful measurement several times a day by the scholars at Yale in the 18th and 19th century, allows this analysis. That the results are broadly consistent with those of the regional and global analyses add confidence that the missing metadata is not an overwhelming problem.

One consequence of this warming is the substantial decrease in the fraction of the year that frost is likely. At the end of the 17th century the frost-free duration was 125 days. Now it is 161 days, an increase of 29%. Gaps between other temperature thresholds have experienced similar increases. Examination of the seasonal temperature cycle in Figure 3.2(a) shows that the transitions form February to June and September to December are almost linear. The effects of warming on the length of an interval above any temperature between 5 and 20 ºC can be easily estimated.

It is also interesting and significant to note that warming appears to be larger in the winter. This is likely due to the radiative equilibrium that occurs in the summer when the loss of heat at night is large. Monitoring in the winter is more likely therefore to yield a detectable effect earlier.

The ecological consequence of the lengthening of the summer have not been very extensively investigated. It appears likely that plant and insects will benefit substantially. For short lived organisms, a few weeks or a month may be enough time to increase the number of generation cycles per year. The long period (decadal) variations in temperature that overlie the long term trend we focus on here may only a have an amplitude of a few degrees, but since we find that a 2-4 ºC warming increases the duration between frosts by 29%, it appears likely that the effects of these decadal-scale variations can be similarly amplified. This effect deserves further attention from ecologists.

3.5 References

Horton, R., G. Yohe, W. Easterling, R. Kates, M. Ruth, E. Sussman, A. Whelchel, D. Wolfe, and F. Lipschultz (2014). Ch. 16: Northeast. Climate Change Impacts in the United States: The Third National Climate Assessment, J.M. Melillo, Terese (T.C.) Richmond, and G.W. Yohe, Eds., U.S. Global Change Research Program, 16-1-nn.

Kirtman, B., S.B. Power, J.A. Adedoyin, G.J. Boer, R. Bojariu, I. Camilloni, F.J. Doblas-Reyes, A.M. Fiore, M. Kimoto, G.A. Meehl, M. Prather, A. Sarr, C. Schär, R. Sutton, G.J. van Oldenborgh, G. Vecchi and H.J. Wang (2013). Near-term Climate Change: Projections and Predictability. In: Climate Change 2013: The Physical Science Basis. Contribution of Working Group I to the Fifth Assessment Report of the Intergovernmental Panel on Climate Change [Stocker, T.F., D. Qin, G.-K. Plattner, M. Tignor, S.K. Allen, J. Boschung, A. Nauels, Y. Xia, V. Bex and P.M. Midgley (eds.)]. Cambridge University Press, Cambridge, United Kingdom and New York, NY, USA.

Loomis, E. and H.A. Newton (1866). On the mean temperature and on the fluctuations of temperature at New Haven, Connecticut, 41º 18'N, 72º 55'W of Greenwich. Connecticut Academy of Arts and Sciences, Volume 1 Article 5 p 194-246.

Chapter 4 – River Discharge

Table of Contents

List of Figures

4. Ecological Driver: River Discharge

4.1 Introduction

The salinity of the Sound is largely determined by the discharge of the Connecticut (O'Donnell et al., 2014). The salinity is extremely important to the Sound ecosystem because the distribution is not uniform and the density gradients that arise drive both very significant horizontal circulation and contribute to the inhibition of vertical mixing. The Hudson River also has an effect since the salinity at the western end of the East River is determined by the flow rate in the Hudson. The net freshwater flux is thought to be small, in an annual average sense, relative to the Connecticut River, but at the western end of the Sound where seasonal hypoxia is common (see O'Donnell et al., 2014), it has an important influence on both the vertical stratification and the non-tidal current structure. The archive of direct salinity measurements in the Sound is very limited; however, long records of flow rate have been acquired and understanding their trends is likely to provide insight into their impact on the ecosystems.

Gay et al. (2004) quantitatively summarized the long-term average discharge of the seven major rivers entering the Sound. They showed that Connecticut River is the dominant source of fresh water and contributes 75% of the total gauged discharge. In winter, precipitation in the form of snow collects in the hills and mountains of the New England states. Much of this area is in the watershed of the Connecticut River. As a result, the Connecticut River usually experiences its smallest river flows in January-March. As temperatures rise in the spring, precipitation turns to rain and the snow and ice melt. This leads to higher runoff. The periods of high flow is termed the spring freshet. Figure 4.1 shows the average seasonal cycle in the discharge measured at the U. S. Geological Survey's gaging station at Thompsonville, CT (from O'Donnell et al., 2014). On average, the peak flow occurs in April. However, the variability in the time of the peak flow is substantial and this leads to the large standard deviations shown in Figure 4.1 and a broad peak in the monthly average discharge that spans March-May. The average annual discharge is approximately 500 m^3/s and this is represented in Figure 4.1 by the horizontal line. Clearly, during nine months of the year the monthly mean flow is below the annual average.

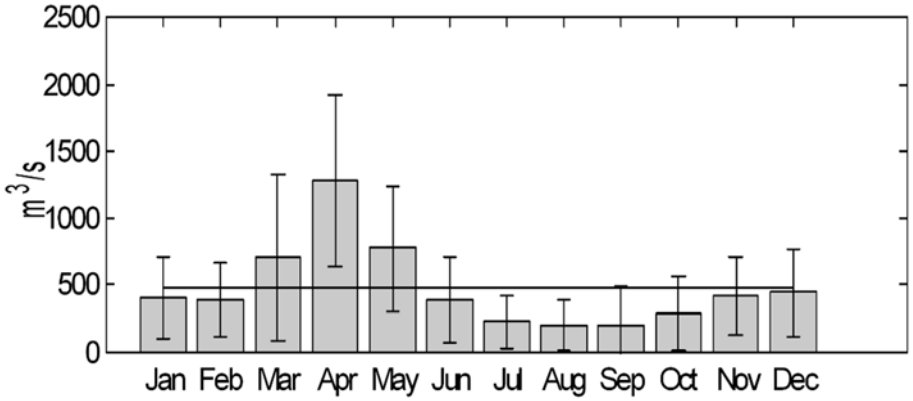

Figure 4.1. Mean and standard deviation of the mean monthly discharge in the Connecticut River measured at Thompsonville, CT. The horizontal line shows the long-term mean.

There is substantial inter-annual variation in the discharge of the river that is driven by regional scale meteorological variability, and Whitney (2010) has shown that the Connecticut and several other rivers of the eastern United States correlate with the North Atlantic Oscillation (NAO) index (Hurrell, 1995). Using the same record, O'Donnell et al. (2010) showed that the day of the year by which 50% of the annual discharge has passed the gauge, the "center of volume flow," has become earlier at a rate of 9 ± 2 days/century. That the fresh water stored in the winter ice and snow pack arrives at the ocean through the Connecticut River earlier than in the past is consistent with the analysis of unregulated New England rivers and streams reported by Hodgkins et al. (2003) and is, therefore, likely to be a consequence of regional meteorological fluctuations rather than changes in watershed management.

Changes in the magnitude and timing of the freshet and the mean annual discharge will have significant implications for patterns of circulation and sedimentation in the Sound, and may also have implications for some aquatic and marsh species along the shore. Flooded fields and marshes during the freshet provide critical feeding habitat areas for migratory waterfowl and fish. The freshet also carries a large fraction of the annual sediment load to the Sound and the timing and magnitude may have long term impacts.

In this analysis, we examine the variability and trends in the flow of the Hudson and the Connecticut Rivers, update the analysis of the center of volume flow, and explore the links to both North Atlantic Oscillation and the Atlantic Multi-decadal Oscillation.

4.2 Data

The primary source of data on river discharge rates in the United States is the U. S. Geological Survey (USGS). The measurements are obtained in a variety of ways but generally flow rates are estimated from water level (stage) measurements that are converted to flow using empirical formulae. The daily mean discharge data is distributed via the National Water Information System (NWIS, http://nwis. waterdata. usgs. gov/nwis). Data can be conveniently downloaded from this site though a web interface. However, downloads are limited to 120 days and acquiring large data sets this way is tedious. Automated procedures using a scripting language and the *wget* (https://www. gnu. org/software/wget/) utility greatly facilitates the process.

The data we use are from the lowest gaging station on the Connecticut River, Thompsonville (USGS ID 01184000) and on the Hudson at Green Island (01358000). The data series are shown in Figure 4.2. The data quality is excellent and no additional screening was necessary. The main substantial data gap was in the Hudson record from February to May, 1998, though some shorter gaps occurred between December 1999 and June 2000.

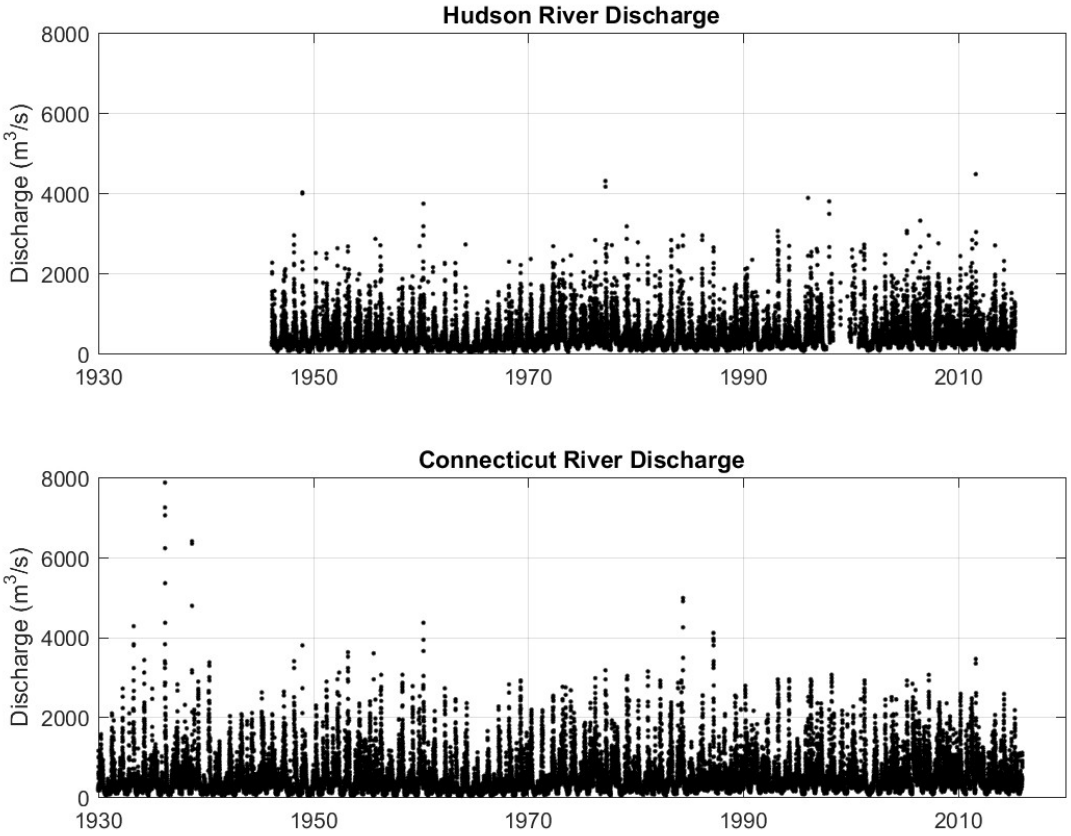

Figure 4.2. The measured daily discharge in the Hudson River at Green Island (01358000) and the Connecticut River at Thompsonville (01184000).

The general character of the two series is very similar, both in the range of values and the dominance of the fluctuations at the annual period. The main difference is that the Connecticut River record is longer and captures the effects of the Hurricane of 1938 when the largest discharge on record was established.

4.3 Analysis

Figure 4.3 shows the long term average flow computed using five-day time bins for the whole record. The long term mean for the Hudson is 410 m^3/s and the Connecticut is approximately 20% larger at 488 m^3/s. The mean peak discharges are in April with the Connecticut River's again being larger by approximately 20%. For both rivers, the annual cycle can be separated into three components. In March-May, the flow is above the long-term annual average. From June until October, the average monthly flow is below average, and then in the winter months, November-February, the flow is close to the average level.

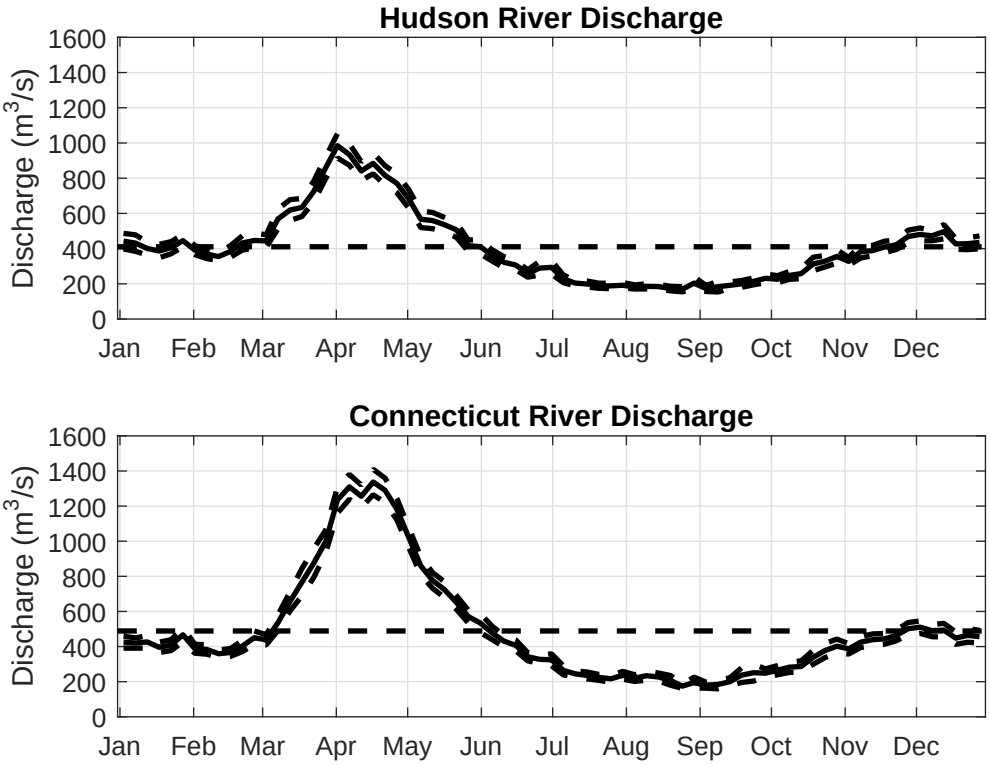

Figure 4.3. The long-term average discharge in the Hudson River at Green Island (01358000) and the Connecticut River at Thompsonville (01184000). Averages were computed in five day intervals. The two standard deviations error interval of the means are shown by the dashed lines. It was computed as $\sigma/\sqrt{N}$ where σ and N are the standard deviation and number of five day means contributing to the estimate.

The long term trend in the annual averages discharges in the two rivers is shown in Figure 4.4. The red and black '+' symbols show the Connecticut River and the Hudson River values, respectfully. There is a clear rising trend in both series which is overlaid by year to year and decadal scale period oscillations. The trends were estimated using linear regression to be 135 m^3/s per century in the Connecticut (see the red dashed line) and 222 m^3/s per century in the Hudson (green dashed line). These were significantly different from zero

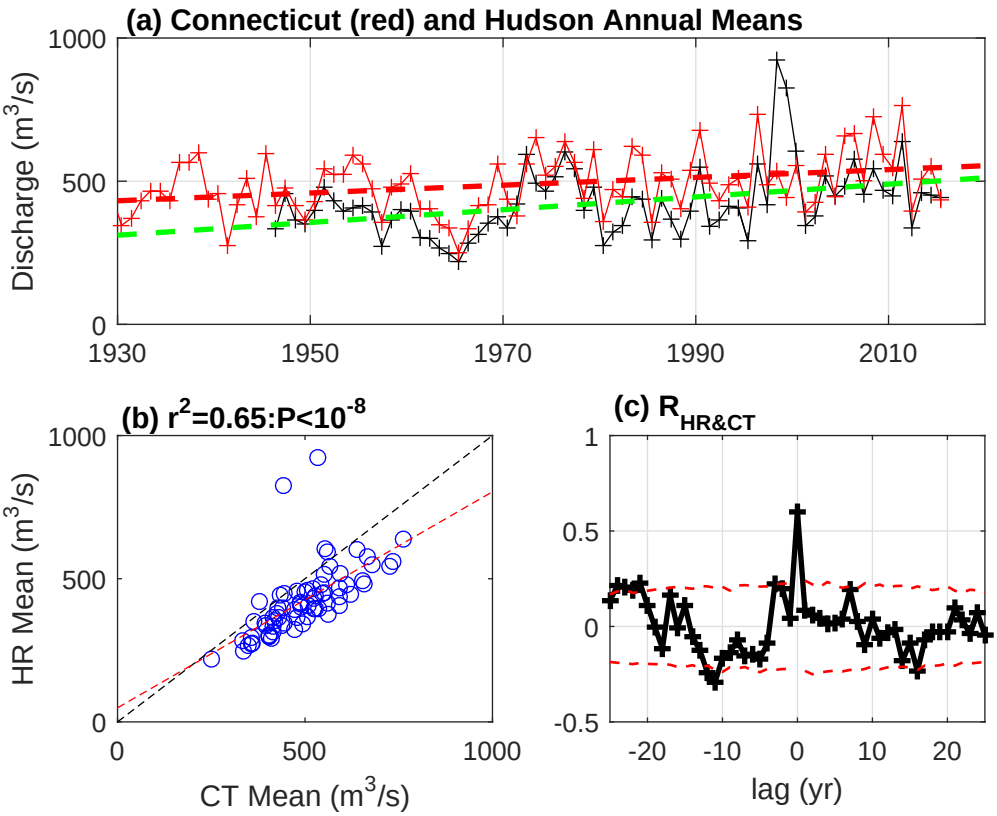

Figure 4.4. (a) The evolution of the annual average discharge in the Connecticut River (red '+') and the Hudson River (black '+') computed form the data in Figure 4.2. The red and green dashed lines show the linear regression-based estimate of the trend. (b) The correlation between the two annual discharge series. The black line shows the trend expected if they were equal and the red line shows the best-fit regression which is significant at the 99% level. The correlation coefficient is 0. 65. In (c) we show the lagged autocorrelation of the discharge series with the confidence interval in red.

Both the annual and longer time scale fluctuations about the trends in Figure 4.4(a) are highly correlated. Figure 4.4(b) displays the pattern. The correlation coefficient is 0. 65 and the slope is less than unity, implying that the variations in the Hudson have a slightly larger amplitude than in the Connecticut. This is consistent with the ratio of the watershed areas.

Figure 4.4(c) shows the lagged autocorrelation in the two series in black. At zero lag, the correlation is 0. 65 as in Figure 4.4(b). The red dashed lines show the interval in which the correlation is not significantly different from zero at the 95% level. This was computed using the bootstrap method (Willmott et al., 1985) since the data distribution is not normal. The negative correlations at approximately +/- 10 years are different from zero and indicate that the river discharge oscillations at 20 years period are correlated.

The long period variations in the annual average river discharge appear to be associated with regional variations in weather. In the northeast, US weather patterns are strongly influenced by the location of the center of the Icelandic Low and Azores High (Hurrell, 1995) and the difference in sea level pressure between them. The NAO index was originally defined as a normalized sea level difference between Lisbon, Portugal, and Stykkisholmur, Iceland. It is proportional to the magnitude of the westerlies in the northwest Atlantic and this index has been

demonstrated to correlate with weather patterns in southern New England. The Hurrell et al. (2009) estimate of the NAO index uses surface pressure maps that take movements of the central pressure into account rather than the data at fixed stations. Bradbury et al. (2002) demonstrated that there were significant decadal-scale period oscillations in the discharge of streams throughout New England. However, they did not investigate the Thompsonville or Green Island records which are the lowest gauges in the two large watersheds. They also found correlation between the fluctuations in discharge in small stream and the winter NAO index. In Figure 4.5 we show by the red 'x' symbols the time series of the deviation of the annual average discharge in the Connecticut from the trend line in Figure 4.4, normalized by the standard deviation of the record. The solid red line is a smoothed version of the anomaly series (computed with a five-year running mean) to clarify the variation. Figure 4.5 also shows a smoothed version of the Hurrell et al. (2009) NAO index. Both series show substantial oscillations and both show a significant minimum in 1965 that attracts attention. However, calculation of the lagged cross correlation shows no significant correlation in the sequences.

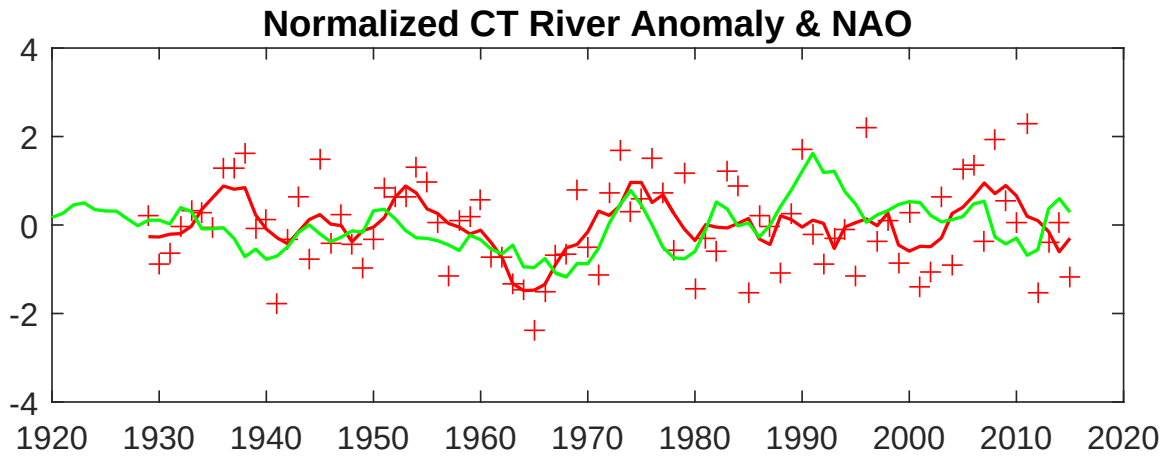

Figure 4.5. The red '+' symbols show the residuals from the regression of the annual mean discharge estimates at Thompsonville and the red line shows the effect of a running average of length five years on the variability. The green line show the smoothed NAO estimate of Hurrell et al. (2009). The correlation between these records is not significant.

The analysis by Hodgkins et al. (2003) suggested that there has been a change in the timing of the delivery of freshwater to the ocean as measured by the winter-spring center of volume (WSCV). This statistic is simply the day of the year when the time integrated stream flow from January 1st exceeds a half of the flux integrated from January 1st to May 31st. Hodgkins et al. (2003) found that the WSCV was advanced by 1-2 weeks in the 11 rivers that were dominated by snowmelt. O'Donnell et al. (2010) followed this and found that even though the watershed of the Connecticut River is dammed at more than 2000 locations, the WSCV exhibited a similar trend.

Figure 4.6(a) shows the total volume passing the Thompsonville gauge before June 1st each year by the blue '+' symbols and a smoothed version of the series using a five-year running average with the red line. The black line shows the results of a linear regression. The mean is 9.3 km^3 and almost no trend is detectable. Figure 4.6(b) shows the winter-spring center of volume flow, the smoothed series, and the regression line using the same symbols and colors. Though there is an

upward trend in the annual discharge in the Connecticut River (see Figure 4.4a), it is evidently not a consequence of the spring discharge since the 85 year record has a slope of 0. 02 × 10^{10} m^3/century. The WSCV has been decreasing at eight days/century as shown by O'Donnell et al. (2010). The same statistics for the discharge in the Hudson River are shown in Figure 4.7. As in the Connecticut, the spring flow has not changed, but the WSCV has reduced but at the slower rate of four days/century.

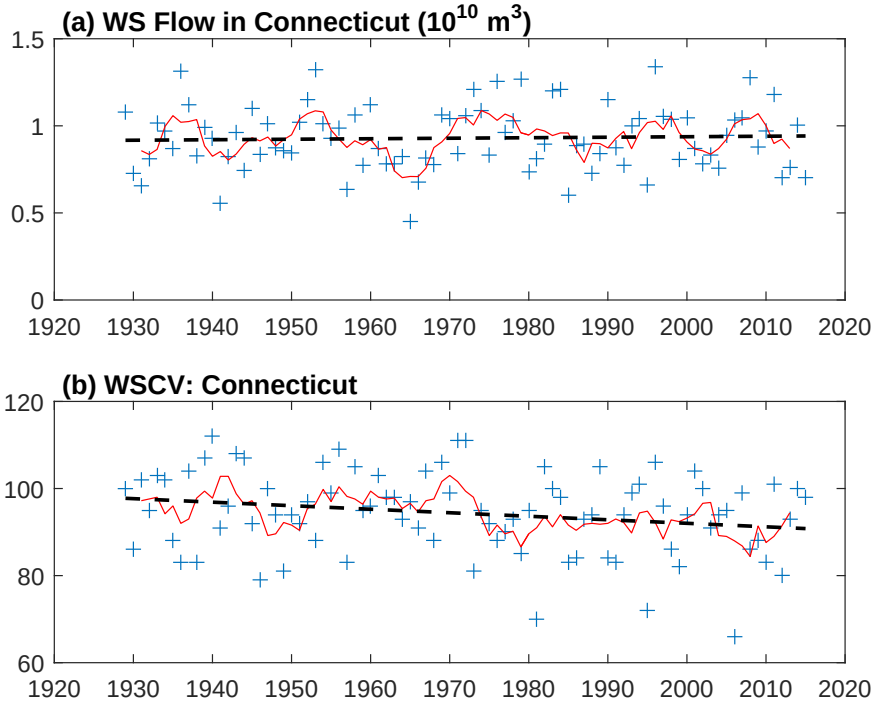

Figure 4.6. (a) The total volume passing the Thompsonville gauge before June 1st each year by the blue '+' symbols and the red line shows a smoothed version of the series using a five-year running average. The black dashed line shows the results of a linear regression. (b) The winter-spring center of volume flow, the smoothed series and the regression trend line.

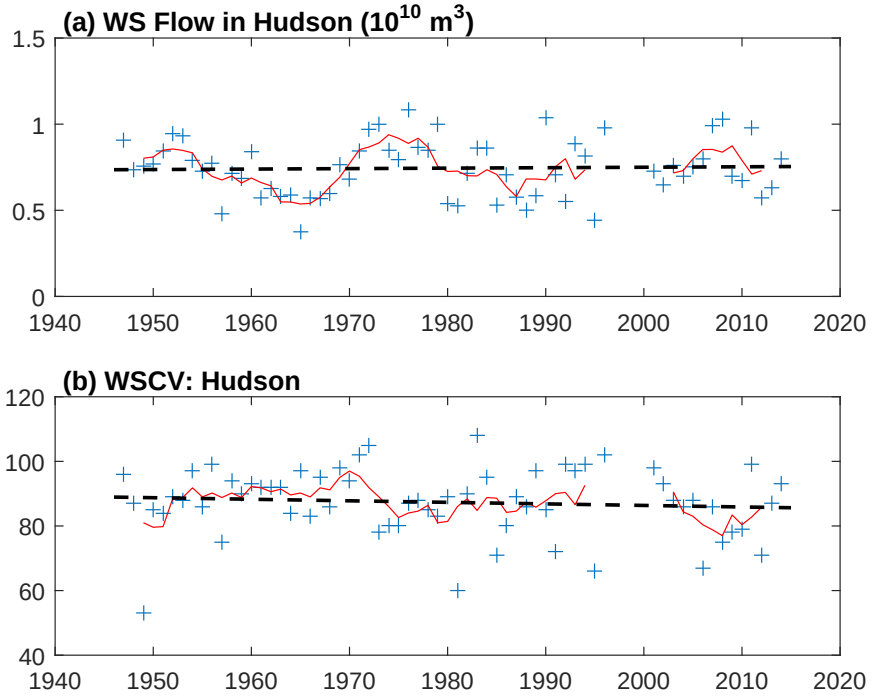

Figure 4.7. (a) shows the same statistics as Figure 4.6(a) but for the Hudson River at Green Island. (b) See Figure 4.6(b).

Since the annual flows are significantly increasing, but the spring flows are not, then obviously the increase in runoff is occurring during the summer and winter discharge. Figure 4.8(a) and

Figure 4.9(a) show that the total amount of water passing the gages after June 1st is, as anticipated, increasing. The rates, estimated by the regression lines shown in the figures are almost identical at 0. 4 × 10^{10} m^3/century. These rates are statistically significant at the 99% level and are large. They have led to almost a doubling of the discharge in the second half of the year in the Hudson and almost as much in the Connecticut. The day of the year when half of the annual flow has passed the gages (ACV) are shown in Figure 4.8(b) and

Figure 4.9(b). These dates have made a much more substantial increase than the WSCV has decreased. The ACV in the Hudson has increased at a rate of 52 days/century and in the Connecticut record the ACV has increase at 22 days/century.

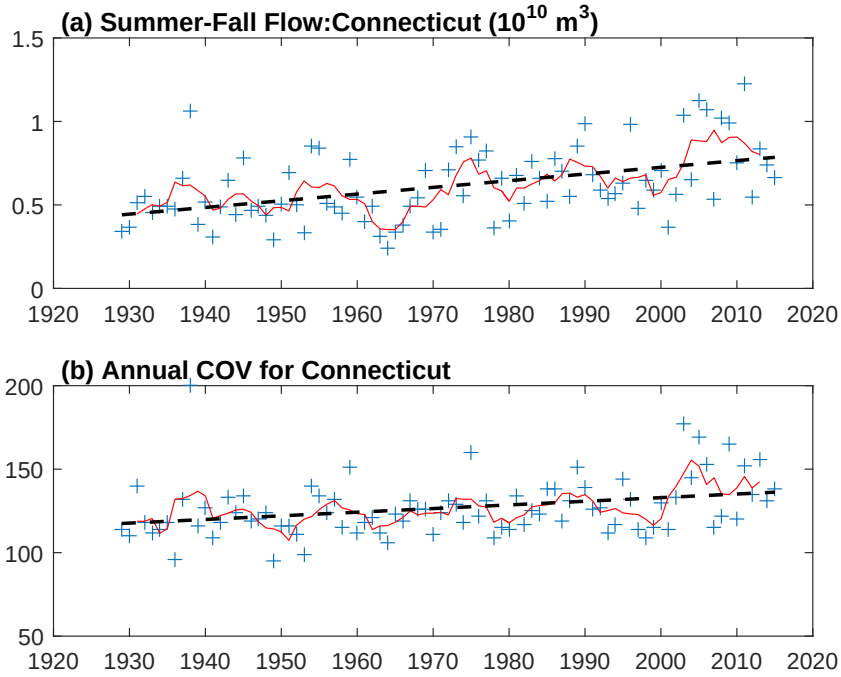

Figure 4.8. (a) shows the total volume passing the Thompsonville gauge each year after June 1st by the blue '+' symbols and the red line shows a smoothed version of the series using a five-year running average. The black dashed line shows the results of a linear regression. (b) shows the annual center of volume flow, the smoothed series and the regression trend line.

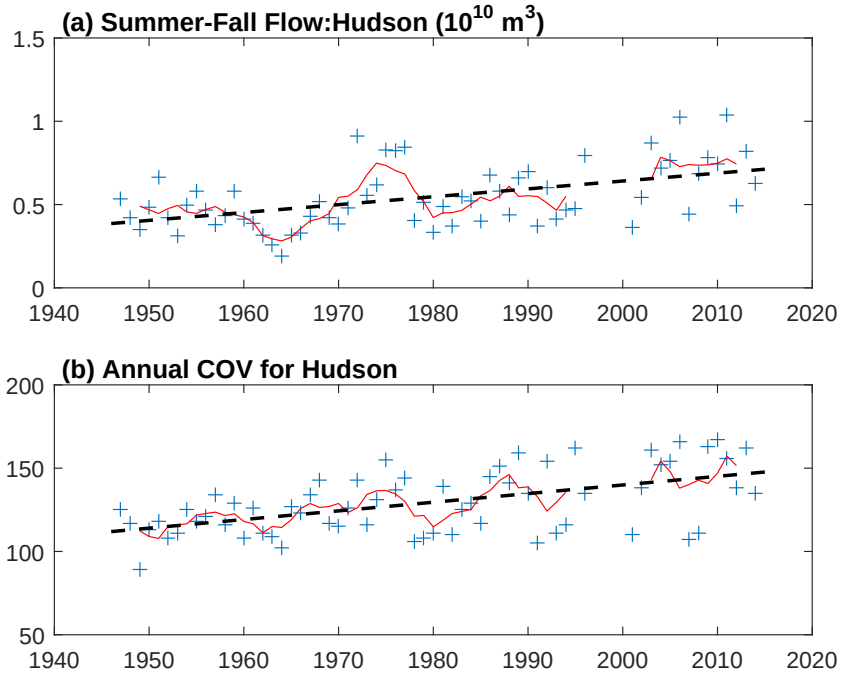

Figure 4.9. (a) shows the same statistics as Figure 4.8(a) but for the Hudson River at Green Island. (b) See Figure 4.8(b).

4.4 Summary and Conclusions

We have examined the trends in the discharge in the Connecticut and Hudson Rivers. These both have a major influence on the salinity in Long Island Sound (LIS) and consequently, the patterns of circulation and mixing. The effects are quite different since the location of the sources and the mechanisms that control the distributions are quite different. Our analysis has demonstrated that the character of river discharge patterns is very similar in the Connecticut and Hudson and that they have exhibited large decadal-period oscillations and secular trends during the last century. We showed that the annual discharge in both rivers was increasing. We also confirmed an earlier finding that the spring freshet was occurring earlier in the spring (the WSCV was decreasing) and was advancing at a rate of eight days/century. The Hudson was shown to be undergoing a similar trend though at a slower rate.

The decadal scale fluctuation in the two rivers were found to be significantly correlated at zero lag and negatively correlated at approximately 10 years, indicating that the forcing of the long period fluctuations affected the watersheds of the two rivers in a similar manner. However, despite the similarity in the character of the variations in the records, the correlation with the NAO index showed was not found to be significant. This seems likely to be a consequence of the highly variable lags in the relationship between precipitation and streamflow in very large basins.

The most significant and novel result of the analysis is that the streamflow in the spring was stable and that the discharge in the low-flow months (June-December) was increasing. The rate of increase has led to almost a doubling of the amount of water reaching New York Harbor and LIS in these months. To more clearly illustrate the magnitude of the changes that have occurred we divided the year in to three phases based on the average seasonal cycle shown in Figure 4.2. The “low” phase extends from June to October when both the five-day and monthly means are below the annual average. The “average” flow interval occurs in November to February and the “high” phase is March to May, when the spring freshet occurs. Note that these intervals are not of equal length. We then computed the total volume passing the gages in the three intervals each year and calculated the fraction of the annual freshwater volume occurring in each.

In Figure 4.10(a) the lower black line shows the fraction of the annual flow occurring in the “low” phase. The boundary between the red and blue areas was obtained by linear regression of the low phase discharge fraction against time. Figure 4.10(b) shows the same property for the Connecticut River. The upper black line in Figure 4.10(a) and (b) shows the evolution of the sum of the discharge fraction during the below-average and average phases, and the boundary between the blue and green areas is the temporal trend in the sum of the fractions. The distance from the upper black line to the top of the graph represents the spring discharge contribution to the annual cycle. The green, blue and red areas then each represent the contribution of the three phases (high, average and low) of the discharge cycle to the delivery of fresh water to the estuaries.

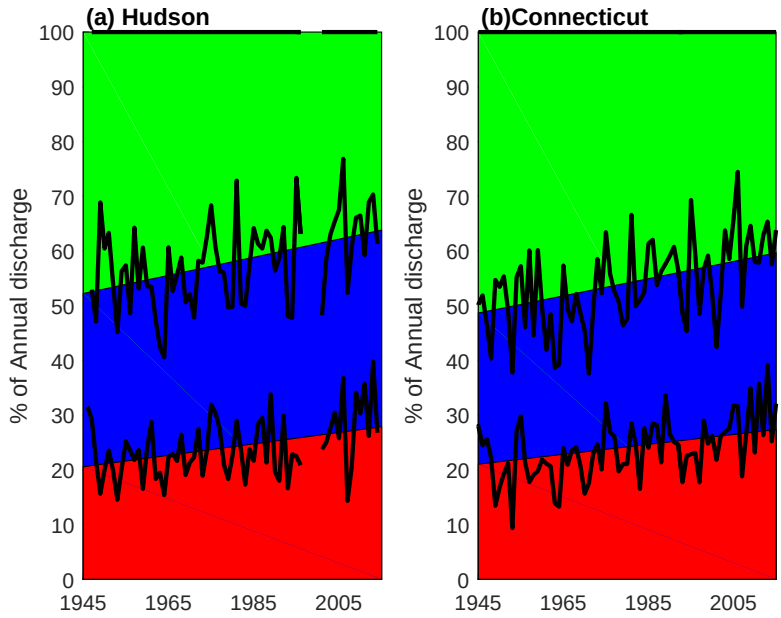

Figure 4.10. The lower black line and red areas shows the fraction of the annual flow in the (a) Hudson and (b) Connecticut Rivers occurring in the "low" phase (June-October). The blue and green areas show the fraction in the average flow period (November to February) and high flow (March-May).

In 1945, approximately 50% of the freshwater arrived in the estuary during the three months of the high phase. As a fraction of the annual flow, it has diminished by almost 15% in the Hudson and 10% in the Connecticut. Both the other phases have expanded their contributions. It is unclear why this has happened. Since patterns are the same in both watersheds, it seems unlikely that there has been a reduction in the diversion and changes in precipitation are more likely. The implications of these changes are unclear and the issue will require further study. The availability of more freshwater in the Hudson in the summer may, for example, decrease the salinity and increase the stratification in the western Sound.

4.5 References

Bradbury, J.A., S.L. Dingman and B.D. Keim. (2002). New England Drought and Relations with Large-Scale Atmospheric Circulation Patterns. Amer. Water. Res. Assc. V 38, No. 5, 1287-1299.

Hodgkins G.A., R.W. Dudley and T.G. Huntington (2003). Changes in the timing of high river flows in New England over the 20th Century. J. Hydrology V278, 244–252.

Gay, P.S., J. O'Donnell and C.A. Edwards (2004). Exchange Between Long Island Sound and Adjacent Waters J. Geophys. Res. 109, C06017, doi: 10. 1029/2004JC002319.

Hurrell, J.W. (1995). Decadal Trends in the North Atlantic Oscillation Regional Temperatures and Precipitation. Science 269: 676-679.

Hurrell, J.W. and C. Deser (2009). North Atlantic climate variability: The role of the North Atlantic Oscillation. J. Mar. Syst., 78, No. 1, 28-41 - See more at:

https://climatedataguide. ucar. edu/climate-data/hurrell-north-atlantic-oscillation-nao-index-pc-based#sthash. 77h8RnZx. dpuf.

O'Donnell J, J. Morrison and J. Mullaney (2010). The expansion of the Long Island Sound Integrated Coastal Observing System (LISICOS) to the Connecticut River in support of understanding the consequences of climate change. Final Report to the CTDEP, LIS License Plate Fund, 20pp.

O'Donnell, J., R.E. Wilson, K. Lwiza, M. Whitney, W.F. Bohlen, D. Codiga, T. Fake, D. Fribance, M. Bowman, and J. Varekamp (2014). The Physical Oceanography of Long Island Sound. In Long Island Sound: Prospects for the Urban Sea. Latimer, J. S., M. Tedesco, R.L. Swanson, C. Yarish, P. Stacey, and C. Garza (Eds.), ISBN-13: 978-1461461258.

Whitney, M.M. (2010). A study on river discharge and salinity variability in the Middle Atlantic Bight and Long Island Sound. Cont. Shelf Res 30:305-318.

Willmott, C.J., S.G. Ackleson, R.E. Davis, J.J. Feddema, K.M. Klink, D.R. Legates, J. O'Donnell, and C.M. Rowe (1985). Statistics for the Evaluation and Comparison of Models. J. Geophys. Res. 90: 8995-9005.

Chapter 5 - Cloudiness

Table of Contents

List of Figures

5. Ecological Driver: Cloudiness

5.1 Introduction

The plankton in Long Island Sound (LIS) harness energy from light. There have been routine measurements made of the concentration of chlorophyll-A in LIS by the CT Department of Energy and Environmental Protection (CT DEEP) and archived at LISICOS.uconn.edu. Several authors (see for example, Dam et al., 2010) have noted that there is a large degree of variation in the concentration of chl-A but that there was an anomalously low period in 1998-2000 that has been unexplained. The data from CT DEEP survey station (see Figure 5.1) illustrate this behavior. Figure 5.2 shows the time series of the near surface measurements. The green and red dots show the data collected in the spring and summer, respectively. The green and red lines show seasonal averages of the log of the data. The period 1998 to 2000 is bounded by vertical lines on the left of the figure to isolate the interval in which the means in both seasons were almost a factor of ten lower than the longer term mean. A second low year occurred in 2010 and it is highlighted by the lines on the right of Figure 5.2.

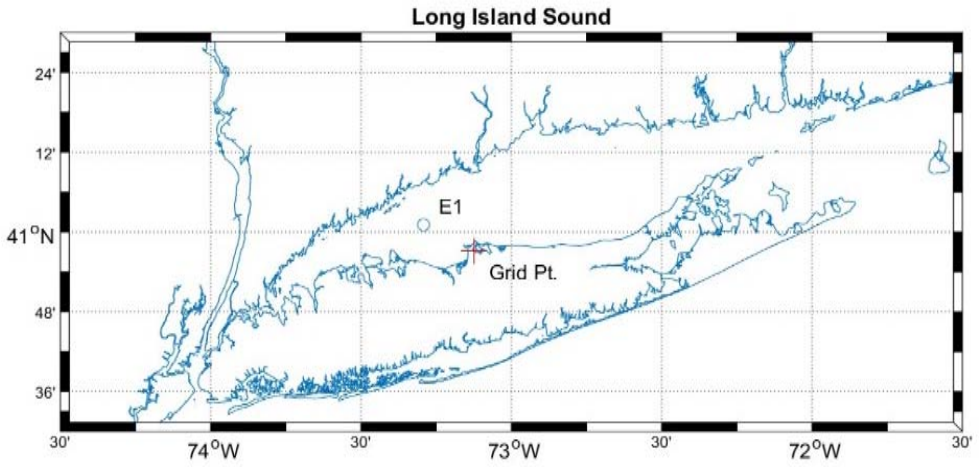

Figure 5.1. Map of the coast of Long Island Sound showing the location of CT DEEP station E1 by the circle and the closest grid point in the NCEP–DOE AMIP-II REANALYSIS model.

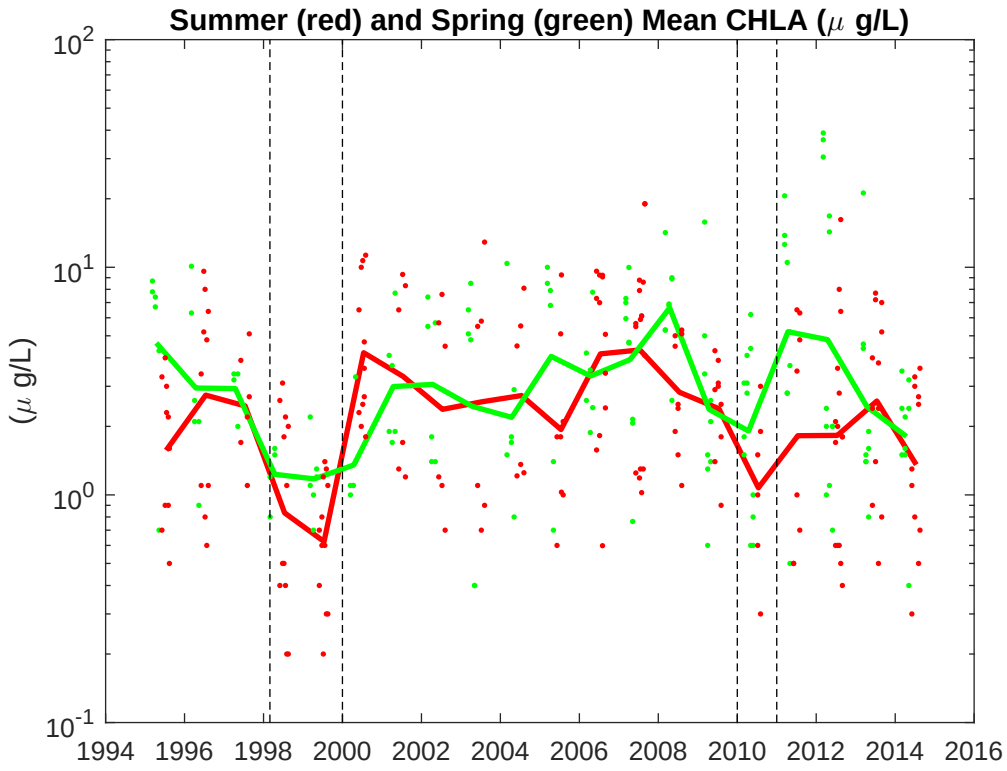

Figure 5.2 The time series of the near surface chlorophyll-A measurements by CT DEEP at station E1 (see Figure 5.1). The green symbols show the spring data and the red symbols show the summer data. The log mean of the spring (March-May) and summer (June-August) are shown by the red and green lines. The vertical lines indicate intervals of low chl-A.

O'Donnell et al. (2014) speculated that large variations in cloudiness which were common in southern New England could impact the inter-annual variability of the primary production in LIS. In the next section, we discuss the availability of cloud data and describe the trends that can be detected.

5.2 Data

The fraction of the sky that is covered by cloud, the type and altitude of clouds have been noted by weather observers for several centuries. Unfortunately the classification and estimates are very subjective and the biases introduced by the sampling times that humans can maintain are quite large. Few high quality records exist. We downloaded the available data from the NOAA data distribution site (http://www.ncdc.noaa.gov/cdo-web/datasets#GHCND). The parameters ACSH - average cloudiness from sunrise to sunset, and ACMH - average cloudiness midnight to midnight were extracted. These are both produced by human observers. Available data spanned the interval 1965 to 1995, and there was a gap in 1988-1990. We examined average conditions by month and found that there was little change from 60%. We concluded that the noise introduced by the estimation system was too large to provide insight.

Quantitative measurements of cloud cover are not readily available, and the data regularity and quality is unreliable. After extensive exploration, we identified a data assimilating model reanalysis product as a useful source. The National Atmospheric and Oceanic Administration's

(NOAA's) National Center for Environmental Prediction (NCEP) executed a program that integrates a sophisticated global atmospheric model with the large and diverse array of weather observations available to create fields of variables that are regularly distributed in space and time and are consistent with both the observation (taking uncertainty in to account) and our understanding of the dynamics of the atmosphere. The fields can then be analyzed to guide interpretation of change. The model is referred to as NCEP Reanalysis-II. The development is described by Kanamitsu et al. (2002) and the results are shared at http://www.esrl.noaa.gov/psd.

5.3 Analysis

We extracted from the archive the cloud cover fraction (%) at the model grid point closest to CT DEEP station E1 in LIS. The location is indicated in Figure 5.1. The time series is available at six-hour intervals from 1979 to 2015. The series vary rapidly between 0 and 100%, so to illustrate the monthly and seasonal scale variability we show in Figure 5.3 the series filtered to remove variations with periods shorter than a week. The annual and inter-annual variations are clear in this view; however, it seems likely that the critical period of the year for productivity is the spring and summer.

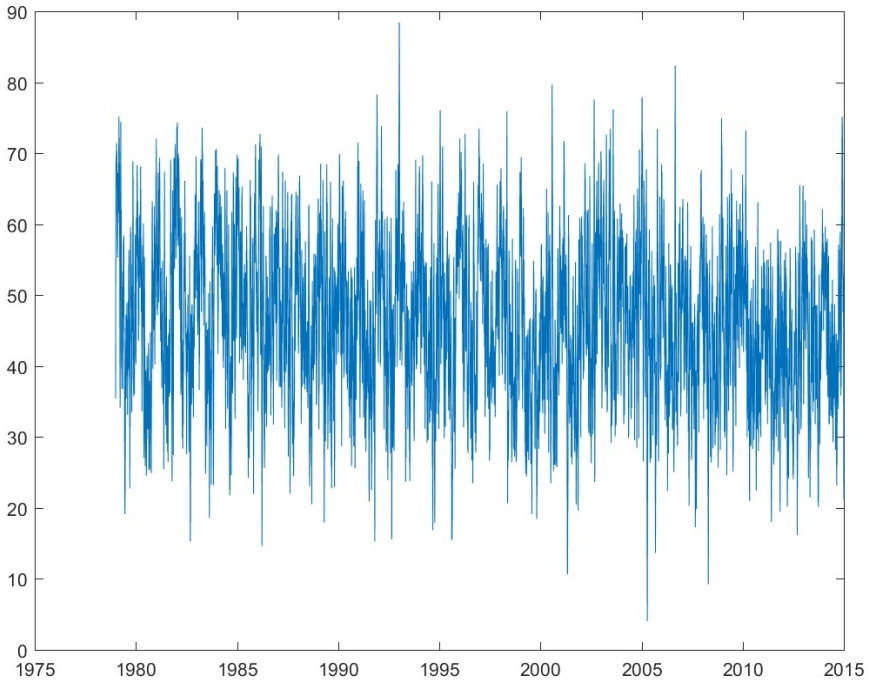

Figure 5.3 Percent cloud cover over Long Island Sound as estimated by the NCEP Reanalysis II.

In Figure 5.4 we show the monthly average cloud cover for each year between 1979 and 2014. The yellow shades show that high cloud coverage conditions are prevalent in the winter months and then, in some years, into the late spring. The periods of low chl-A do not appear to be associated with unusually cloudy spring and summer conditions. Rather, it would be more reasonable to describe 1998-2000 as a relatively clear interval period, and 2010 is the least cloudy year of the reanalysis period.

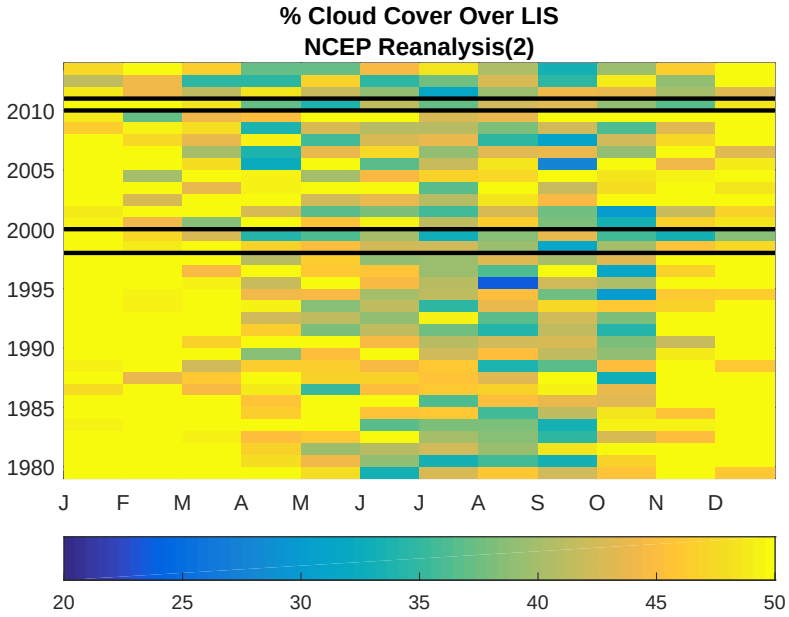

Figure 5.4. Monthly average cloud cover (%) over Long Island Sound between 1979 and 2004. The black horizontal lines show the intervals in 1998-2000 and 2010 in which the surface chl-A concentrations in LIS were low. The color scale is shown at the bottom of the graph.

Figure 5.5 shows the same data but averaged in the spring (March-May) and summer months (June-August) using green and red, respectively. The rapid decreasing trend in the spring cloud cover is readily apparent. This has been observed elsewhere but has not been confirmed by comparison to available human observer reports to-date. Of relevance here is the evident dip in the cloud cover fraction in 1998 and 2010. This is inconsistent with the speculation that there would be a reduction in productivity.

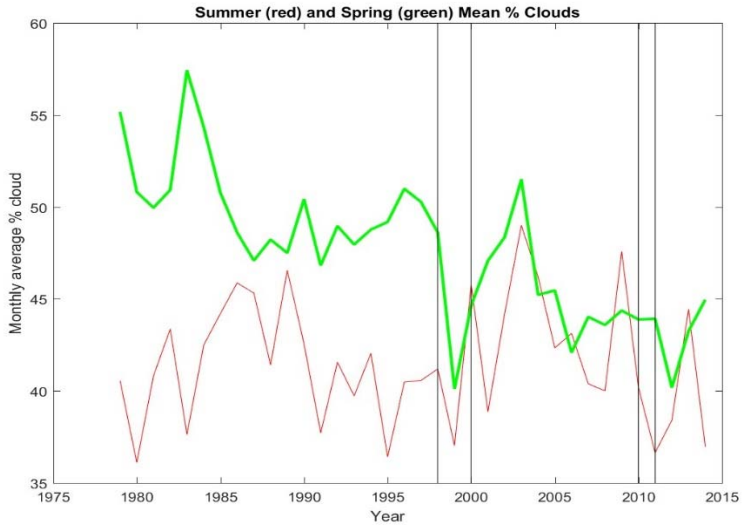

Figure 5.5 The green time series shows the spring (March-May), and red shows the summer (June-August), cloud cover fraction over LIS from the NCEP Reanalysis-II. The black lines outline the intervals when the chl-A was low.

5.4 Summary and Conclusions

We have explored the possibility that the anomalously low concentration of chl-A observed in surveys of LIS in 1998-99 were associated with increased cloud cover in the spring and summer and, consequently, reduced light levels. We used the NCEP reanalysis product from a global atmospheric model to examine the pattern of cloudiness since the NCEP team invested in an extensive data quality review and their products have the advantage of consistency with many other observations. Unexpectedly, we find that the cloud cover was unusually low during the years of anomalously low chl-A.

The concentration of chl-A is commonly used as a measure of plankton density. However, it is also an indicator of the potential for primary productivity. We had assumed that the low concentrations had been a consequence of low productivity and had speculated that perhaps low light levels, due to clouds, was the cause. The analysis of data now suggests light levels were higher than normal and another explanation must be sought. Perhaps the chl-A level was low because the plankton had adapted by raising the carbon to chl-A ratio to exploit the high light levels.

It is also possible that the reanalysis products are not sufficiently highly resolved to predict the cloud cover at a coastal area like Long Island Sound. Though available data is limited, it is likely that a trend of the magnitude predicted (see the green line in Figure 5.5) should be detectable. If the reanalysis is correct, then the ecological consequences of a changing light regime deserve additional attention.

5.5 References

Dam, H.G., J. O'Donnell and A.N.S. Siuda (2010). A Synthesis of Water Quality and Planktonic Resource Monitoring Data for Long Island Sound. Final Rept. Long Island Sound Study, LI-97127501.

Kanamitsu, M., W. Ebisuzaki, J. Woollen, S.-K. Yang, J.J. Hnilo, M. Fiorino, and G.L. Potter. (2002). NCEP-DOE AMIP-II Reanalysis (R-2): 1631-1643, Bulletin of the American Meteorological Society.

O'Donnell, J., R.E. Wilson, K. Lwiza, M. Whitney, W.F. Bohlen, D. Codiga, T. Fake, D. Fribance, M. Bowman, and J. Varekamp (2014). The Physical Oceanography of Long Island Sound. In *Long Island Sound: Prospects for the Urban Sea.* Latimer, J.S., M. Tedesco, R.L. Swanson, C. Yarish, P. Stacey, C. Garza (Eds.), ISBN-13: 978-1461461258.

Chapter 6 - Wind

Table of Contents

List of Figures

6 Ecological Driver: Wind

6.1 Introduction

The wind affects Long Island Sound (LIS) in several different, but very important, ways. The speed and direction of winds over the southern New England Shelf determine the magnitude of the non-tidal sea level fluctuations at the eastern end of LIS. Winds from the northeast (to the southwest) are most effective in generating coastal set-up, a positive sea level anomaly that rapidly propagates throughout LIS. Winds from this direction also cause an additional local set-up in the Sound that raises the water levels in the west relative to those in the east by up to several meters. This is a well-established effect and the mechanisms are comprehensively summarized in O'Donnell et al. (2014). This particular sensitivity to winds from the northeast is a consequence of the coastal geometry. It is responsible for the dramatic flooding that occurs in the western end of LIS during major storms. However, the effects of more modest storms are amplified in the same way and this affects the frequency of flooding of salt marshes.

In the western Sound the surface stratification is modulated by the vector component of the wind to the southwest. This is also now well established by both model results (Wilson et al., 2008) and direct observations (O'Donnell et al., 2008). Basically, the rate of restratification of the western sound can be modulated by wind. Winds from the southwest accelerate the rate, and winds from the northeast slow it. Recently, Wilson et al. (2015) has provided convincing evidence that the frequency of occurrence of wind from the northeast can influence the duration and extent of bottom water hypoxia.

It is clear that the ecosystems of LIS are sensitive to the statistics of the wind field, both in the summer when water column stratification is impacted, and in the winter when saltmarshes are frequently subjected to inundation. There are likely to be other effects as well. It is, therefore, important to characterize the statistics of long term trends and fluctuations. O'Donnell (2010) has already demonstrated that all the meteorological stations reporting more than 50 years observations in the New England states show a decline in the monthly averaged wind speed through 2005. In this chapter, we update that result, and then report the results of an evaluation of the trends in the wind stress components since it is now clear that they are more dynamically relevant to ecological processes.

6.2 Data

The National Climatic Data Center (NCDC) maintains an archive of hourly meteorological observations at a global array of locations. O'Donnell (2010) showed that the trends across all New England were correlated, so here we focus on the station at Bridgeport, CT, USAF ID# 725040 (Sikorsky Memorial Airport, 41°09'30" -73°07'44"). The data formats and quality from 1940 to 2005 were discussed by O'Donnell (2010). The record was updated by downloading the years 2006-2015 from ftp://ftp.ncdc.noaa.gov/pub/data/noaa/. Since this data set is not at uniform time intervals, the data was averaged when there were more than one sample per hour. The wind speed and direction were then screened to eliminate missing data to ensure the calculations of means were not biased.

We would estimate the wind stress over the Sound but the records of wind measurements over the water are relatively short. We must therefore assume that the wind velocity can be

extrapolated from the coastal stations over LIS. We estimated the wind stress with the bulk formula of Large and Pond (1981).

Recently, over water observations have become available from the Long Island Sound Integrated Coastal Observing System (LISICOS) (http://lisicos.uconn.edu) at the Execution Rocks (EXRK), western and central Long Island Sound (WLIS and CLIS) buoys. The locations of these buoys and the Bridgeport weather station are shown in Figure 6.1(a). Figure 6.1(b) and (c), from O'Donnell et al. (2014) show a comparison of the annual mean wind stress vector components computed from wind speed using the Large and Pond (1981) formula. The red symbols show the mean and 68% confidence interval at the CLIS buoy. The blue and green symbols show the components at the WLIS buoy and Bridgeport, respectively. The seasonal cycle is clear in the components of all three records. The monthly mean wind stress is weak from April to September and has a maximum magnitude in February of 0.07 Pa toward the southeast at the CLIS buoy. Note that the amplitude of the cycle at the CLIS site is 0.04 Nm^{-2}, in agreement with the intra-annual variations in the MAB estimated by Lentz (2008). The means and the amplitude of the annual cycle at the WLIS buoy and Bridgeport are approximately 60% and 30%, respectively, of the value at the CLIS buoy. It seems likely that the stress estimated using the Bridgeport winds will be approximately a factor of two less than the stress over the Sound, but the temporal trends will be similar.

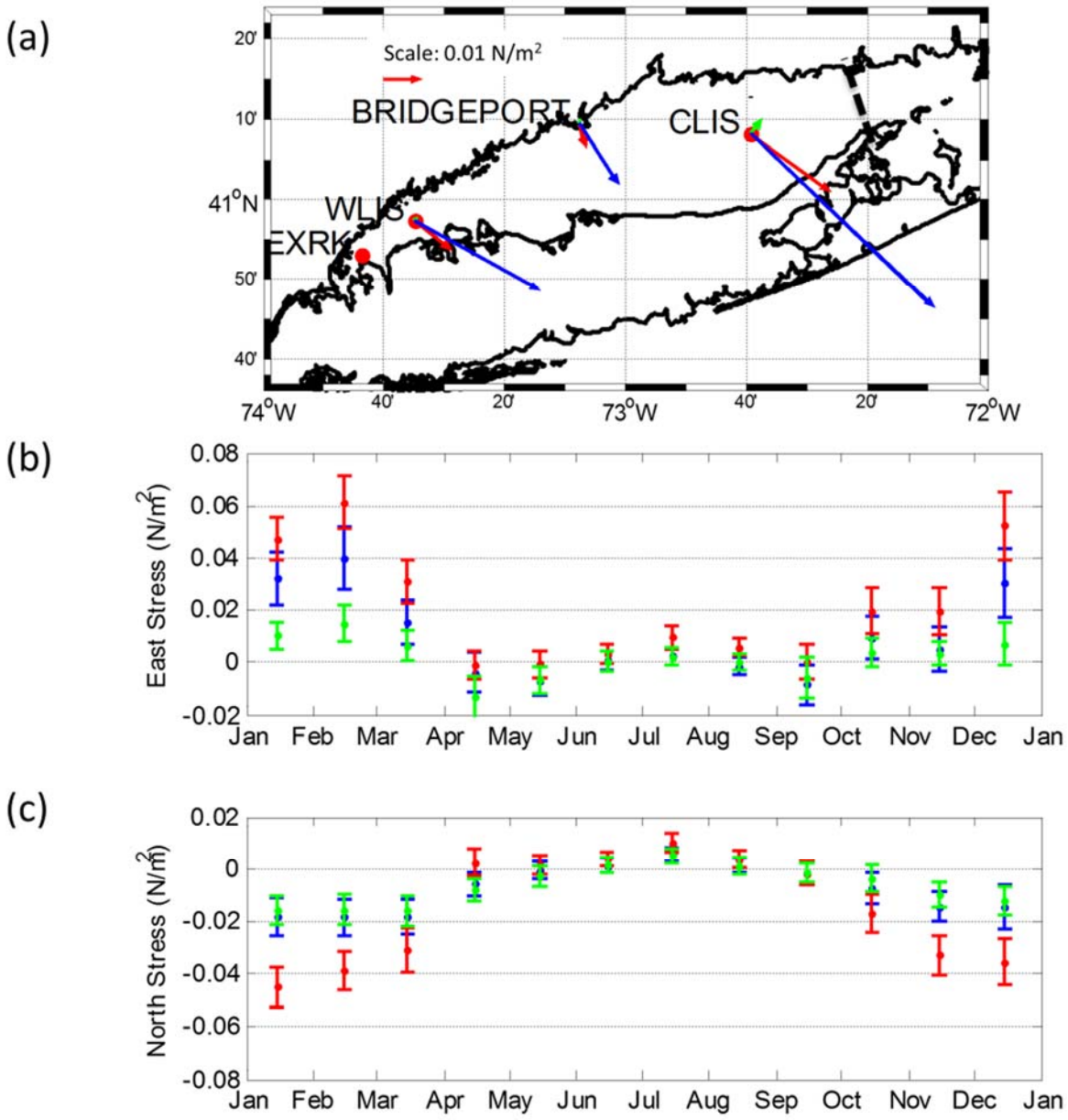

Figure 6.1. (a) A map of the coastline of LIS showing the locations of the EXRK, WLIS and CLIS buoys, and Bridgeport Airport. The red, blue, and green vectors show the annual, winter, and summer mean stress vectors. (b) and (c) show the monthly mean east and north stress components for the period with their 68% confidence interval at Bridgeport, CT (green), WLIS (blue), and CLIS (red).

6.3 Analysis

The analysis of all long wind records in New England by O'Donnell (2010) showed that the annual cycle of the monthly averaged wind speed was substantially the same at all stations and that the maximum occurred in February and the minimum in August. Figure 6.1(b) and (c) show the mean monthly stress also has a maximum in the winter during the February-April interval and a minimum in July-September.

The mean wind speed recorded at the Bridgeport station was computed for the three months in which was the highest (February, March and April, or FMA) and the lowest (July, August and September, JAS) in each year of the record and are shown in Figure 6.2. The FMA graph in Figure 6.2(a) extends the prior analysis of O'Donnell (2010) by a decade and shows that the downward trend in wind speed he identified has persisted. The JAS data in Figure 6.2(b) show almost identical behavior in the summer.

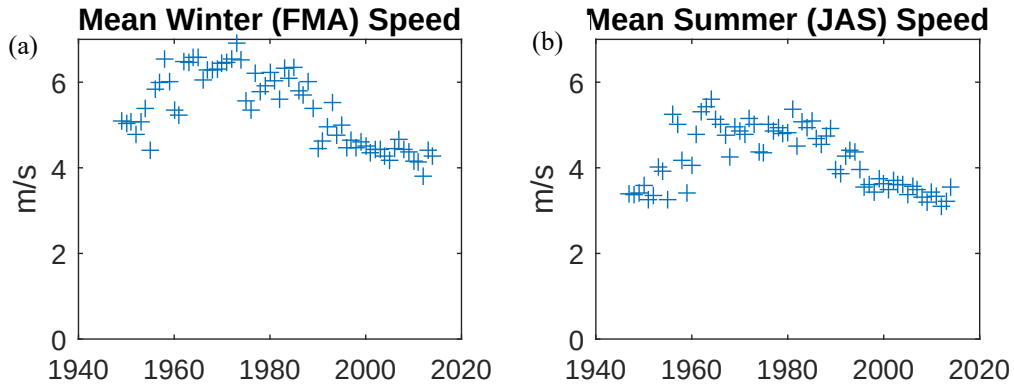

Figure 6.2. The average over February to April (a) and July to September (b) of the wind speed at Bridgeport, CT.

The characteristics of the wind stress are more complicated to assess since the mean is generally very small and the dynamically important characteristic is the magnitude during intermittent periods of "bad" weather. We computed the stress from the Large and Pond (1981) formula and then rotated the vector components 30º into an along and across Sound coordinate system. We take positive stress components to be towards the northeast and northwest. To characterize the seasonal cycle of stress component values, we identified all the samples that were obtained in each calendar month, and then computed the median, and the 50, 80 and 95 percentile interval bounds. In Figure 6.3(a) the blue lines show the monthly evolution of the boundary containing 95% of the along LIS stress component estimates. The green and the red lines show the 80 and 50% bounds. Note that the magnitude of the mean values shown in Figure 6.1 is an order of magnitude smaller than the 95% bounds; however, the pattern of winter maxima and summer minima is the same.

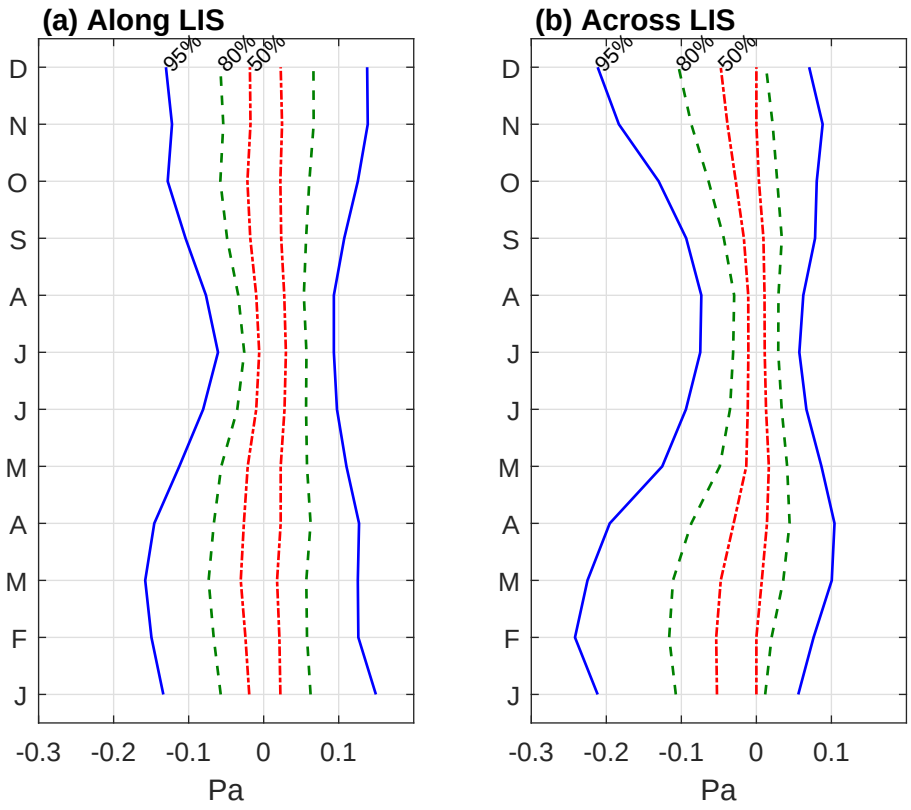

Figure 6.3. (a) shows the boundaries of the stress intervals containing 95% (blue), 80% (green) and 50% (red) of all the along LIS component stress estimates. (b) shows the same statistics but for the across LIS stress components.

The maximum value of the 95% along Sound stress component occurs in March and is directed towards the southwest (negative) at approximately -0.16 Pa. The minimum value occurs in July and is only half as large. The pattern for the 80% bounds (green lines) is similar, but the 50% interval does not have a strong annual cycle. Comparison of the positive and negative bounds shows the pattern is almost symmetric. The infrequent large events can have similar magnitudes in either direction, though there is a slight bias to larger negative events in the winter.

The statistics of the across sound stress components are shown in Figure 6.3(b). Here the distribution is very asymmetric in winter. The 95% boundary has a maximum magnitude in February of -0.24 Pa. The positive 95% boundary is only half as large. Even the frequent events are stronger when from the northwest to the southeast. In the summer, the stress values are generally small. It is important to note, however, that the larger values do occur in the late summer and early fall and are associated with hurricanes. They are so infrequent that the effects do not appear in statistical summaries.

To assess how the long term changes in mean speed that were identified influence the statistics of the stress values, we bin data in the February to April (FMA) and July to September (JAS) periods and then compute the 95, 80 and 50% intervals for each season and stress component. Figure 6.4(a) shows the FMA along Sound stress component trends. As in the previous figure, we use blue to show the boundaries of the 95% interval and the green dashed lines show the 80% interval. The distributions are again most symmetric. The critical feature, though, is the factor of

two reduction in the 95% bounds between 1980 and 2000. Figure 6.4(b) shows that the FMA across Sound component also underwent a radical reduction in the magnitude of the largest events which lead to stress towards the southeast. In the summer period, the stress values are lower and symmetrically distributed, but careful examination of the blue and green curves in Figure 6.4(c) and (d) show that the magnitude of the infrequent events has also been decreasing in the summer.

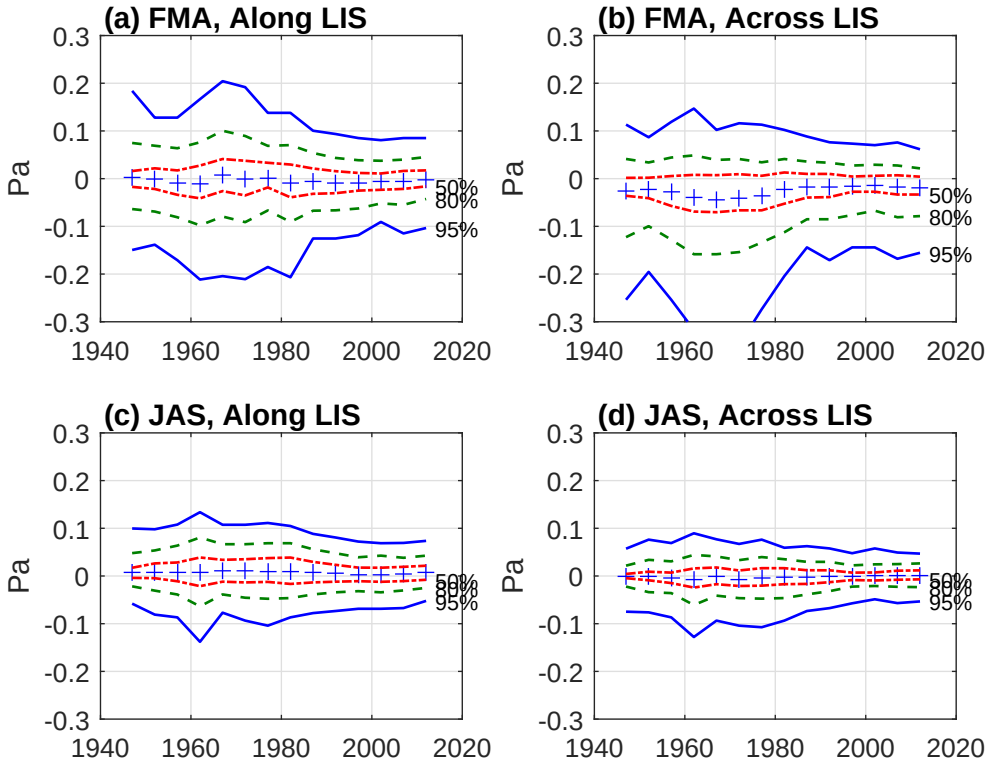

Figure 6.4. (a) shows the boundaries of the stress intervals containing 95% (blue), 80% (green) and 50% (red) of the along LIS component stress estimates in February-April each year. (b) shows the same statistics but for the across LIS stress components. The data distribution evolution for the low wind July-September period are shown in (c) and (d) for the along and across Sound components respectively.

6.4 Summary and Discussion

We have expanded the analysis of wind observations described by O'Donnell (2010) in which he found that there had been a regional reduction in the average wind speeds during the time of year when they are highest, February-April, at stations all across New England through 2005. We show by extending the analysis using the Bridgeport–Sikorski Airport data record that the decreasing trend has continued through 2015. Further, the average wind speeds during the calmer months, July-September, also shows a substantial decrease.

By examining the distributions of the estimates of the vector component of the wind stress, we show that they are also largest in February-April and smallest in July-September. Binning the vector components during these two intervals for each year, we computed the boundaries of the 95, 90 and 50 percentile intervals and displayed their evolution since 1947 in Figure 6.4. A dramatic decline in the 95 and 80% stress level was detected. In February to April of the 1960-80

interval, the magnitude of the stress during events that were less frequent than 5% was approximately 0.2 Pa. Since 2000 it has been 0.1 Pa. Summer statistics show a similar change.

We should be concerned that trends at a single station might be the consequence of some local effect. Small movement of sensors or new buildings can change airflow patterns, for example. But the fact that the reduction in wind speed was regional supports the interpretation that the climate system is responsible for the change.

The record does not show much decadal-scale variation. The trends in wind speed and stress show an increase from the 1940s to the 1960s, and then an almost monotonic decrease. This variation is much more in-keeping with the form of the Atlantic Multi-decadal Oscillation (AMO) that has been described by Schlesinger and Ramankutty (1994). The AMO is manifest as variation in the annual average sea surface temperature in the North Atlantic (30–65°N). Trenberth and Shea (2006) showed that water temperature (positive AMO) led to reduced storm activity and it has been linked empirically, and through models, to several regional ocean and atmosphere trends. For example, above average summer air temperatures in the eastern United States during positive AMO was suggested by Enfield et al. (2001), and Goldenberg et al. (2001) found a positive AMO anomaly was associated with increasing frequency of land-falling hurricanes on the eastern seaboard.

To examine the potential association of the wind forcing of LIS with the AMO, we show in Figure 6.5, the AMO index developed by the NOAA Earth Systems Research Laboratory (ESRL) (http://www.esrl.noaa.gov/psd/data/timeseries/AMO/) using satellite sea surface temperature maps. To simplify the graphics, we divide the index by the record standard deviation. The blue lines in Figure 6.4(a) show $\tau_{AL,95\%}$, the upper and lower value of the along Sound stress component that are greater than 95% of the observations in a particular year. We repeat these lines in Figure 6.5 after dividing by the standard deviation and changing the sign of the upper (positive) bound. The similarity in the in the pattern of the curves is remarkable. Since the wind records only extend from 1947, less than a single oscillation has been captured. This correspondence can only be further investigated through models.

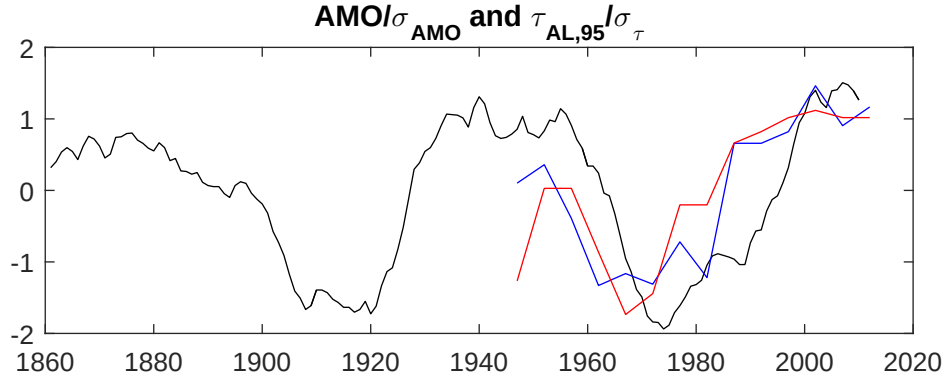

Figure 6.5. The December AMO index from the NOAA ESRL analysis (black line) with the 95% bounds of the FMA along Sound stress distributions. The blue shows the lower bound and the red line is minus the upper bound. All three records have been standardized through division by the standard deviation.

A factor of two change in the stress should be expected to have a significant effect on the ecosystems of the Sound. Reexamination of data with the recognition of these long term changes have been occurring may bring new insights to the understanding of the variability in LIS.

6.5 References

Enfield, D.B.; A.M. Mestas-Nuñez and P.J. Trimble (2001). The Atlantic Multidecadal Oscillation and its relation to rainfall and river flows in the continental U.S.: Geophysical Research Letters, v. 28, p. 2077–2080.

Goldenberg, S.B., C.W. Landsea, A.M. Mestas-Nunez and W.M. Gray (2001). The recent increase in Atlantic hurricane activity—causes and implications: Science, v. 293, p. 474–479.

Large, W.G. and S. Pond (1981). Open ocean momentum flux measurements in moderate to strong wind. J Phys Oceanogr 11:324–336.

Lentz, S.J. (2008). Seasonal variations in the circulation over the Middle Atlantic Bight continental shelf. J Phys Oceanogr 38:1486-1500.

O'Donnell, J., H.G. Dam, W.F. Bohlen, W. Fitzgerald, P.S. Gay, A.E. Houk, D.C. Cohen, and M.M. Howard-Strobel (2008). Intermittent Ventilation in the Hypoxic Zone of Western Long Island Sound During the Summer of 2004. J. Geophys. Res., 113, doi:10.1029/2007JC004716.

O'Donnell, J. (2010). A Change in the Wind: Long Term Trends in the Forcing of Long Island Sound. Proceeding of the 2010 Long Island Sound Research Conference. http://lisfoundation.org/downloads/lisrc_proceedings2010.pdf.

O'Donnell, J., R.E. Wilson, K. Lwiza, M. Whitney, W.F. Bohlen, D. Codiga, T. Fake, D. Fribance, M. Bowman, and J. Varekamp (2014). The Physical Oceanography of Long Island Sound. In *Long Island Sound: Prospects for the Urban Sea*. Latimer, J.S., Tedesco, M., Swanson, R.L., Yarish, C., Stacey, P., Garza, C. (Eds.), ISBN-13: 978-1461461258.

Schlesinger, M.E. and N. Ramankutty (1994): An oscillation in the global climate system of period 65-70 years. Nature, 367, Issue 6465, pp. 723-726, DOI: 10.1038/367723a0.

Trenberth, K.E. and D.J. Shea (2006): Atlantic hurricanes and natural variability in 2005. Geophysical Research Letters 33, L12704, doi:10.1029/2006GL026894.

Wilson, R.E., R.L. Swanson and H.A. Crowley (2008). Perspectives on long-term variations in hypoxic conditions in Western Long Island Sound. Journal of Geophysical Research, 113, C12011, doi:10.1029/2007JC004693.

Wilson, R.E., S.D. Bratton, J. Wang and B.A. Colle (2015). Evidence for Directional Wind Response in Controlling Inter-annual Variations in Duration and Areal Extent of Summertime Hypoxia in Western Long Island Sound. Estuaries and Coasts (2015) 38:1735–1743 DOI 10.1007/s12237-014-9914-2.

Chapter 7 – Sea Level

Table of Contents

List of Figures

List of Tables

7. Ecological Driver: Sea Level

7.1 Introduction

Sea level fluctuations due to winds have received considerable attention recently because of the flooding that often ensues. However, some organisms in coastal ecosystems have evolved to depend upon intermittent flooding to bring prey, nutrients, sediment, etc., while other species are negatively affected. Sea levels have been rising and this will change the frequency and duration of flooding, affecting some places more than others. Most recent work has focused on the return frequency of catastrophic events. Here we exploit the available data to assess what the more subtle effects are likely to be and whether we can detect the influence of changing wind patterns.

7.2 Data

Sea level measurements form the longest data records available to oceanographers because water levels are critical to safe navigation. In Long Island Sound, there are three stations with records exceeding 20 years in length. Figure 7.1 shows their locations and Table 7.1 lists the NOAA station numbers and duration. In the west, Kings Point and Willets Point are very close together. Willets Point was closed in 2000 since Kings Point had started in 1998. For the purposes of the analysis of long term trends in the non-tidal sea level fluctuations, these records can be concatenated. Here we will discuss data from New London and Kings-Willets Point.

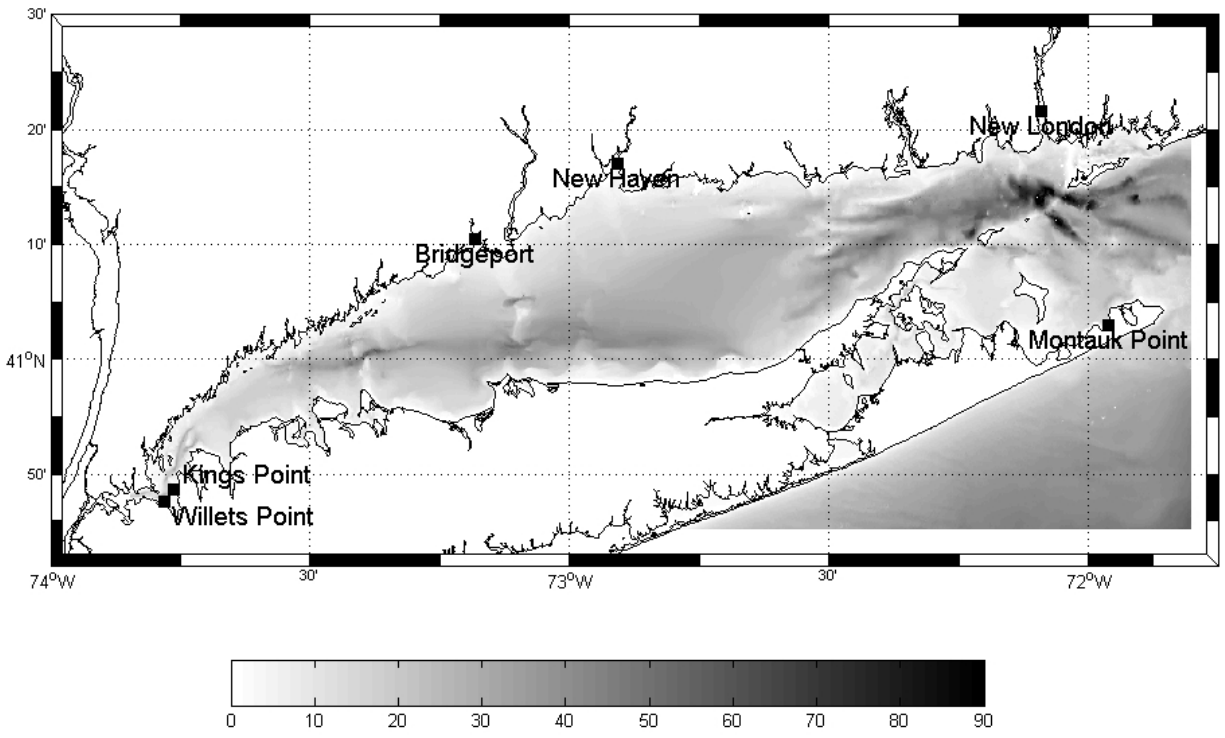

Figure 7.1 A map of the coastline and bathymetry of Long Island Sound showing the locations of long term water level gages maintained by NOAA.

Table 7.1. Tide Station names, ID numbers and data duration

Station	*NOAA ID*	*Start Year*	*End Year*
New Haven, CT	8465705	1999	2015
Bridgeport, CT	8467150	1996	2015
New London, CT	8461490	1938	2015
Kings Point, NY	8516945	1998	2015
Willets Point, NY	8516990	1957	2000

Long records of sea level in Long Island Sound have been archived by NOAA (http://tidesandcurrents.noaa.gov) at the stations, and for the intervals, listed in Table 7.1. Data access is limited; however, access via "webservices" can greatly facilitate the acquisition for long data records. See http://opendap.co-ops.nos.noaa.gov/axis/webservices. Predicted tidal elevations are computed using harmonic analysis (e.g. Foreman, 1989) and both the raw data and the contribution due to the tidal forcing can be obtained. Figure 7.2 shows an example of the non-tidal sea level fluctuations at New London, CT. The record has a few gaps but has been sustained since 1938. The very large positive peaks are mainly the consequence of tropical cyclones but most of the variability arise from winter cyclones. Note that the effects of long term sea level rise are evident at New London.

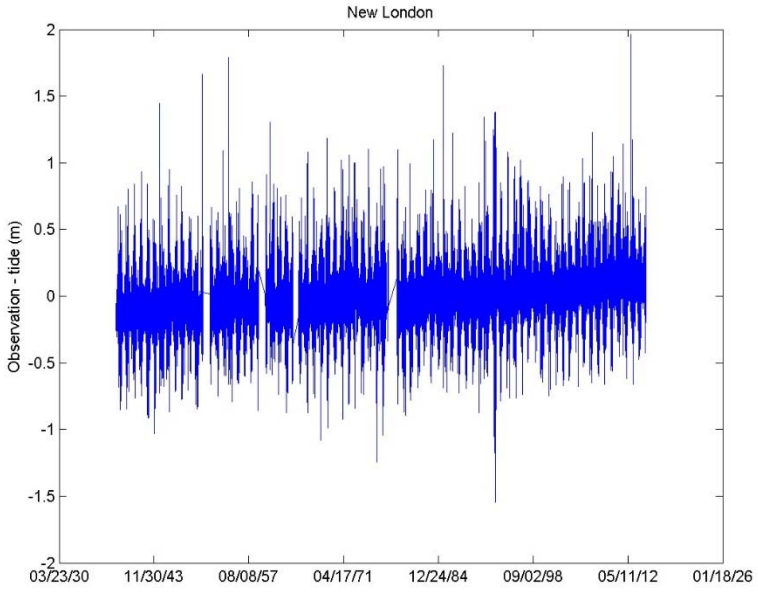

Figure 7.2 The non-tidal sea level fluctuations at New London, CT.

Deviations from the predicted tidal levels are driven mainly by the wind and the interaction of the resulting water motion with land. Garvine (1985) and Wong (1990) demonstrated that the

character of wind forcing in the region led to an amplification in the sea level response in the western part of the Sound. Based on these results, O'Donnell and O'Donnell (2012) demonstrated that of sea level rise will change the risk of flooding more in the eastern part of Long Island Sound than in the west. There is a distinct seasonality to the statistics of wind in southern New England. Consequently, there is seasonality in the sea level fluctuation that the wind creates. Figure 7.3 shows the variance computed from the non-tidal sea level fluctuations at the five stations listed in Table 7.1. It demonstrates both the amplification of the variability in the west and the consequences of seasonality of the winds. At all times of the year, variance at the western station is the highest, and in the winter months, (November –March) the variance is two to four times larger than in the summer, and is proportional to distance west of New London.

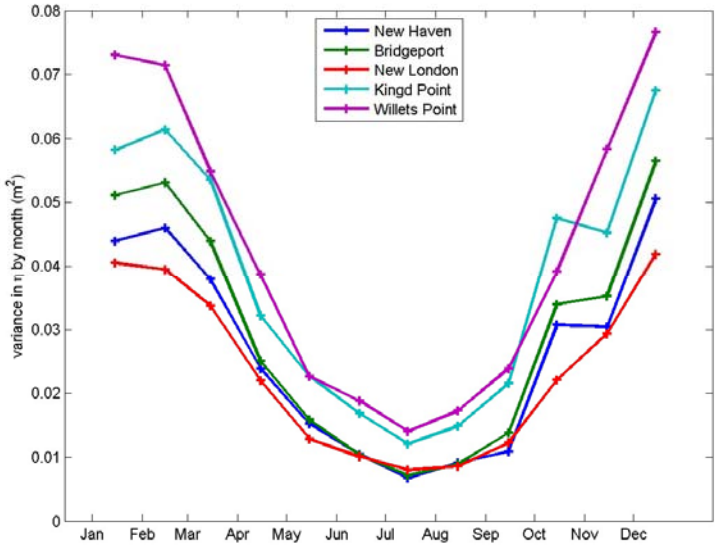

Figure 7.3. The variance in the non-tidal sea level fluctuations by month at the stations listed in Table 7.1.

7.3 Analysis

The main intent of this section is to assess the impact of changes in the characteristics of the wind forcing on the frequency of flooding at the edges of the Sound. Since there is clearly months with large variance and others with smaller variance, and an amplification from east to west, we will examine data in the intervals December-February (DJF) and June-August (JJA) in the records from New London, CT, and Willets-Kings Point, NY.

Figure 7.4(a) shows the distribution of the DJF water level anomalies at New London computed in five year time-bins. The blue lines bound the water level range containing 99% of the observations. The green, red, cyan and magenta lines contain the 98%, 95%, 80% and 50% of the observations, respectively. The tails of the distributions are quite flat so there is greater uncertainty in the estimates of bounds. However, each five year bin is independent and the consistency in time is high.

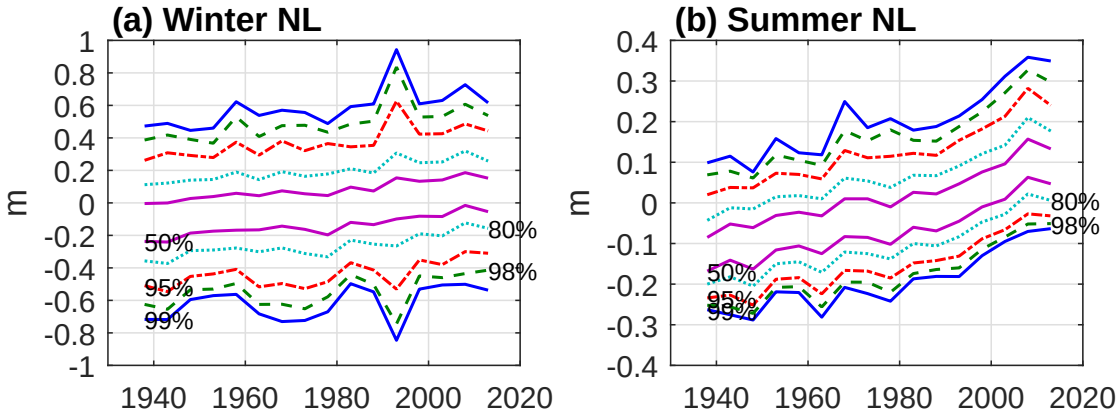

Figure 7.4. (a) shows the distribution of the December to February (DJF) water level anomalies (in meters from the mean water level) at New London computed in five year time-bins. The blue lines bound the water level range containing 99% of the observations. The green, red, cyan and magenta lines contain the 98%, 95%, 80% and 50% of the observations, respectively. (b) shows the same statistics for the June-August interval. Note the change of scale.

The most readily apparent feature of the distribution is the upward trend in all the lines across the record. This is a largely a consequence of sea level rise as will be demonstrated subsequently. But from the perspective of organisms at the edge of the Sound, the mechanism causing increased flooding is not the primary issue. The upper red line in Figure 7.4(a) (95th percentile) takes a value of approximately 0.3 m in 1940. Only 2.5% of hourly level anomalies exceeded 0.3 m in 1940-45. In 2015, the 0.3 m level is close to the cyan line (80th percentile) so 10% of anomalies exceed 0.3 m. Therefore, if a location was at risk of flooding in the winter of 1940 when the water level anomaly reached 0.3 m, then the risk would be increased by a factor of four by 2010-2015. An alternative interpretation is the location should be expected to flood four times more frequently. A similar analysis can be applied to other levels to estimate the change in the expected flooding frequency. Computing the expected frequency (as opposed to the change) is more complicated because the serial correlation in the estimates and the tidal effects must be included. O'Donnell and O'Donnell (2012) discuss this issue with a slightly different approach.

Figure 7.4(b) shows the distribution of the water level anomaly observations the summer (JJA) interval when the variance is much smaller (note the scale is different from Figure 7.4(a)). In this case, the upper limit of the 99% interval (upper blue line) in 1940 is at 0.1 m. In 2015, the 0.1 m level is just below the upper bound of the 50% interval. The expected frequency (or risk) of water levels exceeding the 0.1 m level in the summer has, therefore, increased by at least a factor of 5 (=0.25/0.05).

It is often underappreciated that there are water level negative anomalies due to wind events. These have the effect of exposing sub-tidal mud flats for longer periods and uncovering areas that are normally not exposed. Benthic ecologists may find that there ecological consequences to the reduction in the frequency of exposure to the atmosphere that the data in Figure 7.4 predicts has occurred. Continuing sea level rise will expand the areas impacted in this way.

In Figure 7.5(a) we show the DJF sea level anomaly distribution at the Willets-Kings Point station using the same presentation format as Figure 7.4. Though sea level in this region is increasing at the same rate as in eastern Sound, the upper bounds in the Figure 7.5(a) are level or decreasing. The lower bounds are also increasing with the net effect that the range between the upper and lower intervals of each interval narrows between 1940 and 2015. In Figure 7.5(b), we see that the JJA observations display the upward trend in the interval bounds as at New London.

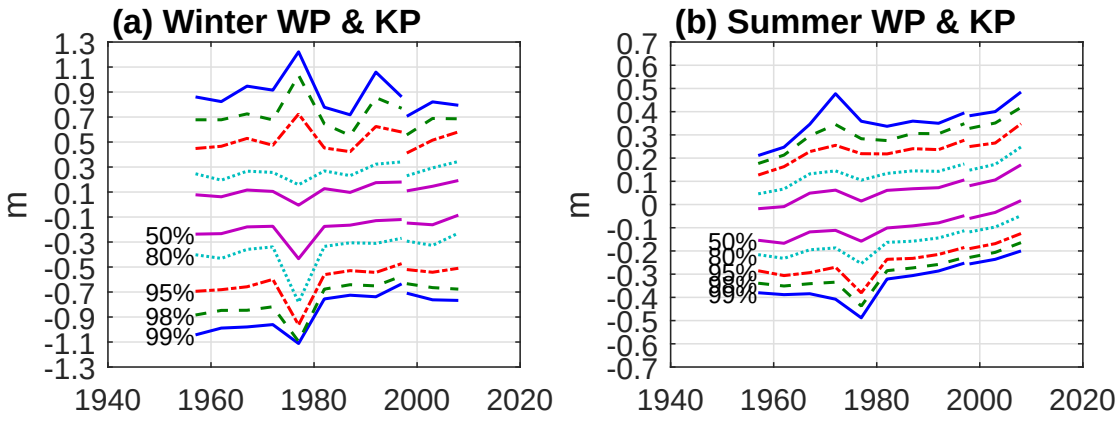

Figure 7.5. (a) shows the distribution of the December to February (DJF) water level anomalies (in meters from the mean water level) at Willets-Kings Point computed in five year time-bins. The blue lines bound the water level range containing 99% of the observations. The green, red, cyan and magenta lines contain the 98%, 95%, 80% and 50% of the observations respectively. (b) shows the same statistics for the June-August interval. Note the change of scale.

To extract the effects of sea level rise from the data records (see Figure 7.2) a linear regression was applied and the data distribution in Figure 7.4 was reconstructed with the de-trended data and the results are shown in Figure 7.6(a) and (b). The upward trend in the percentile bounds in both the DJF and the JJA (see Figure 7.6(b)) is entirely eliminated by the use of the trend removal. Note also that the intervals do not narrow as they appear to do at Willets-Kings Point.

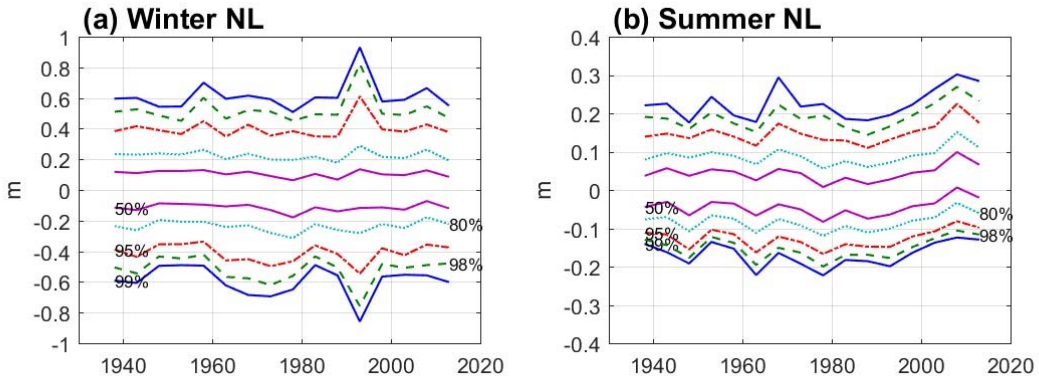

Figure 7.6 (a) shows the distribution of the de-trended December to February (DJF) water level anomalies at New London computed in the same manner as in Figure 7.4(a). (b) shows the same statistics for the June-August interval for comparison to Figure 7.4(b).

Figure 7.7 shows the distribution of the de-trended record from the Willets-Kings Point station. The de-trending procedure had a modest effect on the DJF data in Figure 7.7(a) and made the narrowing of the intervals clearer. In the JJA distribution, the interval bounds were made almost horizontal.

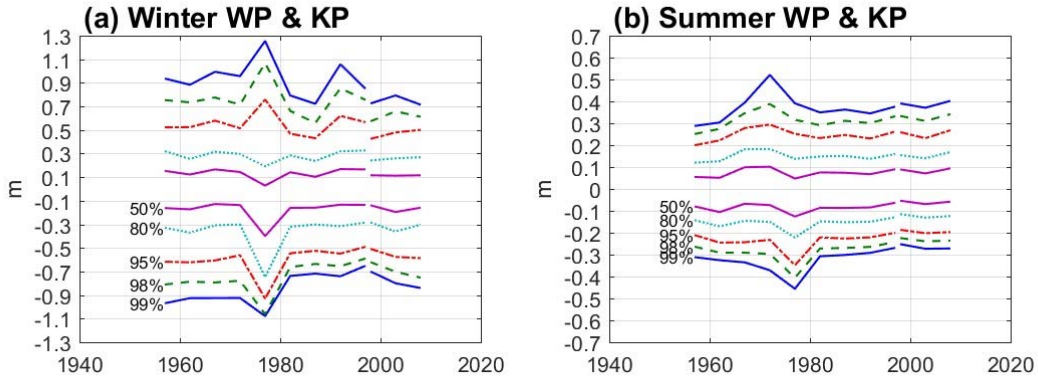

Figure 7.7 (a) shows the distribution of the de-trended December to February (DJF) water level anomalies at Willets-Kings Point computed in the same manner as in Figure 7.5(a). (b) shows the same statistics for the June-August interval for comparison to Figure 7.5(b).

In summary, it appears that the increase in the interval trends is due largely to the increase in sea level over the last 80 years. The significance of small increases in level is that they can have a large increase in the expected frequency of flooding, and a reduction in the frequency of exposure of coast bottom areas to air. The second important feature of note is the narrowing of the percentile bounds in the DJF distribution at Willets-Kings Point. This is the site where the

amplification of the effects of wind is largest and the consequences of reduction in the wind stress would be most readily manifested.

7.4 Summary and Discussion

We have analyzed sea level observations obtained at the eastern and western end of LIS. The tidal effects were extracted using NOAA tidal predictions and the statistics of the anomalies summarized. The theory of Garvine (1985) and Wong (1990) predicts that the amplitude of anomalies driven by winds from the northeast will be large at the western end of LIS compared to those in the east and the distribution of variance in the de-tided records by month of the year is consistent with that prediction. We show that the frequency distribution of the DJF anomalies is significantly impacted by sea level rise, particularly at New London and in the summer at Willets-Kings Point. De-trending the anomalies largely removes this effect. At the Willets-Kings Point station, the DJF percentile bands narrow from 1960 to 2015. This is consistent with a reduction in the magnitude of the along-Sound wind stress driving the local setup in the Sound.

Since the effects of wind on sea level in the winter are so large in the western Sound, the impact of sea level rise is not very significant. In the summer and in the eastern Sound, the impact is large and clearly observable in the anomaly data distributions. The examples of the impacts on the change in the frequency of flooding that the mean sea level change has caused are quite significant. The significance scales with the ratio of the magnitude of the change in mean level to the standard deviation in the wind driven anomalies. When the distribution is narrow, a small change in the mean level can lead to a large change the frequency of flooding. We show the empirical frequency distribution is narrow in the summer and in the eastern Sound. Coastal ecosystems that are sensitive, either positively or negatively, to changes in flooding frequency will be most impacted in the eastern Sound.

7.5 References

Garvine, R.W. (1985). A simple model of estuarine subtidal fluctuations forced by local and remote wind stress. J. Geophys. Res., *90*(C6), 11,945–11,948.

Foreman, M. (1989). The harmonic analysis of tidal model time series. Adv. Water Resources. 12. 109-120.

O'Donnell, J. and J.E.D. O'Donnell (2012). Coastal Vulnerability in Long Island Sound: The Spatial Structure of Extreme Sea Level Statistics. Oceans, 2012, pp.1-4, 14-19 Oct. 2012.

Wong, K.-C., (1990). Sea level variability in Long Island Sound. *Estuaries*, 13, 362-372.

Chapter 8 - Conclusions

Table of Contents

8. Conclusions

The adaptive management of the resources of Long Island Sound (LIS) requires on-going observations to characterize the variability and change of the environment and ecosystem it supports. It is critical that changes that result from local human activities (and therefore can potentially be regulated) be separated from those that are a consequence of natural cycles and global scale processes. In this project we assembled, reviewed, and analyzed existing measurements from LIS and its watershed to determine whether changes that have been observed at the global scale have discernible and important impacts in the region. We have also created a web site to share the results and distribute data that will facilitate further research on long term changes in the LIS ecosystem.

8.1. Temperature Changes

In Chapter 1 of this report we address the important issue of changing water temperatures in LIS. We transcribed old data and aggregated it with results from more recent measurement programs. We then rationalized differences to synthesize a temperature record characteristic of the surface water of the Sound, and the entire Sound in winter. The data were then bin averaged in three year intervals to create records that span 1930 to 2012 in the winter and 1915 to 2012 in the summer.

We conclude that water temperatures in the interval 1960-2010 were anomalously cool in both the winter and the summer, whereas the winters between 1945 and 1955 were anomalously warm. Since 1965, temperatures in both the summer and the winter have been rising. We show that the winter temperature index is very highly correlated with the water temperatures at Woods Hole, MA, and air temperatures at Bridgeport, CT. This allows the LIS temperature index to be extrapolated backwards in time and the recent changes can be then viewed in a longer context. The recent warming trend is rapid, but not inconsistent earlier periods of warming. The long term warming rate is consistent with global trends at 1^{o}C/century.

8.2. Precipitation Changes

Global-scale climate model forecasts have raised concern about the possibility of changes to precipitation patterns in New England. We aggregated available data and find that the mean annual precipitation rate at inland stations in southern Connecticut is significantly higher than at coastal and Long Island stations but there is no evidence of a significant long term trend of the area-wide average. There are, however, long term trends within the region with the annual precipitation in the coastal regions negatively correlated at decadal scales with those inland. The inland stations also show an increasing trend; the coastal and Long Island stations show a negative trend. The number of days of rain and snow were also examined and we find no appreciable change, although there is evidence of fewer rain days in coastal Connecticut in the recent past relative to the 1930s. Finally, we examined the frequency of occurrence of rainfall events leading to more than two inches of rain in a day. We find no evidence of an increasing trend in the frequency of these events.

8.3. Coastal Air Temperature

Using measurements archived by NOAA and transcribed from old reports dating from 1779, we find that there has been a warming in New Haven, CT, of between 2 ^{o}C and 4 ^{o}C over the last

200 years. The larger values apply to the winter months (November-February) and the smaller values to April-August. The larger values are statistically significant. We also examined hourly measurements to determine whether there have been changes in the day of the year that frosts end in the spring, and start again in the fall, relative to 1779-1865. We find that the frosts end 16.1 days earlier and begin again 19.7 days later. This effectively lengthens the frost-free season by almost 36 days. A similar expansion in the duration of days above other temperature thresholds has occurred and can be estimated from the data presented.

8.4. River Discharge

We have examined the trends in the volume flow in the Connecticut and Hudson Rivers, two major contributors of fresh water in the Sound. We find that discharge patterns are very similar in the Connecticut and Hudson. Both records exhibit large decadal-period oscillations and the annual discharges are increasing. We also confirmed that the spring freshet in the Connecticut is occurring earlier in the spring at a rate of 8 days/century. The Hudson was shown to be undergoing a similar trend though at a slower rate. The oscillations in discharged were not found to be linearly correlated with the North Atlantic Oscillation.

An important new insight from our analysis is that the streamflow in the spring has not changed in these rivers and that increases in total discharge are a consequence of higher rates in the low-flow months (June-December). There are been almost a doubling of the amount of water reaching New York Harbor and LIS in these months since 1945. As a fraction of the annual flow, the spring contribution has diminished by almost 15% in the Hudson and 10% in the Connecticut in the last 60 years.

A plausible explanation of the increase in river discharge we detected in the low flow season is that regional atmospheric warming has caused more early winter precipitation to fall as rain and less as snow. The liquid precipitation would quickly augment the streamflow and not be stored until the following spring. Evaluation of this hypothesis could certainly be conducted using an analysis of temperature and precipitation data the upper river watershed. This is a worthwhile follow-on project.

Similarly, the impact of the increased streamflow on the fall density structure in Long Island Sound needs to be assessed. The available salinity distribution data is only almost 30 years in length, however, the ocean salinity variation may not be sufficiently well constrained. The most straightforward approach would be to investigate the potential impact using well calibrated numerical models.

8.5. Cloudiness

The fraction of the sky that is covered by cloud influences the light levels reaching the surface of the Sound. We have explored the possibility that the anomalously low concentration of chlorophyll-A observed in surveys of LIS in 1998-99 were associated with increased cloud cover in the spring and summer and, consequently, reduced light levels. We examined data from weather records but concluded that the results of a data assimilative reanalysis model would be the only source of information that spanned the period of the chl-A records. We find that the cloud cover was unusually low during the years of anomalously low chl-A. This is more

consistent with the hypothesis that the chl-A was low because higher light levels supported the production that could be sustained by available nutrients with less chl-A.

8.6. Wind

Previous work has shown that the mean wind speed in the windiest months in New England (February-April) has diminished since 1960, and we sought to assess the implications for sea level fluctuation and mixing rates in LIS. Using data from the Bridgeport–Sikorski Airport, we demonstrate that the decreasing trend has continued through 2015. Further, the average wind speeds during the calmer months, July-September, also show a substantial decrease. Though the mean speed is a useful summary statistic, it is the vector wind stress that is more directly relevant to important processes in the ocean. We estimate the stress using wind speed and direction and examined the empirical probability distributions of the stress vector components. We find a dramatic decline in the magnitude of the 95% and 80% stress levels. In February to April of the 1960-80 interval, the magnitude of the stress during events that were less frequent than 5% was approximately 0.2 Pa. Since 2000 it has been 0.1 Pa. Summer statistics show a similar change.

The trends in speed and stress do not show much decadal scale variability. However, the pattern does resemble the Atlantic Multi-decadal Oscillation (AMO) index. Since 1970, the AMO has been changing from a low to a high phase which is associated with a warm north Atlantic surface water and reduced storm intensity.

The work of O'Donnell et al. (2006 and 2008) and Wilson et al. (2008 and 2015) demonstrates that wind stress has a strong influence on the intra-annual variation in the area of hypoxia during the summer in western Long Island Sound. The magnitude of the summer winds don't appear to have a large role. This work focusses on the statistics of the infrequent and large events and therefore don't directly address the issue of hypoxia. However, the correlation with the AMO might also be high when only the summer winds are concerned and this is at least worth a preliminary investigation.

8.7. Sea Level

Sea level fluctuations driven by wind dictate the character of flooding around the coast of the Sound and this influences the availability of habitat and population dynamics. Sea level rise and changes in the wind patterns will lead to changes in the statistics of water level fluctuations. We constructed empirical probability distributions for non-tidal water level fluctuation using data from tide gages at New London, in the east of LIS, and Willets Point and Kings Point in the west. Theory and earlier work show that the western locations have an amplified response to wind stress from the east. We show that the frequency distribution of the December to February (DJF) anomalies is significantly impacted by sea level rise, particularly at New London and in the summer at Willets-Kings Point. At Willets-Kings Point, the DJF percentile bands narrow from 1960 to 2015. This is consistent with a reduction in the magnitude of the along-Sound wind stress driving the local setup in the Sound.

We demonstrate using a few examples that small increases in mean sea level can lead to a large increase in the expected frequency of flooding, and a reduction in the frequency of exposure of coastal sea bottom areas to air.

The impact of these long term (decades) variations in the statistics of sea level on the ecological function of salt marshes is likely to be significant. The data show unequivocally that the frequency of occurrence of high water levels has increased due to the increase in mean sea level and, therefore, marsh surfaces are likely to be flooded more frequently. It also appears that this effect has been partially offset by the reduction in the magnitude of the highest wind stresses that occur during storms. The correlation with the AMO index suggests that in the coming 40 years the storms will strengthen again and the frequency of flooding will increase more rapidly. The potential geochemical and ecological impacts of these effects should be evaluated in the near future.

8.8. Concluding Comments

In this project we also examined other data sets but decided not to include the analyses in this report. We acquired and developed computer format files for records from Noank and Milford Laboratories, and from the Riley expeditions. However, these data did not exhibit the spatial correlation that allowed the synthesis of the type we report in Chapter 1. The highly variable and localized sources of freshwater introduce too much noise for sparse data to be useful for broad scale analyses. We also examined the pH record provided by Millstone and decided not to include it here since it requires comparisons with independent data sets that are not available. We expect that others will be better able to exploit that data source in the future.

References

O'Donnell J, Bohlen WF, Dam HG (2006) Wind stress and the ventilation of the hypoxic zone of western Long Island Sound. Proc 8th Biennial Long Island Sound Research Conference, CT Sea Grant Program, New London, CT

O'Donnell J, Dam HG, Bohlen WF, Fitzgerald W, Gay PS, Houk AE, Cohen DC, Howard-Strobel MM (2008) Intermittent ventilation in the hypoxic zone of western Long Island Sound during the summer of 2004. J Geophys Res 113. doi:10.1029/2007JC004716

Wilson RE, Swanson RL, Crowley HA (2008) Perspectives on long-term variations in hypoxic conditions in western Long Island Sound. J Geophys Res113:C12011. doi:10.1029/2007JC004693

Wilson RE, Bratton SD, Wang J, Colle BA (2015) Evidence for Directional Wind Response in Controlling Inter-annual Variations in Duration and Areal Extent of Summertime Hypoxia in Western Long Island Sound. Estuaries and Coasts, Volume 38, Issue 5, pp 1735-1743

Executive Summary

The adaptive management of the resources of Long Island Sound (LIS) requires on-going observations to characterize the variability and change of the environment and ecosystem it supports. It is critical that changes that result from local human activities (and therefore can potentially be regulated) be separated from those that are a consequence of natural cycles and global scale processes. In this project we assembled, reviewed, and analyzed existing measurements from Long Island Sound and its watershed to determine whether changes that have been observed at the global scale have discernible and important impacts in the region. We have also created a web site to share the results and distribute data that will facilitate further research on long term changes in the Long Island Sound ecosystem.

The most important results of this project are:

- Over the last century Long Island Sound has warmed at a rate consistent with global averages. The decade of the 1960s was anomalously cool. Warming since then has been faster that global trends but not inconsistent with warming that occurred between the 1940s and 1960s. (See Chapter 1 – Coastal Water Temperature)
- We find no evidence of changes in annual precipitation across the region or in the occurrence of high rates of rainfall. However, it does appear that the rainfall in the coastal Connecticut and Long Island is decreasing slightly and it is increasing at the more inland stations. (See Chapter 2 – Precipitation)
- Coastal air temperatures have increased at a rate consistent with global averages. This has appreciably lengthened the interval between spring and fall frosts. (See Chapter 3 – Coastal Air Temperatures)
- The annual stream flow in the Hudson and Connecticut Rivers is increasing due to higher flow rates in the low-flow months (June-December) and the spring freshet is arriving 8 days earlier than a century ago. (See Chapter 4 – River Discharge)
- Cloud cover over Long Island Sound in the NCEP Reanalysis-II was unusually low during year of anomalously low Chlorophyll-A. It is possible that the reanalysis products are not sufficiently highly resolved to predict the cloud cover at a coastal area like Long Island Sound. (See Chapter 5 – Cloudiness)
- The highest wind stress events each are lower magnitude than they were in the 1960s. This appears to be associated the Atlantic Multi-decadal Oscillation. (See Chapter 6 – Wind)
- Sea levels are rising and that will lead to an increase in the average frequency of flooding at the edge of the Sound. However, winter winds stress events appear to be getting weaker, partially offsetting the effects of sea level rise in the western sound. Ecosystems that are vulnerable to changes in flooding frequency will be more at risk in the eastern Sound. (See Chapter 7 – Sea Level)